Mold Design in Resin Transfer Molding (RTM) Process Using Point-Voltage Sensors

by

Galip Tarkan Guclu

A Thesis Submitted to the
Graduate School of Engineering
in Partial Fulfillment of the Requirements for
the Degree of

Master of Science
in
Mechanical Engineering

Koc University

November 2007

Koc University

Graduate School of Sciences and Engineering

This is to certify that I have examined this copy of a master's thesis by

Galip Tarkan Guclu

and have found that it is complete and satisfactory in all respects,

and that any and all revisions required by the final

examining committee have been made.

Committee Members:

____

E. Murat Sozer, Ph. D. (Advisor)

____

Mehmet Sayar, Ph. D.

____

Ipek Basdogan, Ph. D.

Date: ______________________________

ABSTRACT

In the Resin Transfer Molding (RTM) process, deviations from nominal resin flow may result in an incomplete impregnation of reinforcing preform by resin. To save the composite part, and also automate the process, the following are needed: (i) monitoring the resin flow, (ii) evaluation of sensor data, (iii) detecting any disturbance, and (iv) taking necessary control actions to correct the flow patterns. This study focuses on the first three items of the list. Resin flow was monitored by using multiple point-voltage sensors, and the sensor data was evaluated by an algorithm developed.

Point-voltage sensors were developed and investigated in recent studies; and they are improved by modifying the sensor circuit in this study. These sensors are integrated with a data acquisition (DAQ) system.

A modular RTM mold was designed and manufactured with the aid of the mold design literature. 30 point-voltage sensors are embedded on the mold: 15 on the upper mold part and 15 on the lower mold part. Repeated injections were done to test the response and reliability of the sensors. By comparing the sensor data with visually recorded data, it was verified that the sensors are working properly.

The next step in automation of the process is to evaluate the sensor data and predict if the resin propagation will deviate from the nominal flow. Corresponding to the major disturbance scenarios, 16 off-line mold filling simulations were done using a mold filling software, LIMS. An algorithm was developed to fit the sensor data to the closest off-line simulation. This algorithm was compared with another algorithm from the literature. As a result of this comparison, it cannot be said that one algorithm is better than the other one, but the algorithm developed in this study gives more realistic results than the other algorithm in some cases.

ÖZET

Reçine Transfer Kalıplama (RTM) yönteminde, nominal reçine akışından sapmalar elyafların reçine tarafından tamamen ıslatılamamasıyla sonuçlanabilir. Kompozit parçayı kurtarmak ve üretim yönteminde otomasyonu sağlamak için şunlara ihtiyaç duyulur: (i) reçine akışının izlenmesi, (ii) algılayıcı verilerinin işlenmesi, (iii) hataların tespit edilmesi, ve (iv) akış gelişmesinin kontrol eylemleri ile düzeltilmesi. Bu çalışmada, reçine akışının izlenmesi noktasal-voltaj algılayıcıları ile yapılıp, algılayıcı verilerinin değerlendirilmesi için bir algoritma geliştirilmiştir.

Noktasal-voltaj algılayıcıları geçmiş çalışmalarda geliştirilip, incelenmiştir. Bu çalışmada ise algılayıcı devresi üzerinde iyileştirilmeler yapılmıştır. Ayrıca bir veri toplama sistemi ile algılayıcılar bütünleştirilmiştir.

Reçine Transfer Kalıplama tekniğinde kullanılan kalıplar ile ilgili detaylı bir kaynak araştırması yapılmıştır. Bu araştırmadan faydalanılarak, yeni bir kalıp tasarlanmış ve üretimi yapılmıştır. Bu kalıpta, 15 tanesi alt kalıp parçasında, 15 tanesi de üst kalıp parçasında olmak üzere toplam 30 adet noktasal algılayıcı kullanılmıştır. Tekrarlanmış deneylerde, algılayıcıların güvenilirliği sınanmıştır. Algılayıcı verileri ve kamera ile kaydedilen akış kayıtları karşılaştırılmış, ve algılayıcıların düzgün çalıştığı onaylanmıştır.

Otomasyondaki bir sonraki adım, algılayıcı verilerinin değerlendirilip, nominal akıştan sapma olup olmayacağının tespit edilmesidir. 16 farklı hata senaryosuna gore, LIMS adlı kalıp akış yazılımı kullanılarak simülasyonlar yapılmıştır. Bu simülasyonlarla gerçek deney verilerini eşleştirmek için, bir algoritma geliştirilmiştir. Bu algoritma daha önce geliştirilmiş başka bir algoritmayla karşılaştırılmıştır. Bu karşılaştırmaya göre, algoritmalardan birinin diğerine göre daha iyi olduğunu söylemek zordur, ancak tarafımızdan geliştirilen algoritmanın bazı durumlarda daha gerçekçi sonuçlar verdiği gözlenmiştir.

ACKNOWLEDGEMENTS

I would like to thank my advisor Murat Sözer for all his help in my studies for these two years. I would also like to thank Assist. Prof. Mehmet Sayar and Assist. Prof. İpek Başdoğan for their participation in the thesis committee; my team mates Murat Danışman, Murat Senan, Tolga Bayrak, Bekir Yenilmez and Muharrem Ceyhun Sözbir for all kinds of support they gave in the laboratory studies and in proofreading this thesis report.

I want to thank my parents, Mehmet and Sema Güçlü, and my brother, Volkan Dağyaran for their endless love and support.

Thanks to Cihan Bilir for sharing his room and thanks to Taylan Bilal and Hüseyin İlker Ocaklı for sharing their home with me. Finally, I would like to thank to my other friends, Mustafa Kaymakçı, Onur Demir, Özlem Tekmek, Kamil Buğra Toga, Özgür Özsun and Mehmet Yılmaz.

TABLE OF CONTENTS

List of Tables ix

List of Figures x

Nomenclature xiv

Chapter 1: Introduction to Composite Materials and Resin Transfer Molding (RTM) Process 1

1.1 Composite Materials…………………………………………………….. 1

1.1.1 Fabric……………………………………………………………… 2

1.1.2 Resin system…………………………………………………………. 4

1.2 Manufacturing Techniques for Composite Materials……………………………. 6

1.2.1 Resin Transfer Molding (RTM) Process………………………………….. 7

1.3 Experimental Set-up and Mold Design………………………………………… 9

1.4 Injection Machine…………………………………………………………… 9

1.5 Resin System and fabric used in the Experiments…………………………... 10

1.6 Organization of the Thesis……………………………………………………... 11

1.7 Contributions Done in this Thesis…………………………………………….. 12

Chapter 2: Sensor Requirement in RTM and Available Sensor Systems 13

2.1 Requirement of Sensors in RTM……………………………………………...... 13

2.2 Available Sensor Systems in the Literature………………...…………………… 14

2.2.1 Thermocouples………………………………………………………. 15

2.2.2 Smartweave……..…………………………………………………… 15

2.2.3 Dielectric analysis……………………………………………………. 16

2.2.4 Ultrasonic sensors………………………………………………………. 16
2.2.5 Fiber-optic sensors…………………………………………………..... 17
2.2.6 Lineal-voltage sensors……………………………………………….. 17
2.2.7 Point-voltage sensors………………………………………………… 18

Chapter 3: Point-Voltage Sensor System 19
3.1 Sensor Configuration………………………………………………………… 19
3.1.1 Sensor bolts………………………………………………………….. 20
3.1.2 Circuit……………………………………………………………….. 22
3.1.3 DAQ System………………………………………………………… 26
3.2 Response of the Sensors……………………………………………............ 28
3.2.1 Flow Front Monitoring……………………………………………… 28
3.2.2 Resin Cure Monitoring……………………………………………… 35

Chapter 4: Mold Design for Resin Transfer Molding 38
4.1 Introduction…………………………..……………………………. 38
4.2 Mold Material Selection.…………………..…………………………… 38
4.3 Clamping Systems and Forces on the Tools…..……………………………... 45
4.4 Ejector Systems…………………..…………………………………... 50
4.5 Sealing of Molds…..……………………………………………………….. 54
4.6 Injection Gates / Ventilation Ports………………………………………..... 56
4.7 Mold Filling and Automation……………………………………………… 58
4.8 Experimental Set-up and Mold Design……………………………………….. 63

Chapter 5: Mold Filling Simulations and Sensor Data Evaluation 70
5.1 Mold Filling Simulations..……………………………………………………. 70

5.2 Permeability Calculation……………………………………………………….. 76
5.2.1 Permeability of Fabric Preform……………………………………….. 76
5.2.2 Permeability of Race-Tracking Channels……………………………...... 77
5.2.3 Permeability of Inlet / Ventilation Pools………………………………... 78
5.2.4 Permeability of the Bumps……………………………………...……… 78
5.3 Results of the Simulations………………………………………………… 79
5.4 Sensor Data Evaluation……………………………………………………….. 96
5.4.1 Time Normalization Algorithm……...………………………………. 98
5.4.2 Sensor Triggering Order Based Algorithm……………………………... 100
5.4.3 Comparison of Algorithms……………………………………...………. 102

Chapter 6: Mechanical Tests of Composite Materials 105
6.1 Introduction………………………………………………………………… 105
6.2 Three-Point Bending Test……..……………………………………………… 106
6.3 Tensile Test………………………………………………………………… 110
6.4 Future Work….……………………………………………………………… 117

Chapter 7: Conclusion 118

Bibliography 120

Vita 124

Appendix A 125

Appendix B 127

LIST OF TABLES

1.1 Mechanical properties of different engineering materials ………………………. 5

1.2 Viscosity values for different materials…………………………………………... 6

1.3 Pot life at room temperature for Polipol™ 336-RTM measured in our laboratory. 11

3.1 Sensor triggering times for the experiment using sensor data (in seconds)………. 30

4.1 Properties of selected engineering materials……………………………………… 44

5.1 Dimensions of regions and number of elements………………………………….. 74

5.2 Permeability of race-tracking channels with a fixed height of $h = 3\ mm$ ………… 78

5.3 Normalized time values of the experiment………………………………………. 99

5.4 Penalty values for the Predefined Scenarios, Scn 1-16…………………………… 100

5.5 Results of the triggering order based algorithm…………………………………... 101

5.6 Penalty values for sensor triggering order based algorithm………………………. 102

5.7 Comparison of two algorithms……………………………………………………. 104

6.1 Equivalent test methods for tensile and bending properties of composite materials…………………………………………………………………………..... 105

6.2 Flexural properties for glass reinforced polyester composites……………………. 108

6.3 Tensile properties of glass reinforced polyester composites……………………… 114

LIST OF FIGURES

1.1 Composite parts in different applications……………………………………. 2

1.2 Different glass fabric types and core material that were used in this study….. 3

1.3 Stages of RTM process……………………………………………………. 8

1.4 (a) Injection machine; and (b) display of Floware software…………………. 10

2.1 SMARTweave……………………………………………………………… 16

2.2 Lineal-voltage sensor on a mold cavity……………………………………… 18

3.1 Sensor configuration from the side view of the mold………………………… 20

3.2 A point-voltage sensor bolt…………………………………………………. 21

3.3 Electrical circuit for the point-voltage sensor………………………………… 23

3.4 Electrical circuit with buffers and multiplexers………………………………. 24

3.5 Differential amplifier………………………………………………………. 25

3.6 Four circuits connected to 30 sensors………………………………………… 27

3.7 Labview user interface snapshot……………………………………………… 28

3.8 Sensor configuration on the lower mold cavity………………………………. 29

3.9 Flow front propagations from sensors of (a) upper mold plate, (b) lower mold plate…………………………………………………………………….. 31

3.10 Snapshots of the flow front propagation……………………………………. 32

3.11 Flow front position at t = 37 s………………………………………………. 32

3.12 Flow front position at t = 66 s………………………………………………. 33

3.13 Responses of sensors 1-2 for resin flow monitoring………………………… 34

3.14 Responses of sensors 3-4 for resin flow monitoring………………………… 34

3.15 Responses of sensors 5-6 for resin flow monitoring………………………… 35

3.16 Curing responses of sensor 10………………………………………………. 36

3.17 Curing responses of sensor 11………………………………………………. 37

4.1 A typical hydraulic press used in RTM………………………………………. 46
4.2 A latch clamp combination for mold closure………………………………… 46
4.3 Bolt and nut system for clamping of mold plates……………………………. 47
4.4 Compression pressure vs. V_f for four layers of stitched random type fabric… 48
4.5 A composite part with 5 layers……………………………………………….. 49
4.6 A pin ejector………………………………………………………………….. 51
4.7 Ejector pin assembled in a mold……………………………………………. 52
4.8 Stem ejector…………………………………………………………………. 53
4.9 Stem ejector embedded in the mold…………………………………………. 53
4.10 Silicon O-ring……………………………………………………………….. 54
4.11 O-ring placed in the mold…………………………………………………… 55
4.12 O-ring channel……………………………………………………………… 55
4.13 A bolt to be used as injection gate and ventilation bolt……………………... 56
4.14 Tube connector with inlet / ventilation bolt………………………………… 57
4.15 Resin pool for lineal injection………………………………………………. 58
4.16 Fabric wash…………………………………………………………………. 59
4.17 Race-tracking channels in a flat mold cavity……………………………….. 61
4.18 A composite part which is not fully filled…………………………………… 61
4.19 RTM mold and its components……………………………………………… 63
4.20 The upper mold plate………………………………………………………... 64
4.21 The lower mold plate……………………………………………………….. 65
4.22 Hydraulic press with the mold……………………………………………… 66
4.23 Clamps and bolts for mold closure with plexiglass upper mold plate………. 66
4.24 Fabric roll and placement of fabric preform into the mold cavity…………... 67
4.25 Sensor locations on the mold cavity (dimensions in mm.)………………….. 69
4.26 Mold cavity dimensions (in mm)…………………………………………… 69

5.1 Top view of the mold with dimensions (in millimeters)……………………… 71
5.2 Potential race-tracking channels in the mold…………………………………. 71
5.3 Meshed view of the mold cavity……………………………………………… 73
5.4 Node and element numbers at the corners of the mold (red numbers inside boxes are element numbers, and black numbers around boxes are node numbers). 75
5.5 Race - tracking channel dimensions………………………………………….. 77
5.6 Race-tracking channel widths in different disturbance scenarios Scn 1-16…... 79
5.7 Simulation results for scenario 1……………………………………………… 80
5.8 Simulation results for scenario 2……………………………………………… 81
5.9 Simulation results for scenario 3……………………………………………… 82
5.10 Simulation results for scenario 4…………………………………………….. 83
5.11 Simulation results for scenario 5…………………………………………….. 84
5.12 Simulation results for scenario 6…………………………………………….. 85
5.13 Simulation results for scenario 7…………………………………………….. 86
5.14 Simulation results for scenario 8…………………………………………….. 87
5.15 Simulation results for scenario 9…………………………………………….. 88
5.16 Simulation results for scenario 10…………………………………………… 89
5.17 Simulation results for scenario 11…………………………………………… 90
5.18 Simulation results for scenario 12…………………………………………… 91
5.19 Simulation results for scenario 13…………………………………………… 92
5.20 Simulation results for scenario 14…………………………………………… 93
5.21 Simulation results for scenario 15…………………………………………… 94
5.22 Simulation results for scenario 16…………………………………………… 95
5.23 Flow front contours of the scenarios 1-16…………………………………... 97
6.1 Three-point bending test……………………………………………………… 106
6.2 Schematic of the three-point bending test…………………………………….. 107

6.3 The three-point bending apparatus in our university……………………………. 109
6.4 Specimen for three-point bending test………………………………………... 110
6.5 A typical stress versus strain plot for reinforced plastics…………………….. 111
6.6 Composite material under tensile test………………………………………… 113
6.7 Specimen manufactured according to ASTM D3039………………………… 115
6.8 Specimen geometries according to ASTM D 638…………………………… 116
6.9 A specimen which fractured with failure……………………………………... 116
6.10 A specimen with tabs………………………………………………………... 117

NOMENCLATURE

V_f	Fiber volume fraction
ϕ	Porosity
R_{media}	Electrical resistance between the two probes of the sensor [Ω]
R_1	Resistance parallel to R_{media} [Ω]
$R_{equivalent}$	Equivalent resistance of R_{media} and R_1 [Ω]
R_2	Resistance serial to $R_{equivalent}$ [Ω]
V	Input voltage of the sensors [V]
V_R	Output voltage of the sensor before amplification [V]
V_{out}	Output voltage of the sensor after amplification [V]
V_{REF}	DC voltage generated for sensor calibration [V]
V_{out2}	Output voltage of the sensor for flow monitoring [V]
SU#	Resin arrival time at upper mold plate sensor [s]
SL#	Resin arrival time at lower mold plate sensor [s]
n	Number of fabric layers in preform
$\rho_{superficial}$	Areal density of fabric preform [kg/m^2]
ρ_{fiber}	Density of fabric preform [kg/m^3]
h	Thickness of the preform [m]
$\bar{u}_x$	Average velocity of resin in x-direction [m/s]
μ	Viscosity [Pa.s]
K_{xx}	Permeability of the fabric preform [m^2]
$\partial P/\partial P$	Pressure gradient in x- direction. [N/m^3]
K	Dimensional permeability [m^2]
K^*	Non-dimensional permeability [m^2]
w	Width of race-tracking channel [m]

w_1	Width of lower race-tracking channel [m]
w_2	Width of upper race-tracking channel [m]
k	Conductive heat transfer coefficient [W/(m. ^{0}C)]
$t_{i,exp}$	Actual arrival time of resin at sensor i [s]
$\bar{t}_{j,\mathrm{exp}}$	Normalized triggering time of sensor j
$P_{Scn\,k}$	Penalty value for scenario k
$s_{i,exp}$	Triggering order of sensor i
t	Simulation time [s]
σ_F	Maximum failure strength under bending [MPa]
E_F	Bending modulus [GPa]
y_M	Maximum bending deflection [m]
F_F	Force when the specimen ruptures or the critical deflection is reached before rupture [N]
L	Distance between two support spans [m]
d	Thickness of the specimen [m]
b	Width of the specimen [m]
E	Modulus of elasticity [GPa]
σ_Y	Yield strength [MPa]
σ_U	Ultimate strength [MPa]
u_t	Modulus of thoughness [MPa]
ε	Strain of the material under load
Δl	Elongation [m]
l_0	Initial gage length of the material [m]
A_0	Initial cross-sectional area [m^2]
e	Initial thickness of the specimen [m]

Chapter 1

INTRODUCTION TO COMPOSITE MATERIALS AND RESIN TRANSFER MOLDING (RTM) PROCESS

1.1 Composite Materials

Composites are combinations of at least two dissimilar materials. Typical examples of these materials are polymer and reinforcing fibers. These composites are called fiber-reinforced polymer composites. Continuous fibers are surrounded by a matrix of cured polymer [1].

Composite materials are not only preferred for their structural properties such as high specific strength (= strength/density), high resistance to chemical interactions or low density, but they are also used for their electrical, thermal or environmental properties. Typical composite parts have much lower electrical and thermal conductivities than many metals. Because of that, food storage units of trains are being manufactured from composite panels.

Composites are used in sporting goods, aircraft parts, automotive components, ship bodies, bridges and many other applications which require high specific strength (see Figure 1.1).

Figure 1.1 Composite parts in different applications [2-5].

1.1.1 Fabric

A fabric is a structure of fibers. Fibers can be continuous or discontinuous. In fiber-reinforced composites, fabric is the component which provides most of the structural support under loading. It is usually made of glass or carbon fibers. In some applications, aramid fibers are used. Also, they can be in different structures such as unidirectional and bidirectional forms. In Figure 1.2, two glass fabric types of this study are seen.

Fiber volume fraction ($V_f = 1 - \phi$, where ϕ is the porosity) is the ratio of the fiber volume to the total volume of the part in composite materials. As V_f increases, structural capabilities of the material increase, but it gets harder to compact the fabric and to inject the resin through the fabric [1]. By embedding a core material (seen in Figure 1.2) in a stack of fabric layers, the overall permeability of "fabric + core" sandwich increases very significantly. In other words, the resistance of the preform decreases against resin flow, when a core material is used as a distribution media. Because a core material is a highly porous media compared to the fabric. When it is compacted together with a fabric preform, the resin flows easily through the core material and saturates the fabric preform.

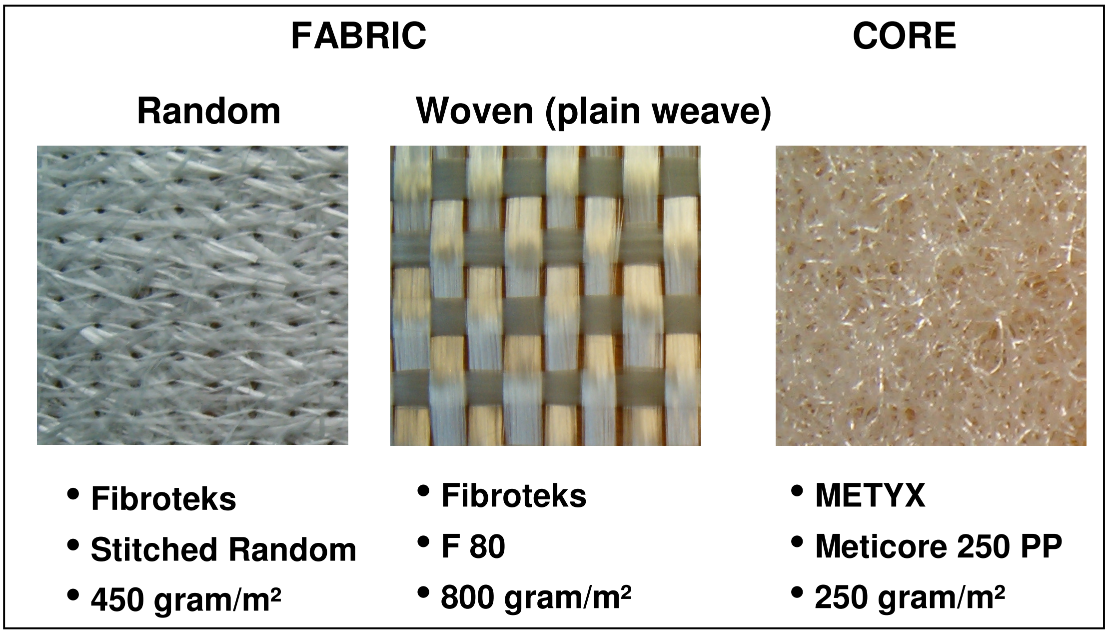

Figure 1.2 Different glass fabric types and core material that were used in this study.

Stitched-random type glass fabric was used in the experiments of this study. Due to its random structure, its permeability tensor and mechanical properties in in-plane directions are expected to be isotropic. In Table 1.1, mechanical properties of different engineering materials are shown including glass fibers.

1.1.2 Resin system

Resin is a polymer with the necessary curing agents and accelerators added in it just before the injection. As resin cures, it becomes a solid matrix around the fibers. The role of the resin to provide the structural properties is not much (see Table 1.1), but it keeps the fibers together and forms the geometry of the part to be manufactured. Also, by choosing a correct resin type, desired electrical, thermal or environmental properties can be provided to composite parts. Another role of the resin is to transfer stresses between fibers if a good contact is achieved between the fibers and the polymer matrix [7].

Two types of resins are used in composite materials: thermosets and thermoplastics. Thermosets are in liquid phase at room temperature, but when additional energy is added into them (by heating or by chemical reactions), molecules form a three-dimensional network structure by cross-linking (covalent bonds). This stage is called *curing*. By curing process, thermosets can be molded. But this curing process is irreversible; they cannot be melted and reshaped once curing occurs. Whereas thermoplastics have weaker bonds between their atoms (van der Waals bonds or hydrogen bonds), and they can be reshaped as many times as required. Despite impact or fracture resistance advantages of thermoplastics, they are not used much in the composite industry due to their high viscosity (see Table 1.2) which makes it difficult to inject the polymer through a fabric preform [7].

As explained above, the formation of covalent bonds between mers (unit cells) is called curing. In case of thermosets, small amount of additives such as peroxide are added into polymer for curing. Also, by adding cobalt solution into the system, the curing process is accelerated. These additives are also called *catalysts*. When the catalysts are added, viscosity of the polymer increases sharply after a *pot life*. This increase in the viscosity corresponds to *gellation*. Pot life is related to the ratio of the additives in the resin system. For mass production of composite parts, pot life has to be set as short as possible in order to decrease the manufacturing time of a single part. But there is a risk that the resin may gellate before the part is filled completely, if the pot life is too short [1,7].

Table 1.1 Mechanical properties of different engineering materials [6].

Material	**Modulus of Elasticity, E [GPa]**	**Ultimate Tensile Strength, UTS [MPa]**
Aluminum	69 - 79	90 – 600
Steel	190 - 200	415 – 1750
Thermoplastic polymer	1.4 - 3.4	2 – 70
Thermoplastic polymer (reinforced with short fibers)	2 - 50	20 – 120
Thermoset polymer	3.5 - 17	35-170
Glass fiber (unidirectional)	73 - 85	3500 – 4600
Carbon fiber	275 - 415	2000 – 3000
Kevlar (Aramid)	62 - 117	2800

Table 1.2 Viscosity of different materials [8].

Material	**Viscosity [Pa.s]**
Air	10^{-5}
Water	10^{-3}
Glycerin	1
Thermosets	0.05 to 0.5
Molten thermoplastics at processing temperature	10^{2} to 10^{6}
Glass	10^{21}

1.2 Manufacturing Techniques for Composite Materials

The manufacturing techniques in composite materials can be divided into two groups: (i) open mold processes, and (ii) closed mold processes. In open mold processes, no conventional mold is used to manufacture the parts. Filament winding and pultrusion are open mold processes in composite manufacturing. In closed mold processes, a fabric preform is placed inside a mold, and it is impregnated with resin. After de-molding, the part might need post-processing such as trimming. Resin Transfer Molding (RTM) is an example of closed molding technique [8].

But, from the view of transport phenomena, manufacturing techniques can be divided into three categories [8]:

- short suspension manufacturing methods,
- squeeze flow manufacturing methods,
- porous media manufacturing method.

In *short suspension manufacturing methods*, fibers are cut into small pieces and mixed with resin (pellets). The pellets are molted (by external heat and friction) before injection stage. The suspension of fibers and resin is then injected into a mold, or it passes through a die (injection and extrusion processes). In another example of short suspension methods, a charge of raw material is placed inside a mold, and it is compressed (by applying heat and pressure) to take the final geometry of the part [8].

Instead of using pellets, if long fiber-reinforcements are used, the processes are called advanced composite manufacturing techniques. For thermoplastics, heat and pressure are applied to highly viscous resin and long fibers to deform them together to take the final shape of the part. These methods are called *squeeze flow manufacturing methods.* Thermoplastic sheet forming, thermoplastic pultrusion and fiber tape laying methods can be classified in this group [8].

The manufacturing of composites using thermosets and continuous fibers is called *porous media manufacturing method*. In this class, fabric preform is impregnated with resin and the part takes its final shape after curing. This class includes: autoclave processing, filament winding, and all liquid composite molding (LCM) processes such as Resin Transfer Molding (RTM), vacuum assisted RTM (VARTM), and wet-hand lay-up [8].

1.2.1 Resin Transfer Molding (RTM) Process

In Resin Transfer Molding (RTM), several layers of continuous glass or carbon fabric are placed in the lower part of a mold. Then, the mold is closed, and a thermoset polymer with curing agents added in it is injected into the mold from a suitable injection gate(s). The resin propagates through the porous media (glass or carbon fabric preform), replaces the air inside the mold and reaches ventilation ports. As propagating in the mold, the resin impregnates the fabric preform. Then, it is left for curing inside the mold at room temperature or in an auto-clave depending on the resin system used. After curing, the mold is opened and the cured part is taken out of the mold [10]. These steps are also illustrated in Figure 1.3.

In our work, RTM was used to manufacture composite panels. It is commonly used in composite industry especially when a high volume production is required. It has some major features in manufacturing such as high fiber volume fraction (V_f) in parts to achieve high-strength, good surface quality, near net-shape manufacturing and complex part shapes [1].

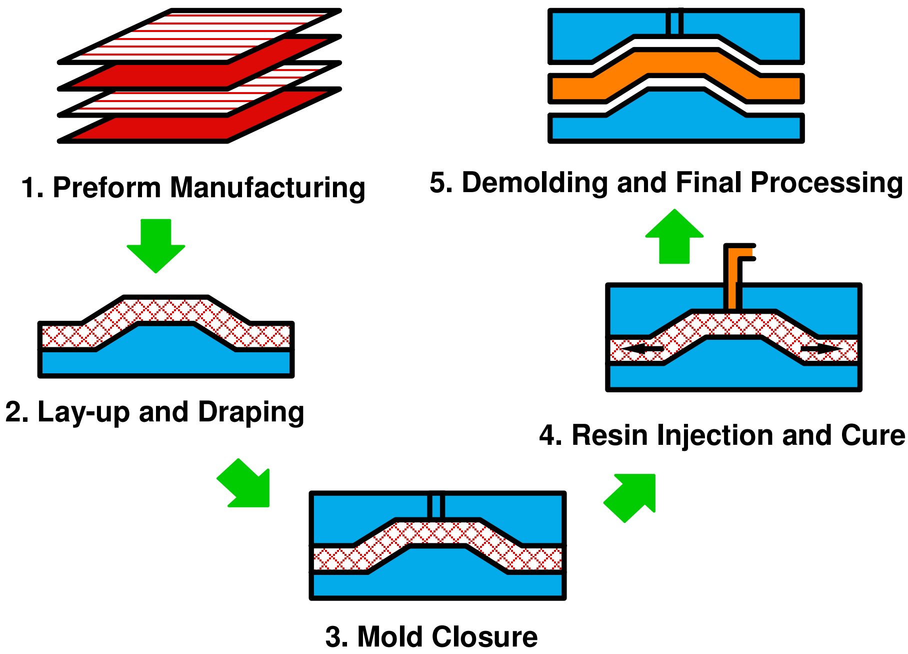

Figure 1.3 Stages of RTM process [1].

1.3 Experimental Set-Up and Mold Design

A mold has been designed and manufactured for TUBITAK MAG 104M290 project. The details about the mold are given in Chapter 4.

1.4 Injection machine

There are two injection machines in our laboratory from Radius Engineering Inc. (see Figure 1.4a). These machines can be operated both from the pad on the machine manually, or using the software Floware (see Figure 1.4b) on a computer. These injection machines are flow rate controlled which means that they can perform injections at a desired flow rate. All the injection parameters and variables can be monitored from Floware (such as resin pressure, flow rate, remaining volume, temperature of the resin, etc). A digital display on the machine shows these parameters and variables in less detail. There is a pressure transducer mounted at the exit of the machine to measure the pressure of the resin. If the resistance of the connecting tube is neglected, this pressure is equal to the inlet pressure of the mold. A control system is integrated to heat the resin and to keep it at a desired temperature inside the cylinder. The volume of the cylinder is 2500 cc. In our experiments, we used low flow rates between 25 and 50 cc/min. The flow rate value is selected in such a way that no micro size voids are entrapped remain in the fabric, and also injection pressure does not reach a critical value.

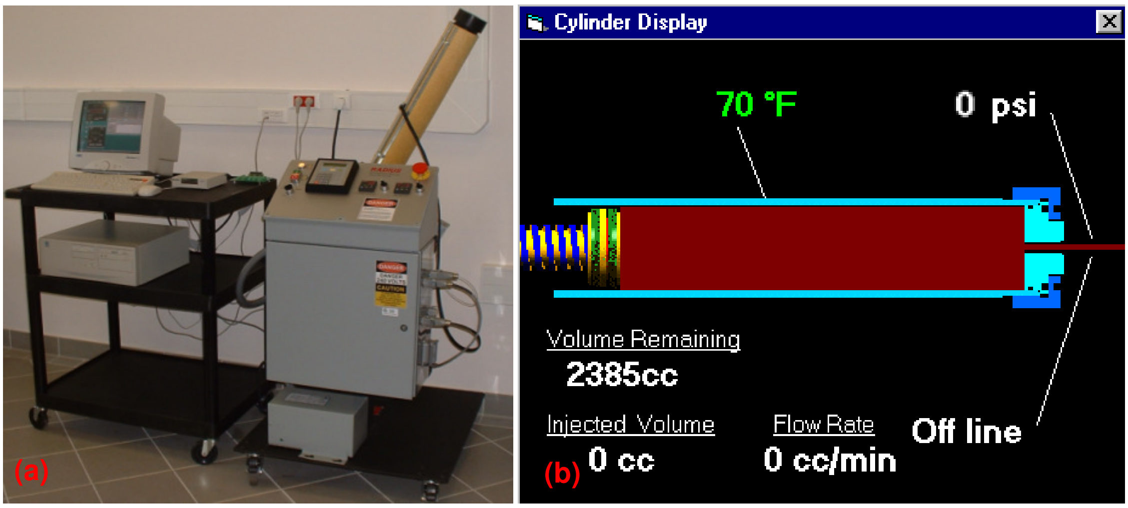

Figure 1.4 (a) Injection machine; and (b) display of Floware software [1].

1.5 Resin System and Fabric Used in the Experiments

There are many kinds of thermosets (such as epoxy, polyester, vinyl ester or bismaleimides) used in composites [7]. In our experiments, we use a general purpose polyester (Polipol™ 336-RTM [9]) supplied from Poliya, Turkey. It has a low viscosity, and low volumetric shrinkage. It has a density of 1.04 g/cm³ and viscosity of 0.300 Pa.s. [9]. Also, the pot life measured in our laboratory for Polipol™ 336-RTM is shown in Table 1.3 for two different additive ratios.

Stitched-random type e-glass fabric is used in this study. It is supplied from Fibroteks, Turkey. Its superficial density (= areal density) is 450 gr/m^2.

Table 1.3 Pot life at room temperature for Polipol™ 336-RTM measured in our laboratory [9].

Polyester	1000 ml	1000 ml
Butanox M60	5 ml	5 ml
Cobalt (1% solution)	5 ml	3 ml
Pot life (min.)	~20	~35

1.6 Organization of the Thesis

In this study, we monitored resin flow and cure using point–voltage sensors. Also, an algorithm was developed to evaluate the sensor data. The organization of the chapters is as follows: a short review of sensors is given in Chapter 2; working principle of the sensor system, details about the sensors and a case study are presented in Chapter 3; issues about mold design in RTM process and a mold designed by us are discussed in Chapter 4; comparison of different algorithms to evaluate sensor data is given in Chapter 5; issues related with standard tests to measure mechanical properties of composite materials are given in Chapter 6 and a conclusion is given in Chapter 7.

1.7 Contributions Done in This Thesis

Automation of RTM process requires monitoring of mold filling. Point–voltage sensors were investigated in a recent study [1] to monitor mold filling and resin cure. In this study, modifications were done on this sensor type. In the previous study, gain factor of the sensors were set to a single value for both resin flow and resin cure monitoring. In this study, gain factor was set to a higher value to achieve a high response rate during flow monitoring. For cure monitoring, a relatively lower gain factor was adjusted for a more sensitive measurement (i.e., sensitivity change on change in resin's electrical resistance).

A new experimental set-up was designed to fully automate the RTM process using these sensors. Experiments were performed to investigate these sensors. They were successfully used to fully monitor the resin flow. By having two sets of sensors on both upper and lower surfaces of the mold, we could investigate the effect of the mold material on the flow front profile.

Also an algorithm was developed to evaluate the sensor data in order to (i) monitor the current position of the flow front and; (ii) predict how the flow front will continue to propagate (i.e., if any macro-size dry region is likely to remain after resin reaches the ventilation port(s)). The latter item is achieved by comparing the in-situ experimental data with some off-line simulation results of mold filling scenarios corresponding to different disturbances. For a full automation of the process control, our research group continues to study on optimal control actions to be taken to fill the mold cavity.

Chapter 2

SENSOR REQUIREMENT IN RTM AND AVAILABLE SENSOR SYSTEMS

2.1 Requirement of Sensors in the RTM Process

RTM is one of the most convenient composite manufacturing processes if a high volume production is aimed. This technique manufactures near-net-shaped parts, fine surface quality and close dimensional tolerances [12]. Another advantage is good mechanical properties due to firm compaction of fabric preform compared to other methods explained in Chapter 1.

Researchers have been working on the RTM process for many years in order to understand the physics of the process steps. Many researches aim to solve the problems encountered during manufacturing. The major problem in the process is incomplete impregnation of the preform by resin. This problem is a result of these situations: (i) deviation from nominal flow propagation due to race-tracking channels or non-uniform fabric compaction and/or structure, (ii) immature gellation of resin due to temperature variations. Other problems in RTM process are long-cycle time and high cost compared to metal forming techniques [12].

To overcome these problems, automation of the process is necessary. Automation consists of (i) monitoring of the mold filling during injections to ensure that the mold has been completely filled, and (ii) monitoring the resin cure for shortest de-molding time.

Monitoring of resin flow means determining which segments of the mold cavity are impregnated by resin. So, actual resin flow can be compared with off-line flow simulations during injections. Off-line flow simulations are predictions about how the flow will propagate in different conditions. Some of these simulations will be successful. In other words, the resin is going to fill the part completely; but in some simulations, it will not fill. If it is predicted that the actual injection is going to be unsuccessful, the flow propagation can be changed by control actions. Control actions are some adjustments in the process parameters such as changing the flow rate, injection pressure or opening and closing injection gates / ventilation ports [12]. Off-line flow simulations are going to be investigated in more detail in the following chapters.

Curing has been shortly described in Chapter 1. It needs to be monitored for the shortest cycle time. If the part is de-molded before it reaches a *green strength*, it will probably deform. However, when the part reaches the green strength, it will not be damaged when it is taken out of the mold. At green strength, even though the full cure is not obtained yet, the part gets strong enough to be handled. So, by monitoring the resin cure, the part can be de-molded when the optimal partial resin cure is reached [12]. This way, cycle time can be kept as minimum as possible for a high-volume production.

2.2 Available sensor systems in the literature

There are many sensor types used to monitor / control the composite manufacturing processes. They might have some benefits, constraints and limitations over other ones. Danisman et al. [12] and Tuncol et al. [13] conducted literature surveys on sensor systems used in the RTM process. These sensors will be summarized in this section with their advantages and disadvantages.

2.2.1 Thermocouples

Thermocouples are widely used as temperature sensors. They convert thermal potential difference into electrical potential difference. They are used in RTM process for resin flow and cure monitoring. Resin cure of thermosets is an exothermic reaction, so thermocouples are typically used for resin cure monitoring. If there is a significant temperature difference between the mold walls and the resin, it is also possible to use thermocouples for resin flow monitoring. Some features of thermocouples are listed below [13]:

+ Low-cost.
- Temperature difference between the resin and mold walls is required for flow front propagation monitoring.
- Not reliable with molds made of materials with high thermal conductivity (such as aluminum).

2.2.2 SMARTweave [39]

SMARTweave is a two-dimensional grid of electrically conductive wires embedded into the preform. The wires overlap each other at sensor locations. Conductive fibers can be used instead of wires not to change the material properties of the preform [14]. For 9 sensors inside the mold cavity, a 3 by 3 array of fibers are needed (see Figure 2.1). These sensors can be used both for resin flow and resin cure monitoring [14]. Some advantages and disadvantages of these sensors are given:

+ A mesh of sensors for detailed flow front monitoring [15].
- Time-consuming wiring process [14].

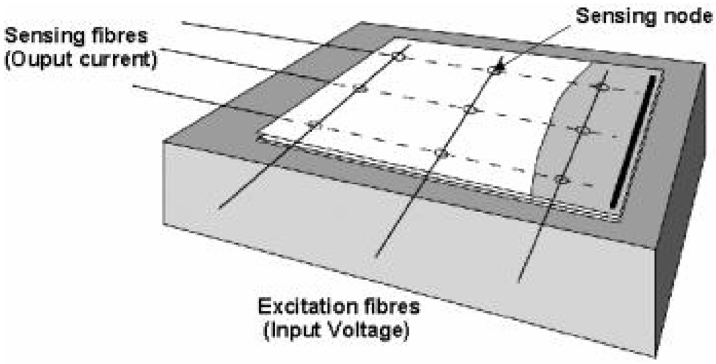

Figure 2.1 SMARTweave [31].

2.2.3 Dielectric Analysis

In dielectric analysis, electrical characteristics of materials such as conductance and capacitance are measured. Using this information, especially resin cure can be monitored efficiently in RTM process [16]. In order to do measurements, parallel plate or comb electrodes which are connected to a DAQ system are embedded into bulk material [1].

2.2.4 Ultrasonic sensors

In ultrasonic sensors, an acoustic signal is given by an impulse generator, and it is detected by an ultrasonic sensor. Properties of sound such as its velocity are measured by the ultrasonic sensor. Curing and flow front arrival can be detected by the changes in these variables. The sensors do not contact the fabric. So, resin propagation is not disturbed, and the part is not defected [17]. But, these sensors require thin mold plates [1].

2.2.5 Fiber-optic sensors

Lim and Lee [18] used an optical-fiber to sense resin arrival and resin cure. A light is transmitted through an optical-fiber; intensity of the light is monitored. When resin reaches a sensor location, the intensity of light changes. This change is the resin arrival signal in the monitoring system. Fiber-optic sensors can be used for cure monitoring as well [19].

2.2.6 Lineal-voltage sensors

Lineal-voltage sensors have two electrically conductive wires placed at a few millimeters distance. A voltage is applied to the wires. A circuit measures the voltage value between the wires. As resin propagates through the gap between the wires, electrical resistance of the media between them changes. So, by measuring the voltage value, it can be detected how much of the gap is covered with the resin if calibration data is known previously [20]. In Figure 4.2, a lineal-voltage sensor is seen schematically. In the figure, the contours represent flow front positions at different times. Its advantages and disadvantages are [12]:

+ It can detect only the fraction of the wetted area, but can not monitor which segment is dry or wet.
- They can be used only once.
- Sensor removal from the part is needed.

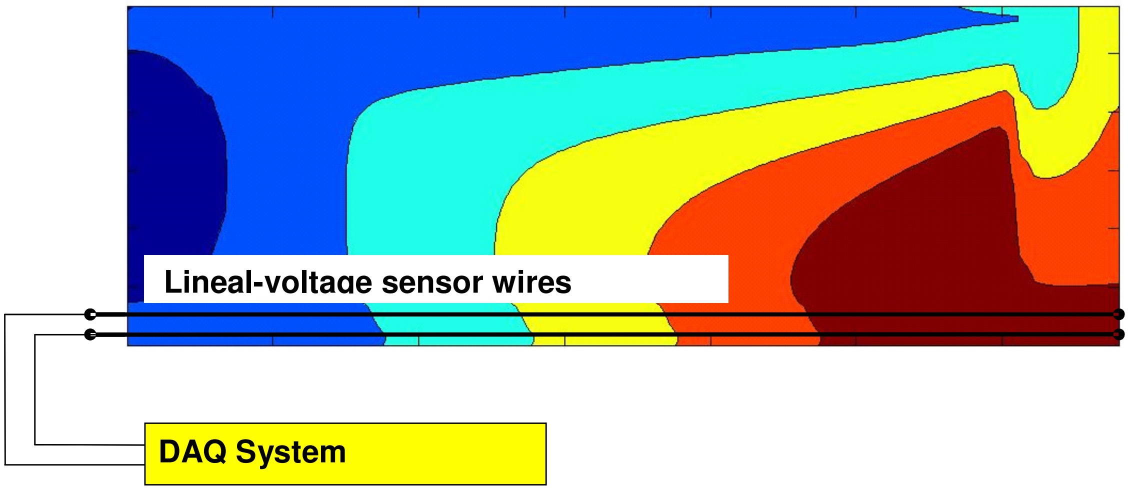

Figure 2.2 Lineal-voltage sensor on a mold cavity.

2.2.7 Point-voltage sensors

Point-voltage sensors are based on DC voltage measurement. When electrically conductive resin arrives at a sensor tip, the resistance between the two poles of the sensor decreases. Using this phenomenon, both flow front and resin cure are monitored. Point-voltage sensors have been investigated by Lawrance et al. [21], Bickerton et al. [22] and Sozer et al. [23]. It has the following features:

- \+ Used for both resin flow and cure monitoring.
- \+ Low cost and reliable.
- \- Many sensors are needed for a detailed resin flow monitoring.

Chapter 3

POINT–VOLTAGE SENSOR SYSTEM

This chapter intends to introduce the point-voltage sensor system. Each component of the system is going to be explained to make it clear how the sensors work. Then, a case study experiment is going to be shown.

3.1 Sensor Configuration

In Figure 3.1, sensor configuration is seen from the side view of the mold. There are 30 sensor bolts embedded on the mold; 15 on the upper mold plate and 15 on the lower mold plate. Sensor bolts are connected to a circuit which evaluates the signal from the sensors. This circuit is connected to the data acquisition (DAQ) system. The DAQ system consists of a DAQ card and a computer with the software Labview installed on it. Responses of the sensors are monitored from the computer. The contributions of each of these components in the sensor system are clarified in the following sections.

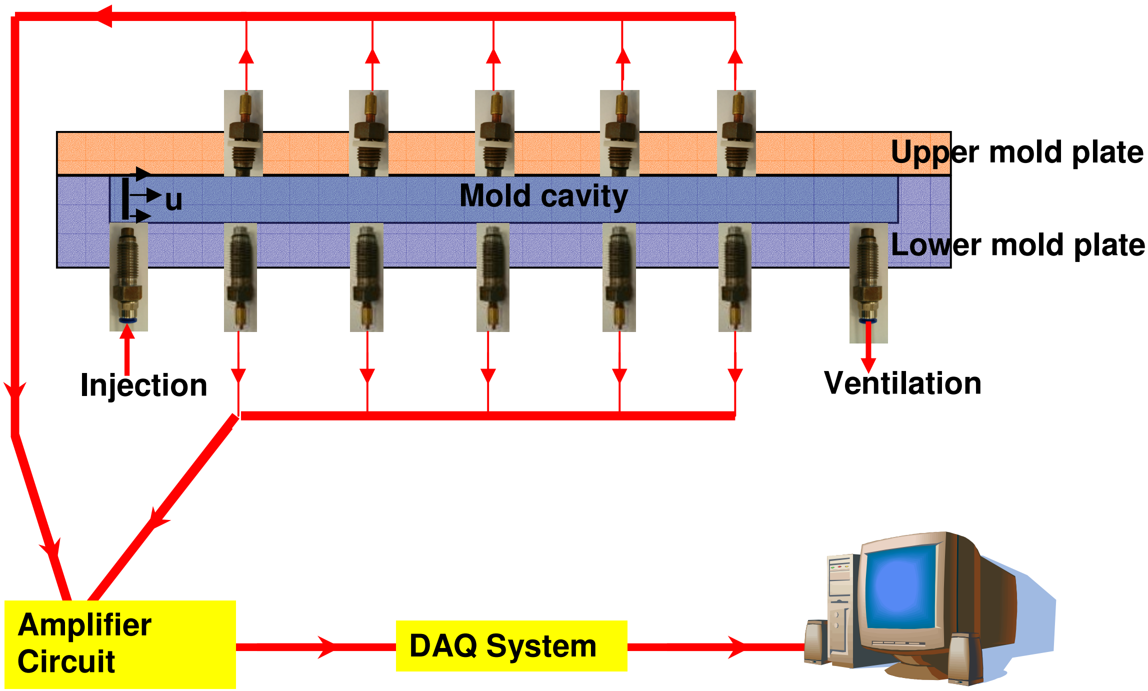

Figure 3.1 Sensor configuration from the side view of the mold.

3.1.1 Sensor bolts

A point–voltage sensor is shown in Figure 3.2. This is the part where the sensing process occurs physically. These bolts are assembled into the threaded holes on the mold. Their tips are at the same level with the mold cavity surface. Thus, sensors do not affect the resin flow during injections. A copper tube and a copper rod (probes) are inserted into a bolt. The probes are electrically conductive, and they are isolated from each other by using insulating tubes made from Delrin (a polyacetal polymer by DuPont). The probes are connected to a circuit that will be analyzed in the next section. There is no electrical connection between these probes of a sensor, if the probes are adjacent to a fabric made of typical glass fibers, which save practically perfect insulators .In other words, electrical resistance of the media between the probes is almost infinite. When the resin arrives at the sensor tip, the two probes are covered with relatively more conductive resin, and electrical resistance of the media decreases. This resistance decrease results in a voltage jump in the circuit. Thus, resin arrival can be monitored.

In the next section, it is going to be explained how this resistance decrease is evaluated in the circuit. Sensor locations, their dimensions and other physical features of the bolts are described in Chapter 4 and in the appendix.

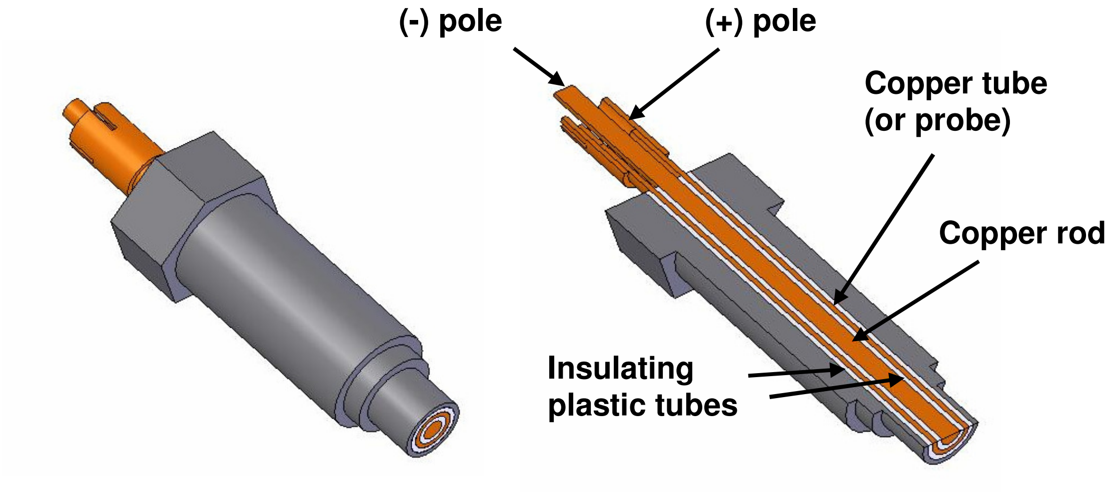

Figure 3.2 A point-voltage sensor bolt.

3.1.2 Circuit

In Figure 3.3, the circuit which is connected to two probes of the point-voltage sensor is shown. In this circuit, let's call the equivalent electrical resistance of the two parallel resistors (R_{Media} and R_1) as $R_{equivalent}$

$$R_{equivalent} = \frac{R_{Media} \cdot R_1}{R_{Media} + R_1} \tag{3.1}$$

R_{Media} is the resistance of the media between the two probes. A voltage value of V (in this study, V = 15 V was used) is applied. Then, the voltage (V_R) between the nodes b and c is given by:

$$V_R = \frac{V}{R_{equivalent} + R_2} \cdot R_2 \tag{3.2}$$

It is clear that V_R value is directly related to the R_{Media}. If V_R is measured during an injection, the value is going to change when the resin arrives at the sensor tip. Also, it is going to change as resin cures, because conductivity of resin decreases as it cures. Obviously, these sensors can only be used with electrically conductive resin systems. Also, preform placed inside the mold must not be conductive. If conductive fibers (such as carbon fibers) are used, it is not possible to monitor the resin arrival.

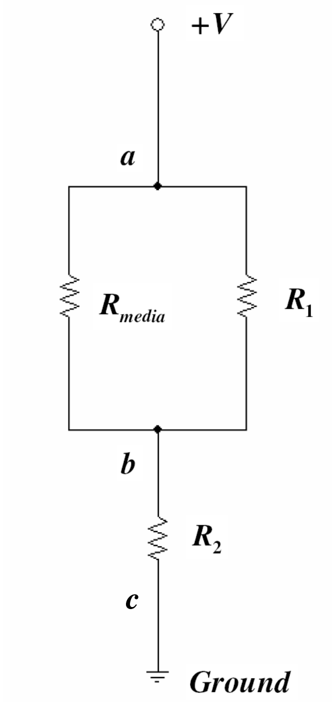

Figure 3.3 Electrical circuit for the point-voltage sensor.

But, this circuit alone is not convenient for measurements with a DAQ system. The voltage difference of V_R is too low to be used as a detection signal. Amplifiers and a multiplexer are needed. The circuit used in this work is seen in Figure 3.4. There is a larger scale circuit schematic in the appendix section.

In **Buffer #1** (see Figure 3.4), the electrical circuit which was shown in Figure 3.3 is connected to a buffer amplifier which is an op-amp. There is no voltage gain in this part; the op-amp is used as a voltage follower. If a voltage follower is not used, the circuit parts are going to use the voltage source which is applied to the sensors. This condition will result in false measurements. There is also a potentiometer in this part to set the voltage to a desired reference value at the beginning of the experiment.

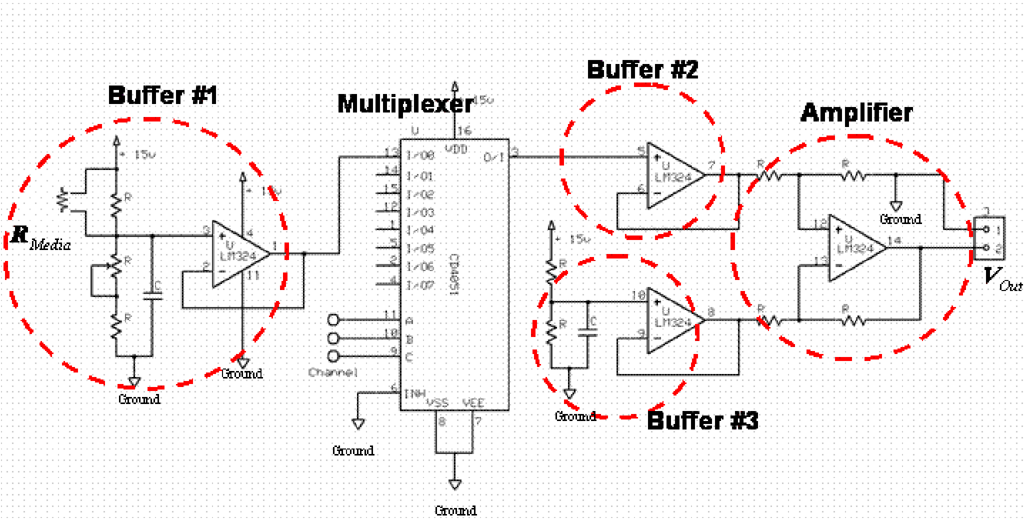

Figure 3.4 Electrical circuit with buffers and multiplexers.

After the voltage follower, a multiplexer is used. So, in a single circuit on the board, many sensors can be used. In our case, an 8-channel multiplexer is used. We can connect up to 8 sensors on one circuit board. Multiplexer also reduces the need for channels on the DAQ card. These 8 sensors can be connected to a single DAQ channel.

Buffer #2 and **Buffer #3** are also voltage followers. A voltage source is connected to Buffer #3 to be used in the final amplifier. Buffer #3 provides an additional DC voltage of about 0.65 V to the amplifier.

When the adjacent fabric is dry, typical value for V_R is 755mV. And when resin (Polipol™ 336-RTM) arrives at the sensor, V_R becomes 771mV. The 16mV difference is amplified for a more sensitive measurement. In the amplifier part, the V_R value passing through the voltage followers and the multiplexer are amplified. A differential amplifier is shown in Figure 3.5. Output voltage V_{OUT} is given by

$$V_{OUT} = V_2\left(\frac{(R_f + R_1)R_g}{(R_g + R_2)R_1}\right) - V_1\left(\frac{R_f}{R_1}\right) \tag{3.3}$$

In this study, $V_1 = V_{REF}$, $V_2 = V_R$, R_g = 47 KΩ, R_F = 470 KΩ and $R_1 = R_2$ = 1 KΩ (see the circuit schematic in the appendix section). The final amplification becomes

$$V_{OUT1} = 461V_R - 470V_{REF} \tag{3.4}$$

where V_{REF} is the voltage source from Buffer #3 which is used to set sensors' output to zero when the mold cavity is empty or, the fabric is dry.

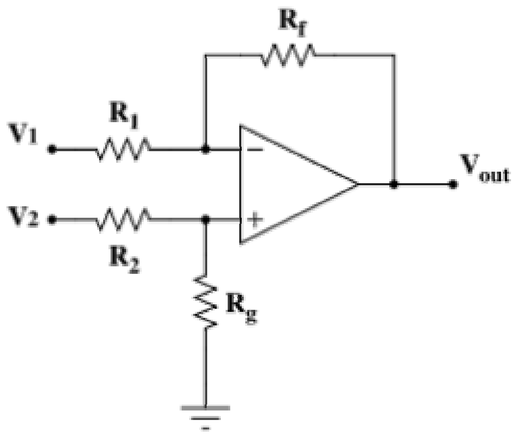

Figure 3.5 Differential amplifier [40].

3.1.3 DAQ System

A DAQ system is needed to measure the voltage values from the circuits and to evaluate the voltage. Four sensor circuits are used in our study (see Figure 3.6). Each circuit has an 8-channel multiplexer. Thus, for 30 sensors, 8 channels in the DAQ system are occupied, because each circuit has two outputs (V_{OUT1} and V_{OUT22}) with different gain values. V_{out} has the amplification given in Equation (3.4). This output is used for cure monitoring. The second output is given as

$$V_{OUT2} = 4V_{OUT1} \tag{3.5}$$

This output is for flow front monitoring. An additional differential amplifier (not shown in Figure 3.4) is used for V_{OUT2}. The reason for this amplification is going to be explained in the following sections.

The DAQ card used in our work is National Instruments, 200 kS/s, 16-Bit, 16 Analog Input Multifunction Card (NI PCI 6035E) [1]. Its specifications can be seen in the appendix section. The card is integrated with Labview.

A Labview code has been written in order to monitor flow front and resin cure. A snapshot from Labview user-interface is seen in Figure 3.7. This Labview code enables the user to monitor the voltage readings of all sensors. The voltage value is also recorded to an output file to be processed. After turning the sensors on initially, the voltage values are set to a reference value such as zero using the potentiometer on the circuit. The typical electrical noise is at a low level such that it does not affect the sensor's output data significantly. Arrival of the electrically conductive resin triggers the sensors, and the voltage values jumps up to 10 V. A threshold value such as 9.5 V is defined in Labview. When the voltage exceeds 9.5 V, a cyber Labview LED is turned on. So, the operator understands that, the sensor is triggered by the resin. In other words, resin reaches the sensor location. As seen in Figure 3.7, the arrival time is shown above each sensor's LED.

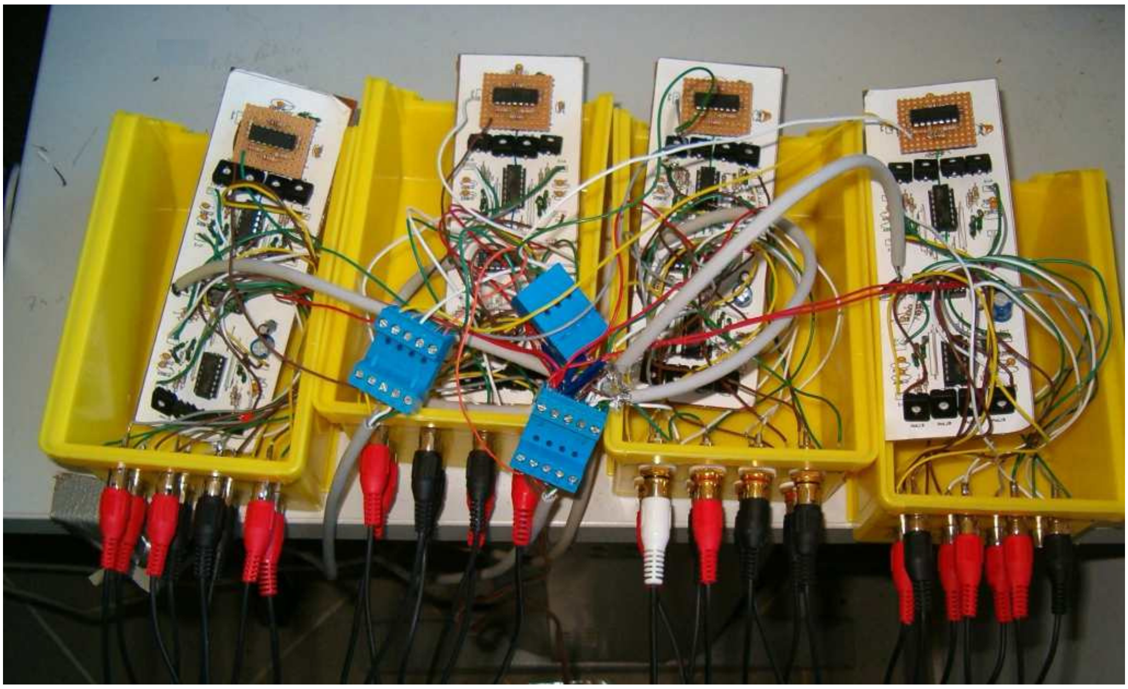

Figure 3.6 Four circuits connected to 30 sensors.

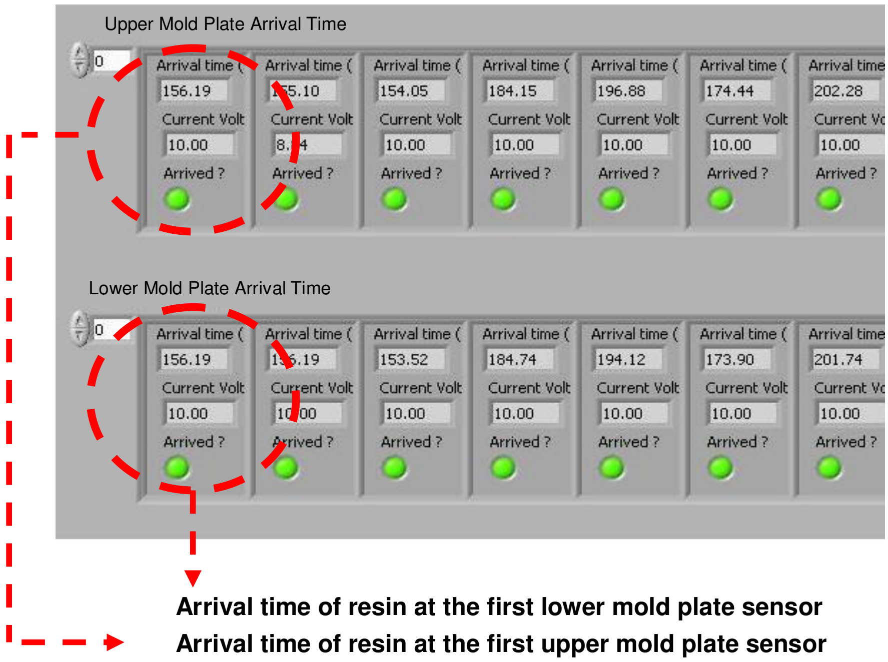

Figure 3.7 Labview user interface snapshot.

3.2 Response of the Sensors

There are two objectives to achieve with the sensors: (i) flow front monitoring, and (ii) resin cure monitoring. In this section, sensor data of a typical experiment will be studied.

3.2.1 Flow front monitoring

In Figure 3.8, configuration of 15 sensors (SL1, SL2, …, SL15) on the lower mold cavity is shown. There are also 15 sensors (SU1, SU2, …, SU15) on the upper mold plate at the same in-plane x,y coordinates.

Figure 3.8 Sensor configuration on the lower mold cavity.

To enhance its visibility through upper transparent mold part, a polymer based dye is added into the resin system. Then, it is injected at 50 cc / min flow rate into the mold. Resin flow is recorded with a camera through the transparent plexiglass upper mold plate. All the voltage readings are recorded. The aim of camera recording is to verify the data from the sensors with the visual data.

In Table 3.1, sensor triggering times obtained from Labview are listed. It is seen that triggering times for sensors at the same in-plane locations (SLi and SUi) are almost identical. But at some locations, there is a delay of up to 2 seconds. This delay is caused by a velocity profile that is not constant along the thickness direction. This might have been caused by dissimilar mold materials at the upper and lower plates.

Using the data from Table 3.1, in-plane (i.e., 2D) flow front contours are plotted in Figure 3.9 using Matlab. There are two plots; one belongs to the data from the lower mold plate and the other one belongs to the data from the upper mold plate. In the figure, also resin propagation times at some locations are given in seconds. Both plots look quite similar.

Table 3.1 Sensor triggering times for the experiment using sensor data (in seconds)

Sensor #	Arrival time [s]	Sensor #	Arrival time [s]
SL 1	29	**SU 1**	29
SL 2	27	**SU 2**	26
SL 3	28	**SU 3**	28
SL 4	52	**SU 4**	51
SL 5	51	**SU 5**	49
SL 6	57	**SU 6**	57
SL 7	77	**SU 7**	76
SL 8	88	**SU 8**	86
SL 9	82	**SU 9**	83
SL 10	104	**SU 10**	101
SL 11	117	**SU 11**	113
SL 12	119	**SU 12**	118
SL 13	137	**SU 13**	135
SL 14	147	**SU 14**	146
SL 15	150	**SU 15**	150

In Figure 3.10, snapshots of the recorded video are shown. The snapshots are taken when resin is around each column of sensors. The similarity between the contour plots and snapshots is clearly seen. Due to race-tracking channels, sensors in the mid-points are triggered later than the ones on the sides, especially after second column of sensors.

a. Flow front propagation on upper mold plate.

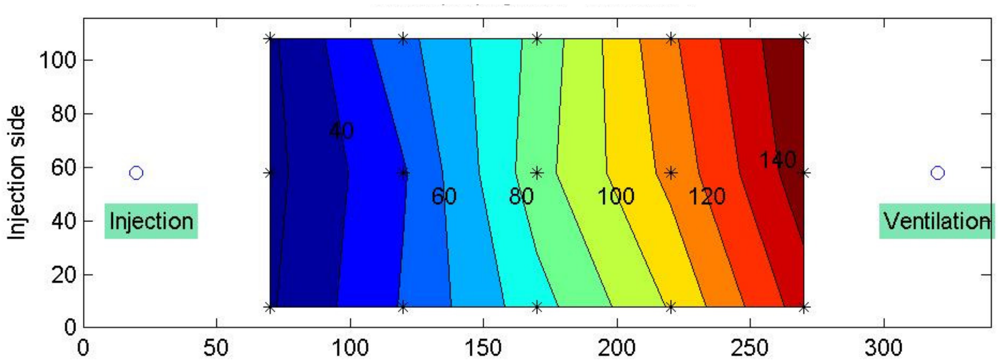

b. Flow front propagation on lower mold plate.

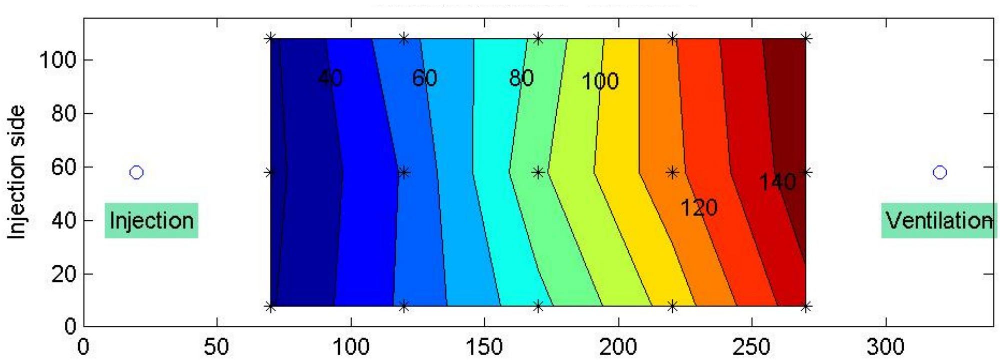

Figure 3.9 Flow front propagations from sensors of (a) upper mold plate, (b) lower mold plate.

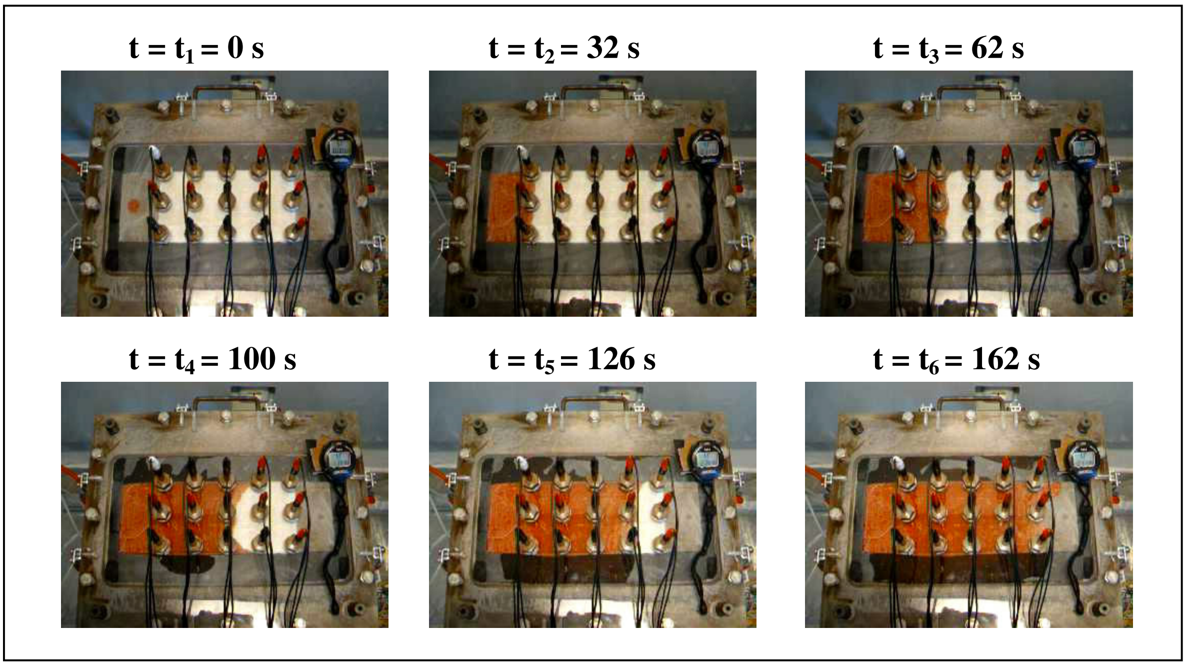

Figure 3.10 Snapshots of the flow front propagation.

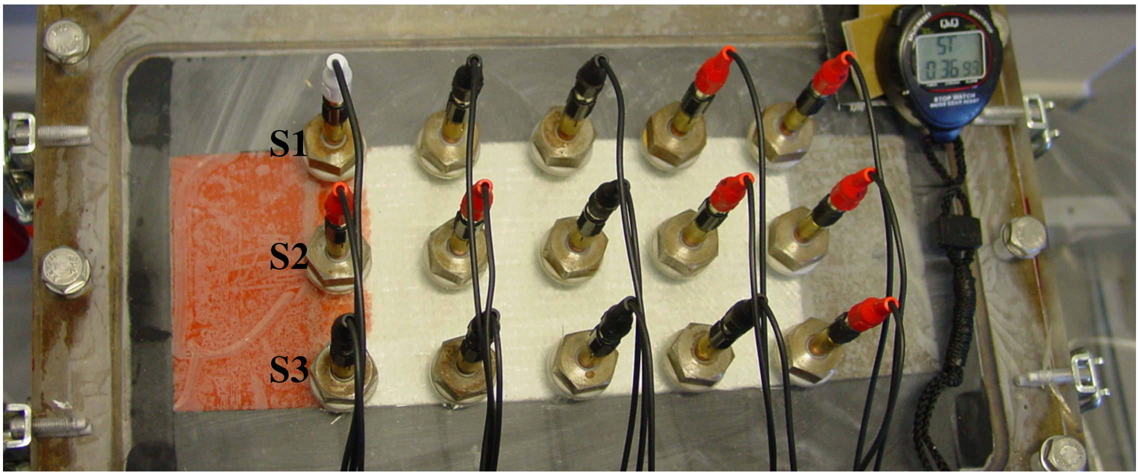

Figure 3.11 Flow front position at t = 37 s.

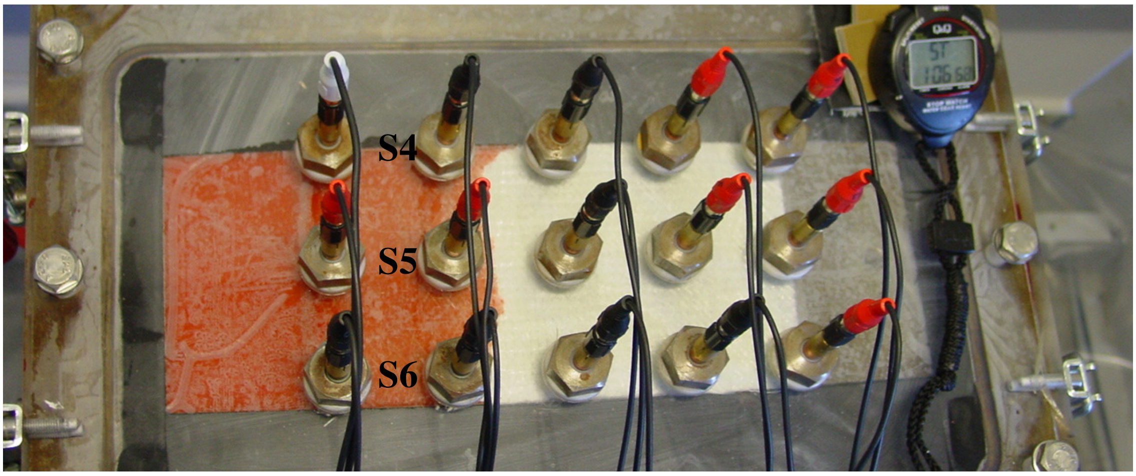

Figure 3.12 Flow front position at t = 66 s.

The snapshots of the flow front positions at t=37 s. and t=66 s. are shown in Figures 3.11 and 3.12, respectively. In Figure 3.13, the responses of the first six sensors are shown. It is clear that the responses of the sensors are prompt.

In Figures 3.13 – 3.15, the voltage value for all sensors is about zero before resin arrival. There is a sharp jump of the voltage reading at the time of resin arrival. When the voltage is over 9.5 V, the LEDs turn on (see Figure 3.7). This threshold value is appropriate because due to DC voltage gain in the circuit, the jump is actually higher than 10 V. But, the maximum voltage reading of the system is 10 V. So, by setting the threshold voltage value to 9.5 V, it is guaranteed that the resin arrival is detected and false detection is prevented. The responses of the remaining sensors are similar and not shown here due to brevity.

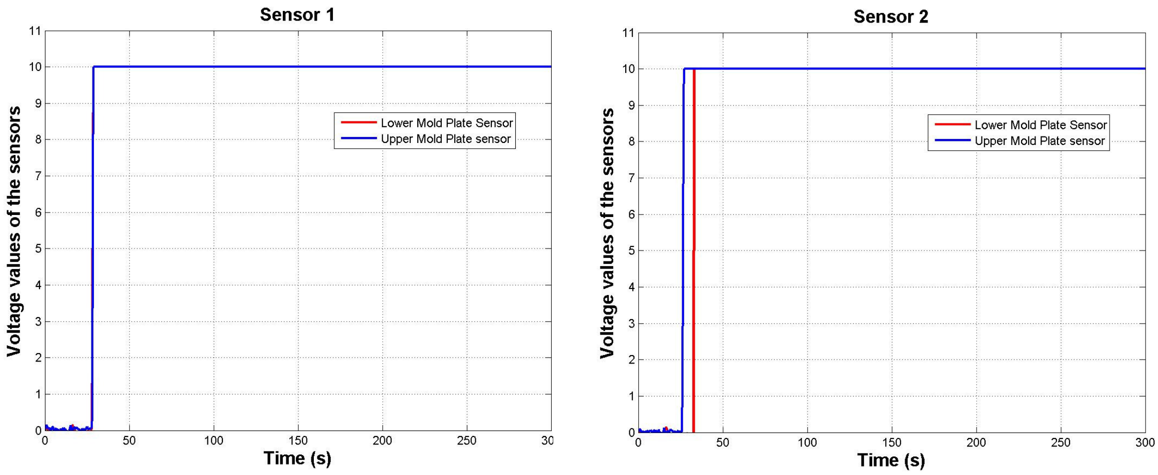

Figure 3.13 Responses of sensors 1-2 for resin flow monitoring.

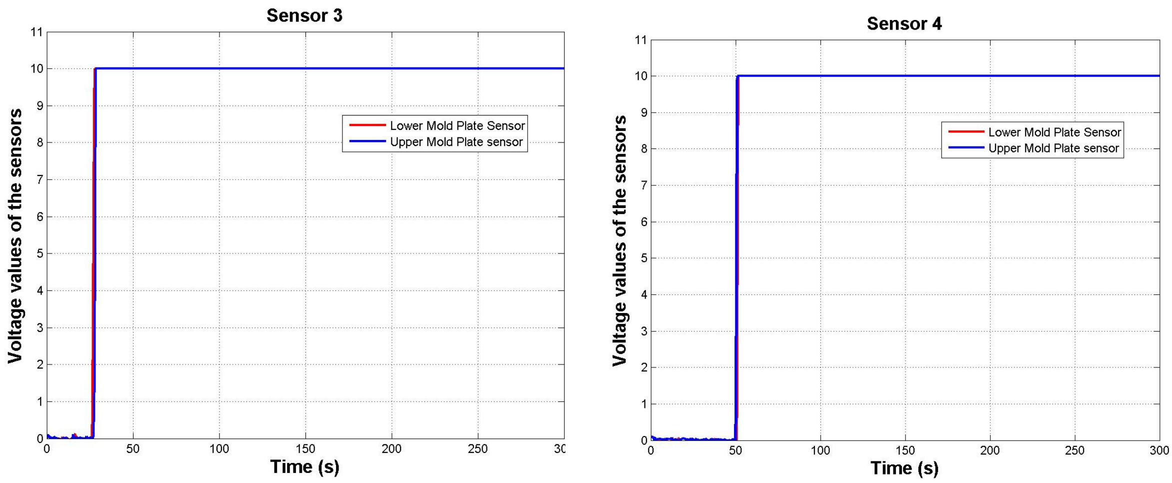

Figure 3.14 Responses of sensors 3-4 for resin flow monitoring.

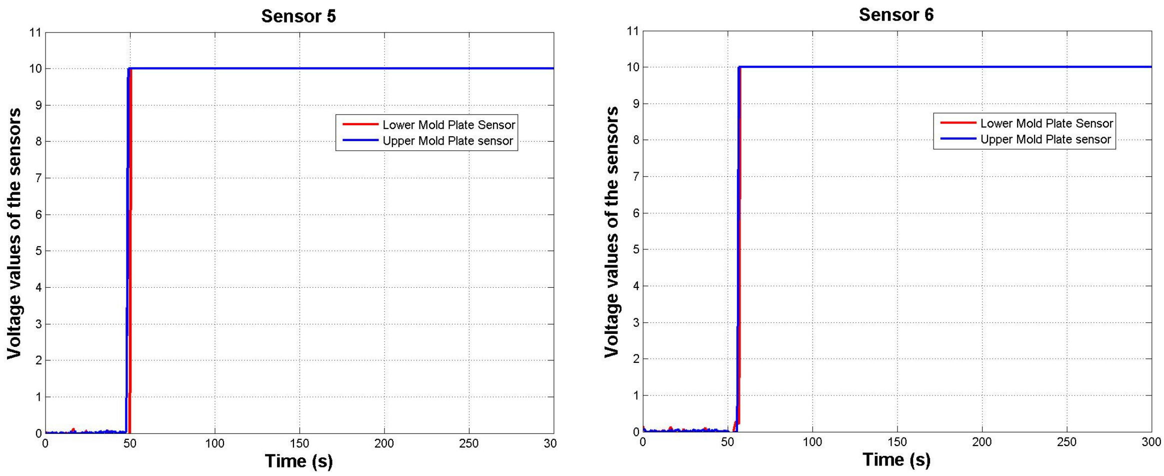

Figure 3.15 Responses of sensors 5-6 for resin flow monitoring.

3.2.2 Resin Cure Monitoring

It was discussed earlier that resin cure monitoring is an important issue in RTM process. Point–voltage sensors can be used for cure monitoring, as well as flow monitoring.

The electrical resistance of the polyester is too high that it is not possible to measure it with the tools available in our laboratory. But it is observed that electrical conductivity of resin decreases as it cures. In other words, its electrical resistance increases. This phenomenon enables the point–voltage sensors to monitor the resin cure. This situation was also observed in the literature [12].

As the curing starts, the voltage readings of the sensors start to decrease and eventually reach a steady value.

In Figures 3.16 and 3.17; curing response at two sensor locations, S11 and S12 are shown. In each plot, responses of upper and lower mold plate sensors are shown. If these sensors are desired to be used for curing monitoring, the user must know the curing history of resin. This means that it needs to be known at what voltage reading of the sensor, the part reaches the green strength. So, the part can be de-molded after the desired properties are achieved. In order to do that, mechanical tests must be previously done on the specimen which are de-molded at different voltage readings. When the required mechanical properties are satisfied, the actual part can be de-molded at that voltage reading.

It must be noted that the amplification factor for curing is different than the amplification factor for flow monitoring. Actual DC amplification for curing is given in Equation (3.4). For flow monitoring, Equation (3.4) has additional amplification with the gain of four (see Equation (3.5)). That is the reason that the voltage reading for curing starts from about 8 V, whereas for flow monitoring, it jumps up to 10 V.

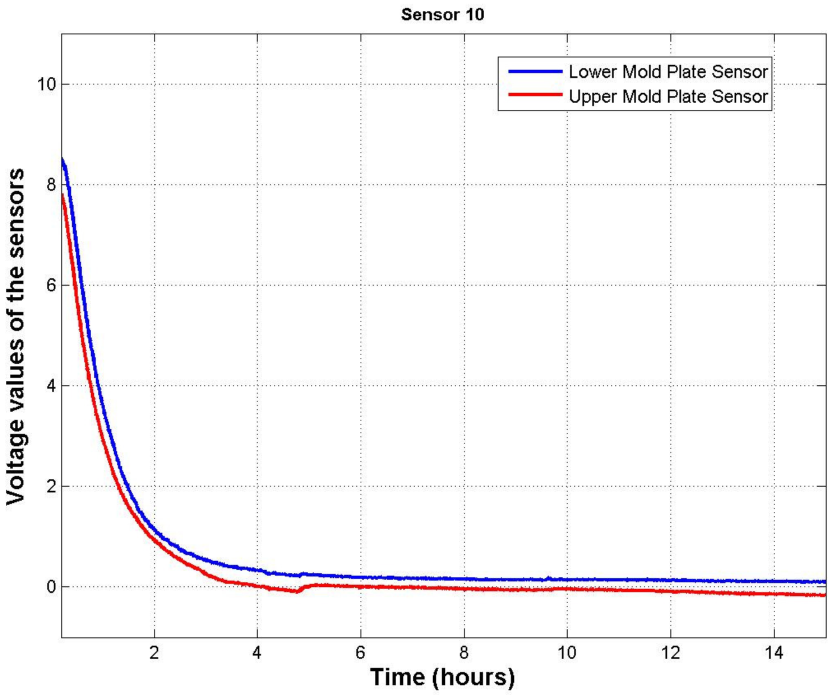

Figure 3.16 Curing responses of sensor 10.

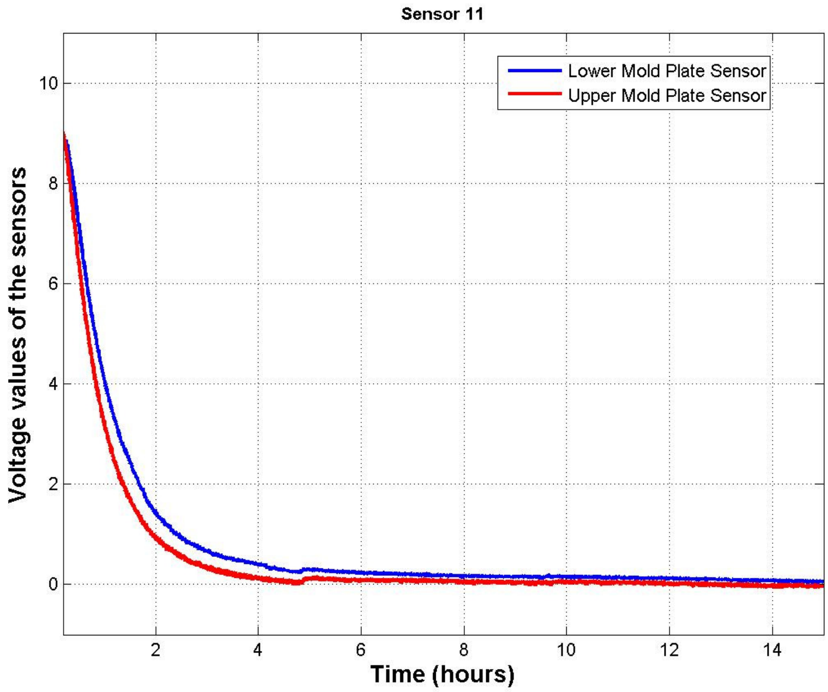

Figure 3.17 Curing responses of sensor 11.

Chapter 4

MOLD DESIGN FOR RESIN TRANSFER MOLDING

4.1 Introduction

Mold design for RTM covers aspects such as mold material, mold geometry, sealing of the mold, ejectors, injection gate / ventilation port placement and etc. It is a critical work; faulty tooling may result in scrap, even for a simple flat part.

An engineer responsible for a mold has to consider many features of the mold during the design work. Manufacturing parameters such as properties of fabric and resin have to be known. Because all the decisions made about the mold are affected from these parameters.

This chapter intends to give the reader a guideline about what to consider during mold design. In this chapter, different aspects are explained step by step beginning with the mold tool material selection.

4.2 Mold Material Selection

In order to decide on the mold material, some physical, mechanical, chemical and machinability properties of common mold materials have to be known [10].

Using a material, which may chemically react with the resin and its catalyst, is not appropriate. Also, the material must be resistant to other corrosive agents in the production environment. Shortly, the chemical interaction of mold material with the resin is one of the issues to be considered [10].

Mechanical properties of the material must be known so the mold can be designed strong and stiff enough to resist against mold closure forces and resin pressure during injection. Also, the mold material has to resist against defects which may occur during handling of the mold. Dropping appliances on the mold surface, or bumping the mold while moving it, are examples of handling sourced defects [10].

High thermal diffusivity of mold material is desired if heating / cooling of the resin-fabric system will be carried. This is done by either (i) circulating hot / cold water through internal channels; or (ii) placing the mold in an autoclave. By heating the mold, the resin will cure in a shorter time which reduces the cycle time. On the other hand, the mold is cooled to extract the heat induced by exothermic reaction. Otherwise, excessive local temperature might cause degradation or deformation.

The density of the material is also important so that the weight of the mold can be calculated, and excessive weight can be avoided or adequate support frames can be constructed. This is especially important if the mold is planned to be operated manually.

The manufacturing process and machinability of mold material affect (i) the machining time, (ii) dimensional tolerances, and (iii) surface roughness.

Three different manufacturing methods can be used for tool construction:

- machining the mold cavity by using CAD/CAM,
- casting the mold by using castable materials,
- combination of machining and casting.

Machining and casting both have advantages over the other one. In general, better dimensional tolerances and good surface quality can be obtained by machining. In case of molds with deep cavities, casting is advantageous over machining. Because, machining of deep cavities results in excessive material removal [10].

Properties of common mold materials are tabulated in Table 1. In addition, some features of different materials used in mold tool construction are listed below:

Steel

Advantages [10]:

- Steel has great toughness.
- If case-hardened steel or tool steel is selected, the mold becomes resistive to damages that may occur during handling or cleanup.
- Steel molds can be machined with good tolerances.
- Very good surface finish.
- Almost infinite service life.
- Compatible with almost any resin systems.

Disadvantages [10]:

- High cost makes steel attractive for only small tools with complex shapes and for high-volume productions.
- Steel has higher specific weight compared to many other materials.
- Thermal diffusivity of steel is too low. Cooling or heating channels usually have to be machined.

Aluminum

Advantages [10]:

- Very good tolerances can be obtained (better than steel).
- Aluminum can have a good surface finish, but great attention must be paid (such as keeping the mold surface free of residuals) to maintain the quality over a long time.
- Aluminum can have very long service life if the surface is not damaged.
- Very high thermal conductivity.

- It is compatible with any resin systems, but damp environment conditions must be avoided to prevent corrosion.
- Lighter than steel and cast iron.

Disadvantages [10]:

- Aluminum is a very soft material, and it can be easily damaged or scratched during cleanup or handling.
- Plastic scrapers should be used during clean up to maintain surface quality.
- The sensitive surface requires trimming or polishing time to time. This causes the dimensions of mold cavity to be out of the tolerances.

Cast iron

Advantages [10]:

- Very high toughness, resistant surface to toughest production environment.
- Cast iron tools can have small tolerances if machined. Also, tool dimensions hardly change by usage.
- Very long service life.
- Machining the complete mold cavity is not required if casting process is used instead of machining the block. This results in lower mold costs.

Disadvantages [10]:

- Surface quality is not as good as aluminum or steel.
- Low thermal conductivity. Requires heating channels in the mold.
- The surface may be defected in damp environment due to corrosion.
- Heavy material.

Glass Reinforced Plastic (GRP)

Advantages [10]:

- Low cost.
- Good choice for low production volumes. Also the composite manufacturers have their own workforce to construct the tool.
- If harsh production conditions (heat, pressure, etc.) are not used, GRP tools can be in service for a long time.

Disadvantages [10]:

- Can be easily damaged or scratched by impacts during handling.
- Cure shrinkages during the tool production prevents to have small tolerances.
- They cannot be used under high pressure, or with excessive tool heating.
- Maximum pressure that the tool can resist prevents some resin types to be used with the tool.

Carbon Fiber Reinforced Plastic (CFRP)

CFRP are mostly used in the RTM of carbon fiber reinforced parts, because the mold is also manufactured by the manufacturer of CFRP parts. The properties of CFRP as a tool material are mostly like GRP. However, some advantages and disadvantages exist [10]:

- Better mechanical performance than the GRP.
- CFRP tools have longer service life than GRP tools.
- Chemically compatible with any resin system unlike the GRP tools.
- Better dimensional tolerances can be obtained compared to the GRP tools.
- It is difficult to make complex shaped CFRP tools.

Ceramics

Even though ceramics are a wide group from machinable to castable ones, they have some common properties.

Advantages [10]:

- They are chemically compatible with any resin systems and solvents.
- They can be used at elevated temperatures.
- Very good surface quality in machined ceramics.
- They can be machined to small tolerances and dimensions stay stable during the service life.

Disadvantages [10]:

- Some ceramic types can be easily scratched.
- They have no resistance to impacts due to their low toughness.
- Lifetime is limited to an impact on the tool in the production environment.

Table 4.1 Properties of selected engineering materials [24].

	Steel *	**Aluminum ** **	**Cast Iron *****	**Glass Reinforced Plastics *******	**Carbon Fiber Reinforced Plastics *********	**Ceramics ***********
Density (g/cm^3)	7.85	2.77	7.30	1.7	2.1	1.71
Modulus of Elasticity (GPa)	207	72.4	90-113	220 (Longitudinal)	45 (Longitudinal)	11
Yield Strength (MPa)	355 (Annealed @ 785^{o}C)	75 (Annealed)	X	X	X	X
Tensile Strength (MPa)	520 (Annealed @ 785ºC)	185 (Annealed)	207	1020 (Longitudinal)	760 (Longitudinal)	13.8 - 34.5
Percent Elongation	30.2	20	X	2.3	0.3	X
Coefficient of Thermal Expansion [10^{-6} (^{o}C)$^{-1}$]	11.3	22.9	11.4	6.6	-0.5	2.0 - 2.7
Thermal Conductivity (W/m-K)	51.9	190	46	0.19	0.19	130 - 190
Specific Heat (J/kg-K)	486	875	544	1050	1050	830
Electrical Resistivity (Ω-m)	1.60×10^{-6}	3.4×10^{-8}	9.5×10^{-7}	10^{10}-10^{13}	10^{10}-10^{13}	7×10^{-6}

*	Steel alloy 1040
**	Alloy 2024
***	Grade G3000
****	E glass fibers-epoxy matrix ($V_f = 0.60$)
*****	High modulus carbon fibers-epoxy matrix ($V_f = 0.60$)
******	Graphite

4.3 Clamping Systems and Forces on Tools

In RTM, necessity of the clamping force arises from the combination of two forces. First one is the force required to compress the reinforcement to the desired fiber volume fraction (V_f). The second one is the dynamic force induced by the resin pressure. Forces also may be generated due to thermal changes caused by the chemical reactions in the resin system [25].

In order to balance the force developed, a clamping system must be designed. In RTM industry, clamping is usually done by using a hydraulic press as shown in Figure 4.1. Capacity of hydraulic presses may vary from a few to thousands of tons depending on the part size, fiber volume fraction and needed resin pressure.

As seen in Figure 4.2, special latch clamps are used for manually operated molds. The clamp seen in the figure has two separate parts. These two parts are fixed on both sides of mold parts. A single clamp may hold up to 27000 N [27]. A combination of latch clamps on the mold is advised. As the number of clamps increases, the compression becomes more homogenous. Necessary compression force should be calculated as shown in the next section. The choice of clamps should depend on this calculation.

The simplest method for clamping is seen in Figure 4.3 where bolts and nuts are used. This method is laborious, and also proper clamping and sealing may not be obtained all the time. Torque on bolts must be carefully adjusted to create adequate and homogenous clamping pressure.

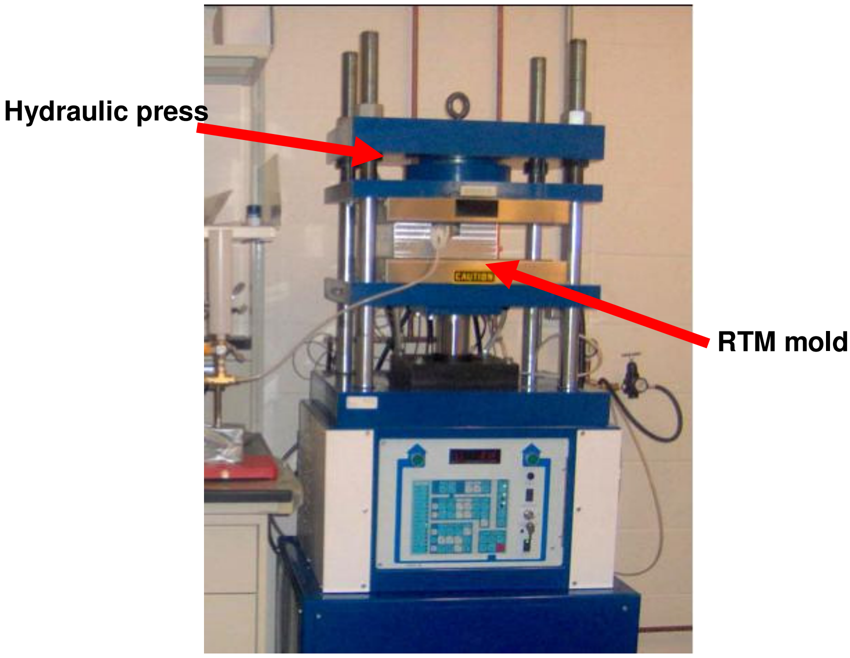

Figure 4.1 A typical hydraulic press used in RTM [26].

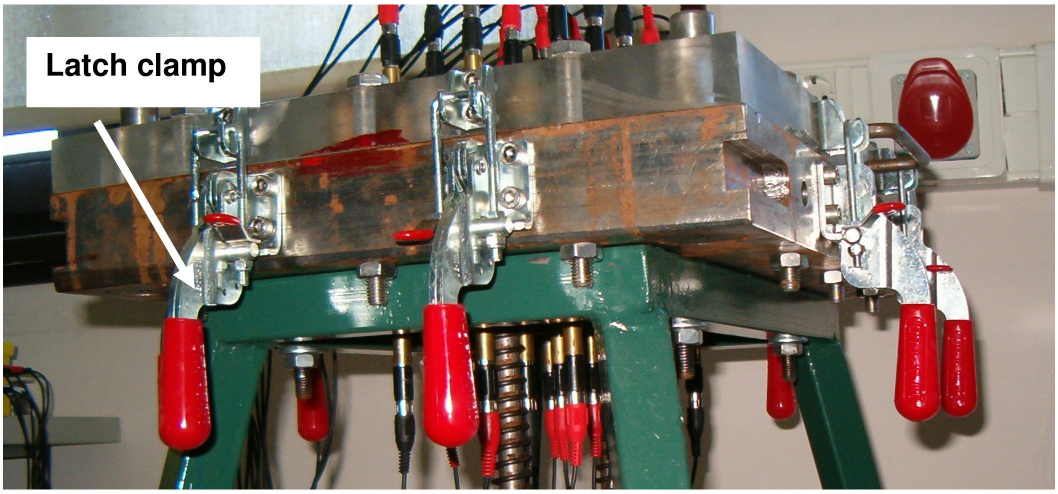

Figure 4.2 A latch clamp combination for mold closure.

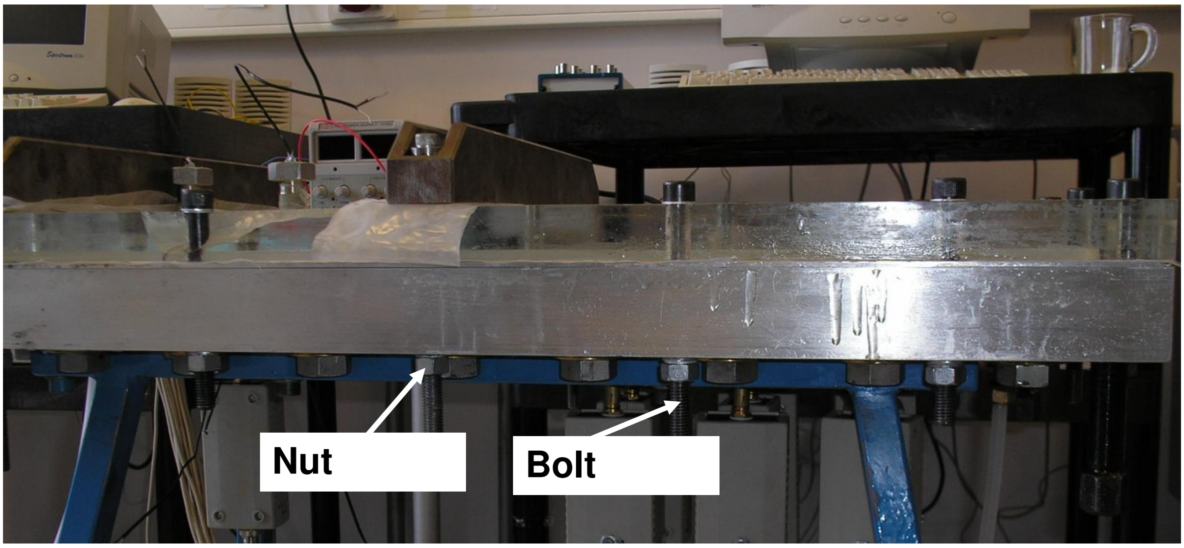

Figure 4.3 Bolt and nut system for clamping of mold plates.

Compression stress and inner fluid pressure have to be calculated for two reasons: (i) to design a clamping system, and (ii) to design mold plate thickness which will not bend significantly.

As described above, the reinforcement has to be compressed to the desired V_f. The question is that how much compression stress is necessary. There is not an exact solution to this question but throughout the literature [28,42], different experiments have been performed for different types of reinforcements, so that reference databases can be used.

Senan [42] did fabric compression experiments to find a correlation between fabric thickness and compaction pressure applied on the fabric. In one of these experiments, 4 layers of stitched random type fabric were compressed at different compaction pressure and the thickness of the fabric at each load degree. The corresponding compaction data is shown in Figure 4.4.

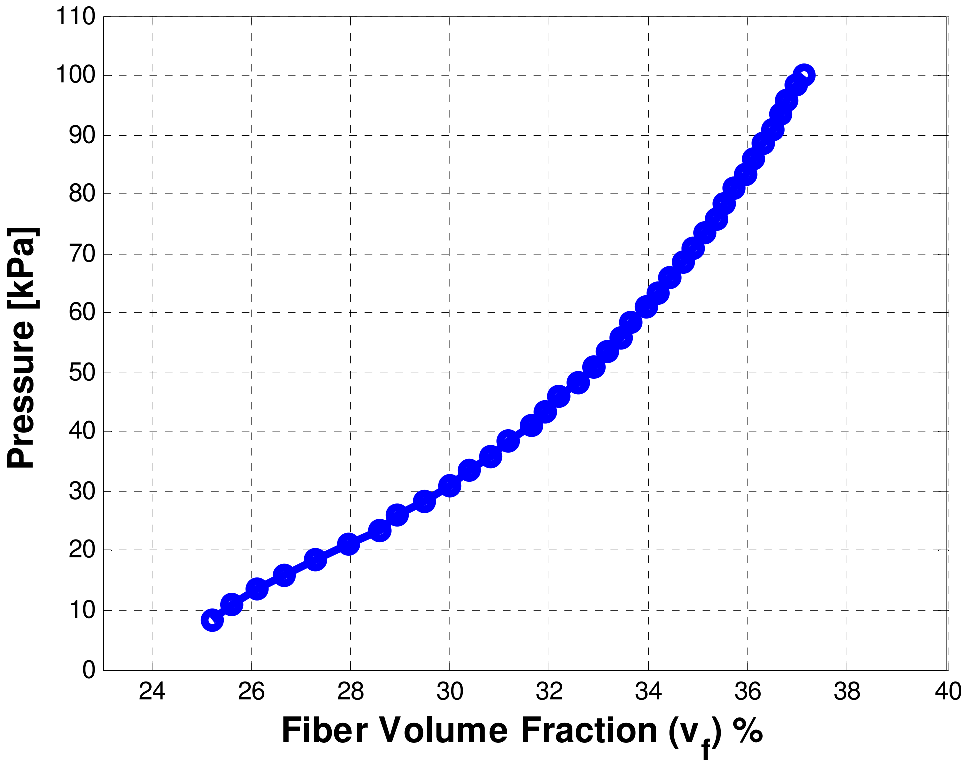

Figure 4.4 Compression pressure vs. fiber volume fraction for four layers of stitched random type fabric [42].

Required V_f of a composite part has to be calculated before the design of the mold. So that, corresponding compression stress can be estimated. Fiber volume fraction is calculated as follows.

$$V_f = \frac{n\,\rho_{superficial}}{\rho_{fiber}}\frac{1}{h} \qquad (4.1)$$

where

n = number of fabric layers in the preform,

$\rho_{superficial}$ = superficial density of one-layer-fabric, [kg/m^2]

ρ_{fiber} = density of glass fibers, [kg/m^3]

h = thickness of preform. [m]

There are many kinds of glass fibers. Their densities vary from 2110 kg/m^3 to 2720 kg/m^3. The most commonly used fiber type, E-glass fiber has a density of about 2540 kg/m^3. In the example part which is schematically shown in Figure 4.5, $\rho_{superficial}$ = 0.5 kg/m^2 and h = 0.003 m. 5 layers of fabric is used. Then the fiber volume fraction is [42]:

$$V_f = \frac{(5)(0.5)}{2540}\frac{1}{0.003} = 0.33 \Rightarrow 33\% \qquad (4.2)$$

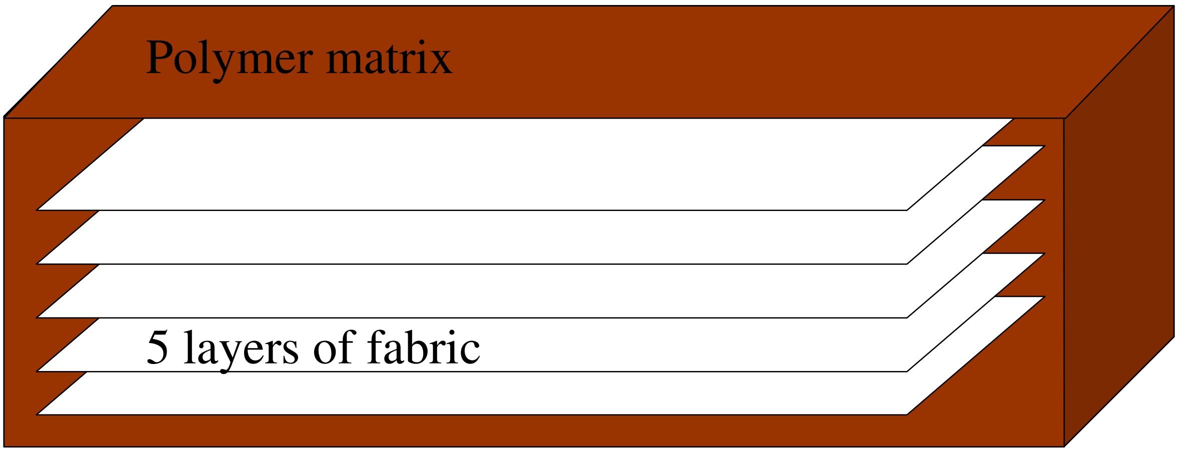

Figure 4.5 A composite part with 5 layers.

The fluid pressure inside the mold cavity during injection depends on many parameters such as permeability, viscosity, flow rate of the fluid and the dimensions of the mold cavity. The injection pressure may vary from a few kPa to hundreds of kPa. Most injection machines have the capability to inject the resin at a constant pressure. With the control of the injection pressure, leakage of the resin and the bending of the mold plates can be prevented. The pressure is set not to exceed a critical value. Otherwise, resin might leak from the sealings of the mold or the tube connections; or the mold parts might bend significantly.

The sum of (i) the estimated fabric compression pressure and (ii) injection pressure is the total clamping pressure required. Clamping system should be designed accordingly.

4.4 Ejector Systems

After injection and complete mold filling, the part is still kept in the mold for a partial or full resin cure. During curing, the part might stick to mold walls. This causes a problem to remove the part from the mold. When the upper mold plate is separated from the lower part, the composite part is ideally expected to be lifted up from the lower mold plate. However, wet surface of the part might stick to the lower mold part which prevents the part to be removed easily. If the part geometry has any ribs or irregular surfaces, lifting the part can be easy; otherwise, it might be a difficult job.

One possible solution to this problem is to apply release agents on the mold surfaces before placement of the preform. Release agents are chemicals used to prevent sticking of molded parts to the mold walls. However, release agents alone are not enough for part removal. Hammers, wedges, screwdrivers are used to remove the part, but they degrade both the mold and the molded product [10].

If the RTM process is desired to be automated, the part must be removed from the mold without consuming too much time. For this purpose, ejector systems must be designed and constructed on the mold. Ejector systems push the part out of the mold cavity [30]. This section introduces ejection systems briefly.

The most common ejector system in the RTM industry is the pin ejector. The pin has a head, a body and a face. The face is the section which contacts the composite part. The body passes through the mold wall and the head is the section which is at the backface of the mold (see Figure 4.6) [30].

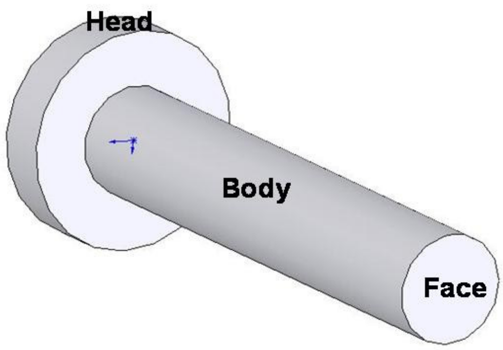

Figure 4.6 A pin ejector.

The ejector pin embedded in a mold is shown in Figure 4.7. When the composite part is cured and green strength is achieved, the upper plate is lifted up. Then, the ejector is pushed up from the head. The applied force from the ejector face to the part breaks the bonds between the part and the mold, and the part is removed.

Molds have other components assembled under them to keep the pin in the mold, and to provide sealing at injection pressure. Also, a combination of ejectors may be used to remove the part effectively, and to prevent the jamming of the part while ejecting it. The pins may be pushed up manually, or they can be actuated hydraulically or pneumatically [30].

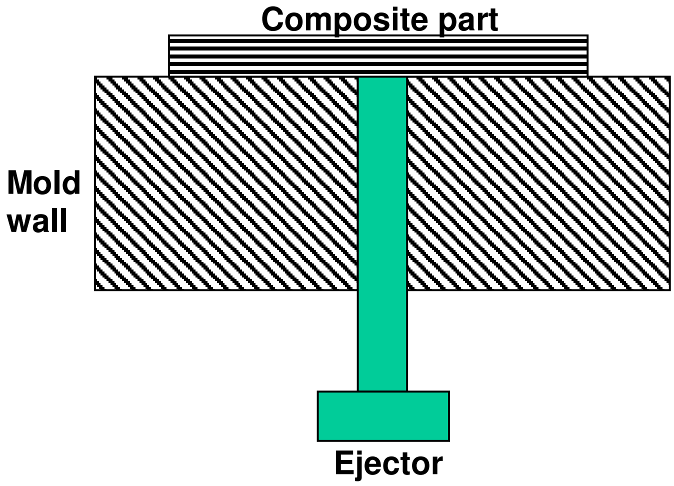

Figure 4.7 Ejector pin assembled in a mold.

The problem with this ejector system is the area of the face. The area of the pin face must be as large as possible. A small face area applies highly localized pressure on the part. This pressure results in ejector marks on the final part, or it may even cause a fracture of the part [30].

The ejector types with the head at the backface of the molds are called backface ejectors [10]. There are many types of backface ejectors used in the RTM industry. A stem ejector used in our laboratory is shown in Figure 4.8. The o-ring provides sealing during the resin injection. Compression of the spring applies a downward force to the face. So, the ejector does not move unless the head is pushed upwards. In Figure 4.9, the ejector is seen both at the frontface and backface of the mold.

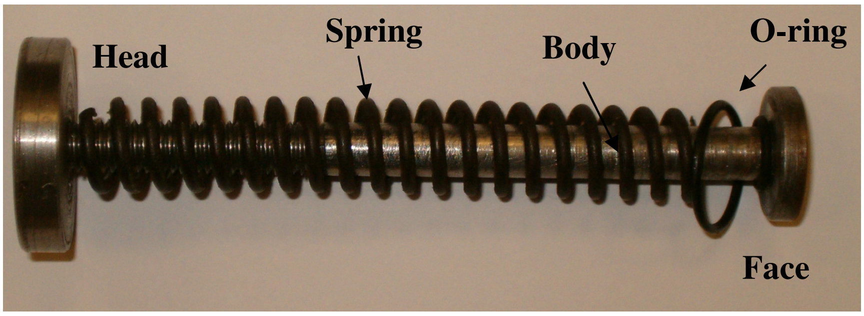

Figure 4.8 Stem ejector.

a. Top view of the lower mold part

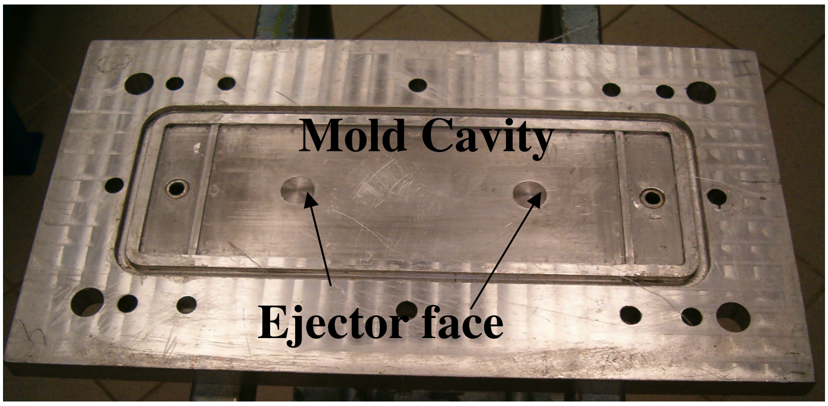

b. Bottom view of the lower mold part

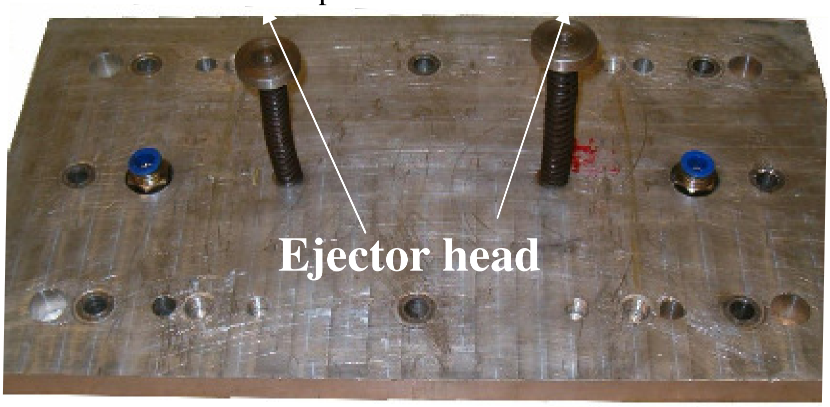

Figure 4.9 Stem ejector embedded in the mold.

4.5 Sealing of Molds

Leakage of resin between the mold plates must be prevented. By sealing, resin flow can be directed as designed, and also contamination of the production environment is prevented.

In our laboratory, a silicon O-ring (seen in Figure 4.10) is used as sealant. The diameter of the O-ring is 7 mm.

In Figure 4.11, one of the molds we use is shown. On the left, the mold has an empty channel for the silicon O-ring. On the right, the O-ring is placed in the mold. When the upper mold is placed on the lower mold, the compaction pressure compresses the silicon O-ring and prevents leakage at high pressure values.

The dimensions of the channel are 5.80 to 7.00 mm (see Figure 4.12). The O-ring can resist up to 6 bars of resin pressure in our laboratory.

Figure 4.10 Silicon O-ring.

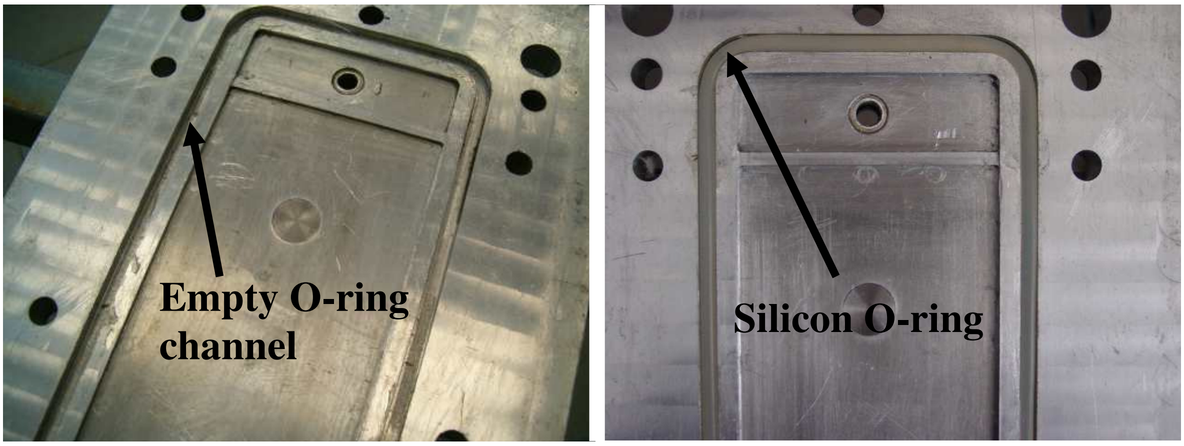

Figure 4.11 O-ring placed in the mold.

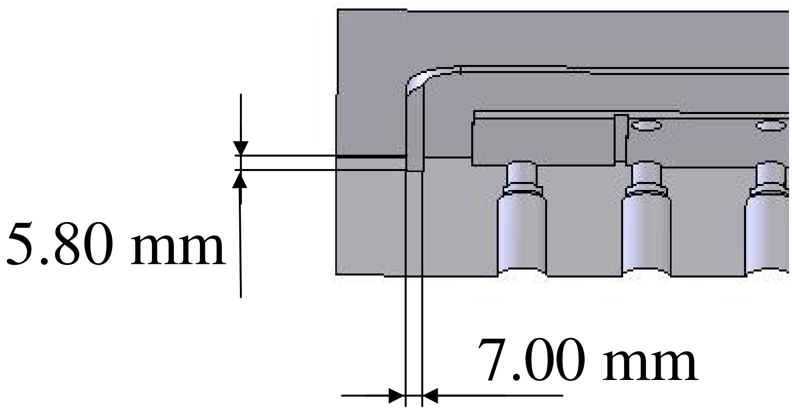

Figure 4.12 O-ring channel.

4.6 Injection Gates / Ventilation Ports

An RTM mold must have injection gates (inlet) and ventilation ports. Resin enters into the mold cavity through exit. Ventilation port allows the trapped air inside the mold cavity exit the mold [30].

In Figure 4.13, inlet / ventilation port used in our laboratory is seen. The bolt is assembled on the mold wall. The brass connector is used to tighten the tube to the bolt. If a point inlet or point ventilation port is desired, the bolt seen in Figure 4.13 can be directly connected to the mold cavity.

In Figure 4.14, a coupling is seen. This part is available in the market with many dimension options. The couplings can resist up to 6 bars of resin pressure.

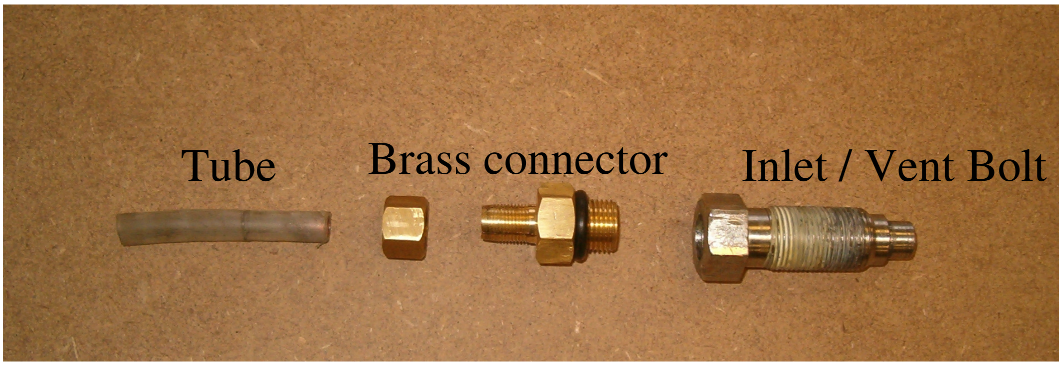

Figure 4.13 A bolt to be used as injection gate and ventilation bolt.

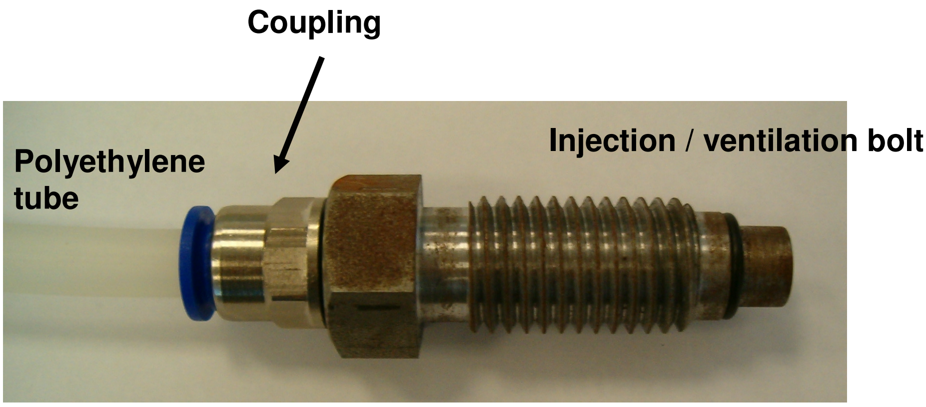

Figure 4.14 Tube connector with inlet / ventilation bolt.

When a lineal injection is designed instead of a point injection, resin pools can be used as seen in Figure 4.15. Mold cavity has a lower permeability than the resin pool due to the fabric placed in it. Practically, resin does not start to flow through the mold cavity before filling the pool completely. So, resin flow is ideally expected to be a 1-D flow, but race-tracking channels usually disturb flow and it becomes 2-D flow.

Different inlet / ventilation port accessories are available in the market. JHM Technologies. Inc., Scott Bader and Magnum Venus are some of the companies selling RTM accesories. The key point in the design of these gates is to have adequate sealing. Injection in RTM is done at high pressure. Without having a proper sealing, the injection cannot be done and the production area might be contaminated.

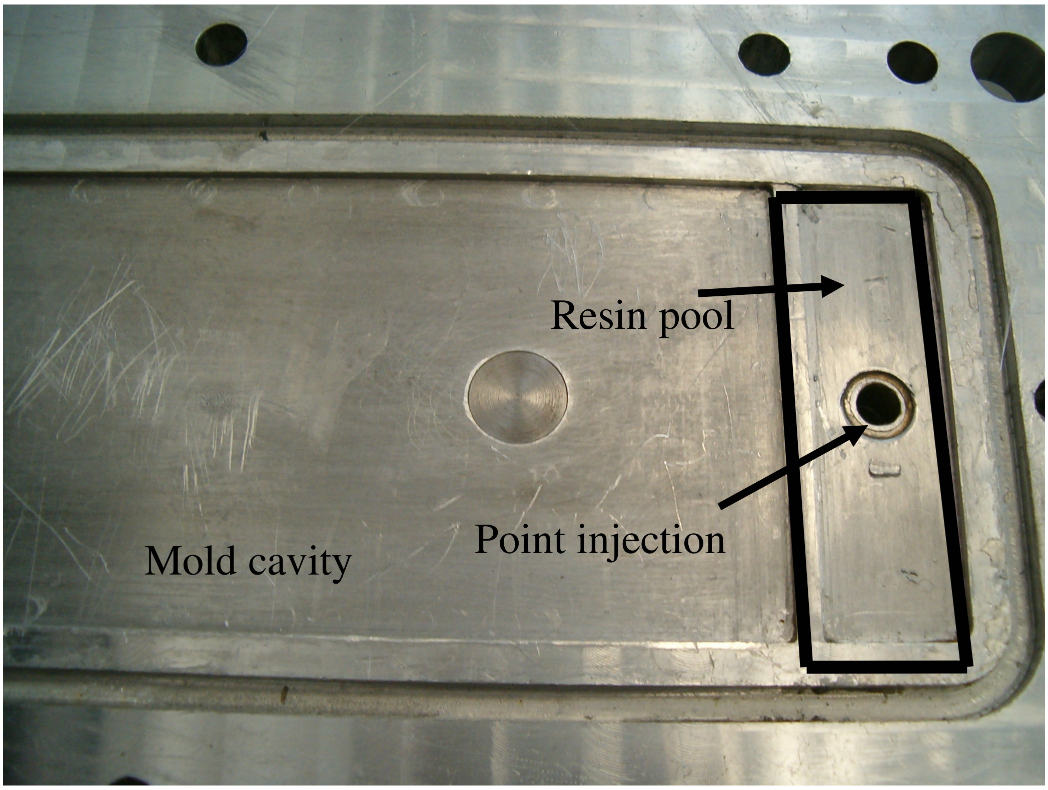

Figure 4.15 Resin pool for lineal injection.

4.7 Mold Filling and Automation

There are two major problems that an engineer may come across in RTM. These are (i) wash of the fabric, and (ii) incomplete filling of the mold cavity [1].

Wash of the fabric is undesired movement of fabric layers inside the mold. During injection process, the fabric may move from its initial position due to high resin pressure and insufficient compaction pressure [1]. In Figure 4.16, resin pressure pushed the fabric layers, and the composite part has an unwanted resin reach section as shown.

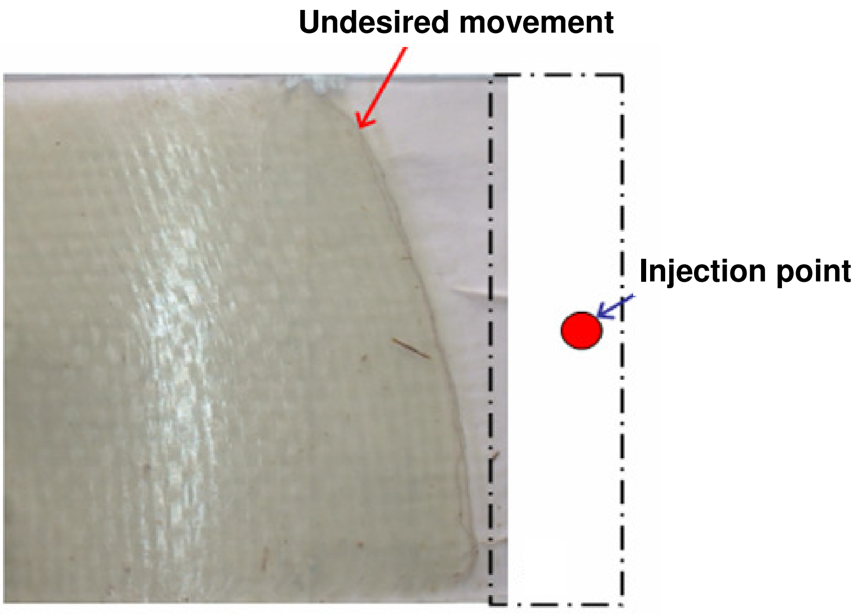

Figure 4.16 Fabric wash [1].

Incomplete mold filling is another major problem in RTM. Dry or partially unsaturated regions (voids) might be in either micro- or macro-scale.

Usually, micro-scale dry regions are caused by the too fast propagation of resin. Even though the flow front might have passed from a region much earlier, the saturation might not be full.

Macro-scale voids might be caused due to entrapment of air within a macro-scale region. Two major reasons might cause macro-scale voids: (i) immature gellation of resin before reaching the ventilation ports (misrun); (ii) flow front propagation which deviates from the designed propagation. The second phenomena might occur due to (a) racetracking channels and/or (b) inappropriate locations and injection conditions of gates.

Race-tracking channels are gaps between fabric preform and mold cavity walls. It is not always possible to cut the fabric layers at desired dimensions exactly. The presence of these gaps changes the local permeability of the mold cavity. The resin flows easily through the high permeable race-tracking channels and reaches ventilation gates before the part is fully wetted. So, air is entrapped in the fabric layers and the part is not filled completely [1]. In Figure 4.17, race-tracking channels in a mold cavity are seen. This part has a lineal inlet gate, but the race-tracking channels prevent the flow propagation to be linear. The part is not fully filled as seen in Figure 4.18. The part is a scrap because it has a macro-scale dry spot in it. For a successful injection, the final product must be void-free [1].

A control system is necessary in the RTM process due to the issues above. With a control system, the followings can be achieved [1]:

- void-free parts can be manufactured,
- cycle time and cost can be decreased,
- the process can be fully automated.

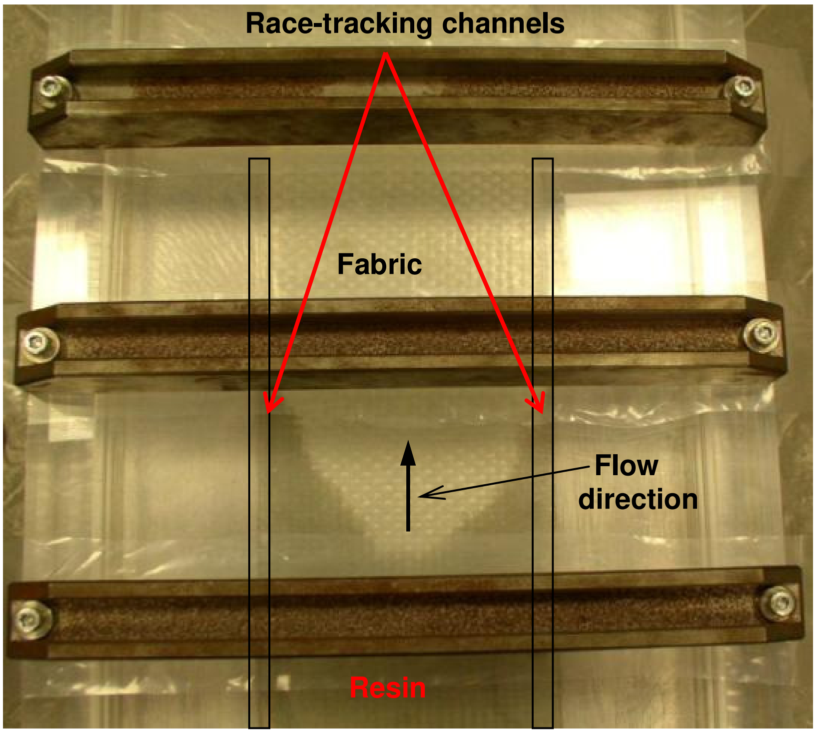

Figure 4.17 Race-tracking channels in a flat mold cavity [1].

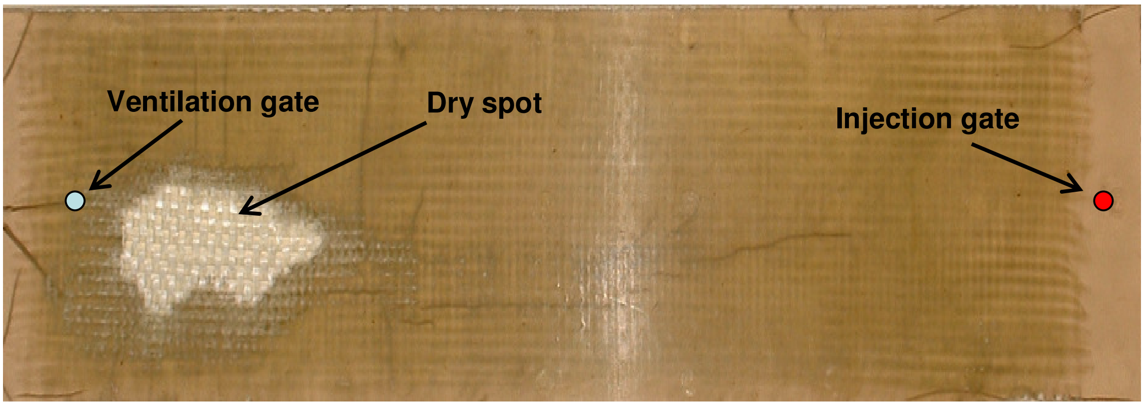

Figure 4.18 A composite part which is not fully filled [1].

For a control system, the followings are needed [1]:

- mold,
- injection machine,
- sensors,
- mold filling simulations,
- data acquisition system.

Sensors embedded on the mold are needed to monitor the mold filling and resin cure. There are many types of sensor systems in the literature; a suitable one has to be chosen. Sensors must be connected to a data acquisition system so that resin propagation and cure can be monitored.

Simulations help the engineers predict how the flow front will propagate will be during the injection. Consider that the sensors detected an unexpected flow front propagation. According to this flow scenario, computer simulations must already have been done. So, the best solution to correct the flow must be applied automatically. Additional inlet / ventilation ports should be opened or existing ones should be closed. For different scenarios, simulations are done and the control actions are saved in the computer for each scenario. Also, during the design of the mold, simulations must be done for the appropriate inlet / vent locations or types. Simulations are described in the following chapters.

4.8 Experimental Set-Up and Mold Design

The RTM mold used in this work was designed and manufactured for TÜBİTAK MAG 104M290 Project. The mold has a constant mold cavity of 3.00 mm, and the geometry of the cavity is flat and rectangular. In Figure 4.19, components of the mold can be seen. The functions of the parts are listed as follows:

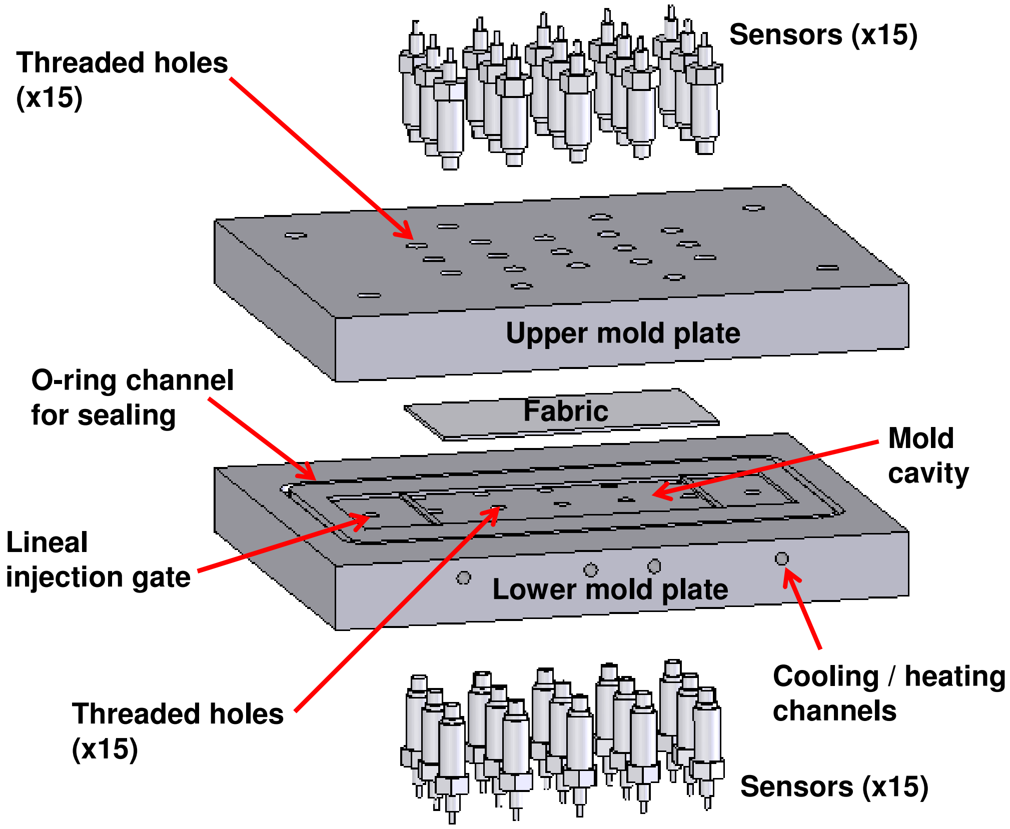

Figure 4.19 RTM mold and its components.

1. *Upper and lower mold plates:* The upper and lower mold plates are machined from tool steel. During resin injection, high injection pressure is necessary to fully impregnate the fabric. Due to high pressure, the mold plates are made from steel for its high strength and stiffness. Also, there is an additional plexiglass upper mold plate for its transparent property, thus the resin flow can be recorded by a camera for verification purpose. Plexiglass has a low specific weight which is necessary for the handling of the mold in the laboratory. The lower and upper mold plates are shown in Figures 4.20 and 4.21, respectively.

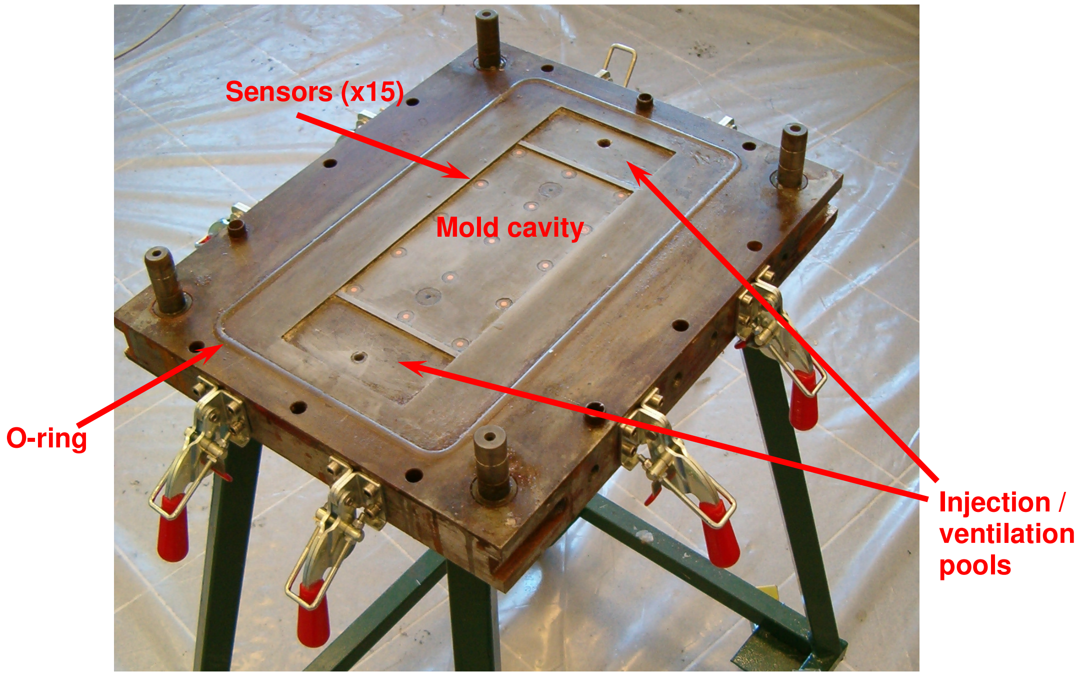

Figure 4.20 The upper mold plate.

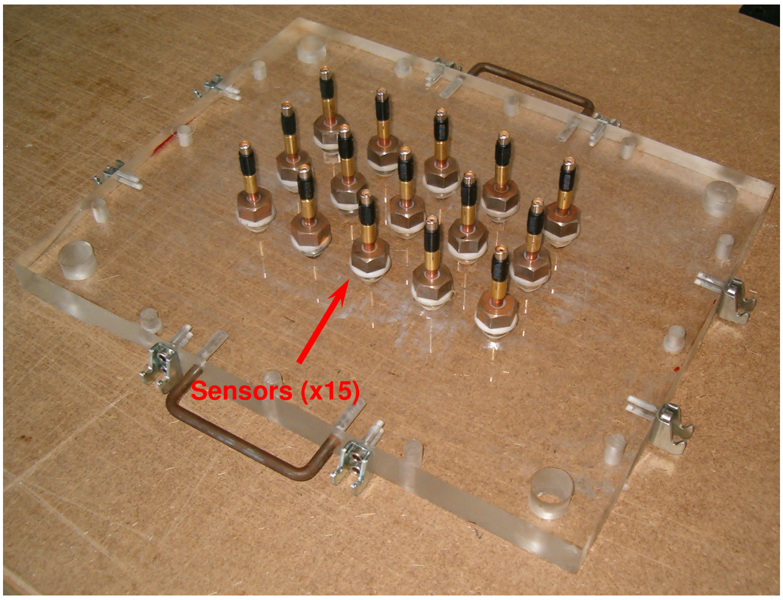

Figure 4.21 The lower mold plate.

2. *Mold closure and fabric compression:* As explained above, an upper mold plate from steel is available. A hydraulic press machine for mold closure was manufactured (see Figure 4.22). The hydraulic press provides up to 20 tons of compression force. But, when the plexiglass upper mold plate is used, compaction is provided by 8 clamps and 12 bolts around the mold. Each clamp has a holding capacity of around 3000 N. Bolts and nuts provide further compaction of the preform (see Figure 4.23).

Figure 4.22 Hydraulic press with the mold.

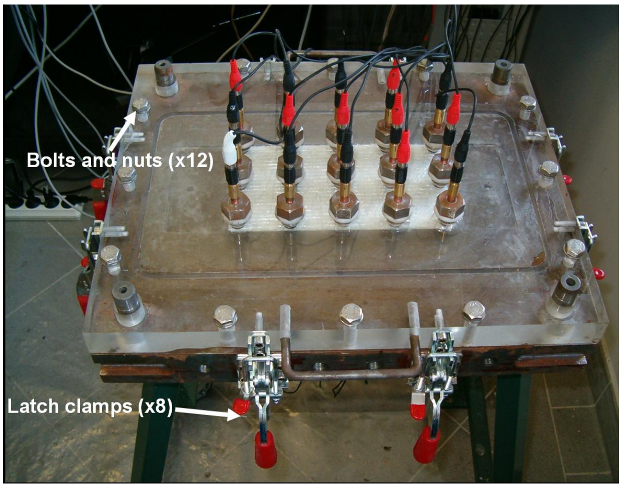

Figure 4.23 Clamps and bolts for mold closure with plexiglass upper mold plate.

3. *Fabric preform:* Fabric preform is cut from a roll at desired dimensions and desired number of layers. Then, it is placed inside the mold cavity. In our work, we usually used a preform by stacking 5 layers of random fabric. In Figure 4.24, a fabric roll with cutting tools and the placement of the fabric into the mold cavity are shown.

Figure 4.24 Fabric roll and placement of fabric preform into the mold cavity.

4. *Injection and Ventilation Tubes:* Resin is transferred from the injection machine to the mold through injection tube(s) [11]. Single or multiple injection and ventilation ports can be used.

5. *Sensor bolts and sensor locations:* 30 point-voltage sensor bolts are embedded into the mold. 15 of them are on the upper mold plate and 15 on the lower one. The upper and lower mold sensors are at the same in-plane x,y coordinates. These sensor bolts are easy to use. They do not act as an obstacle against resin flow. In Figure 4.25, sensor locations on the lower mold plate are shown. With more sensors, flow front propagation can be monitored in more detail, and possible race-tracking channels can be detected more accurately.

6. *Injection / ventilation ports:* The tubes are connected to the mold by using injection / ventilation bolts (see Figure 4.14). Sensor bolts can be replaced by these ports at any sensor location of the mold.

7. *Mold cavity dimensions:* Mold cavity dimensions, pool dimensions and distance between the sensor tips are seen in Figure 4.26. The depth of the cavity is 3.00 mm.

8. *Ejectors:* Two identical ejector stems have been used in this mold. In Figure 4.25, the faces of the ejectors are seen in the mold cavity. Their face diameter is 20 mm.

9. *Sealing:* Sealing is provided by silicon o-ring. The dimensions of the O-ring channel are given Figure 4.12. No leakage has been detected up to 6 bars of resin pressure.

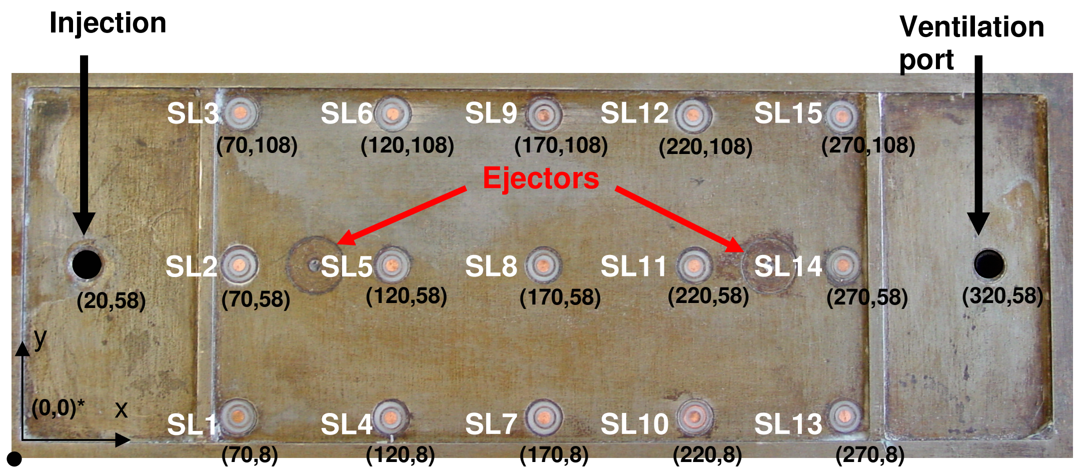

Figure 4.25 Sensor locations on the mold cavity (dimensions in mm.).

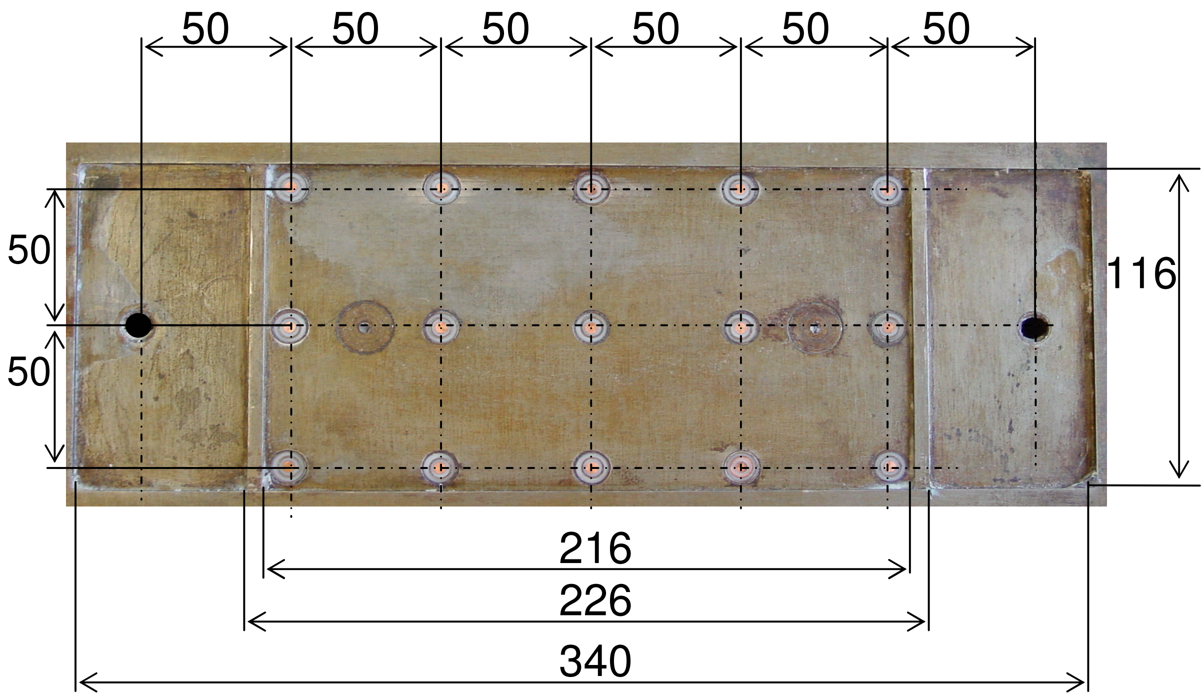

Figure 4.26 Mold cavity dimensions (in mm.).

Chapter 5

MOLD FILLING SIMULATIONS AND SENSOR DATA EVALUATION

5.1 Mold Filling Simulations

In this chapter, mold filling simulations are done using LIMS (Liquid Mold Filling Simulations) [41]. The simulations are performed for the geometry of the RTM mold designed in our laboratory. The dimensions of the mold cavity and the sensor locations are shown in Figure 5.1.

The aim of the simulations is to see the effect of race-tracking channels with different thicknesses. In the mold, 15 point-voltage sensors are embedded to monitor the mold filling process. Flow front contours are compared with the simulated ones to decide which of the previously considered scenario is taking place.

Race-tracking channels are one of the most important disturbances that has to be considered in modeling of the RTM process. Gaps between fabric preform and mold edges form small air channels that are called race-tracking channels. These low resistant (high permeable) channels, through which resin can flow easily, may seriously alter the flow front propagation (see Figure 5.2) [32]. Sensor locations are given in Figure 4.25.

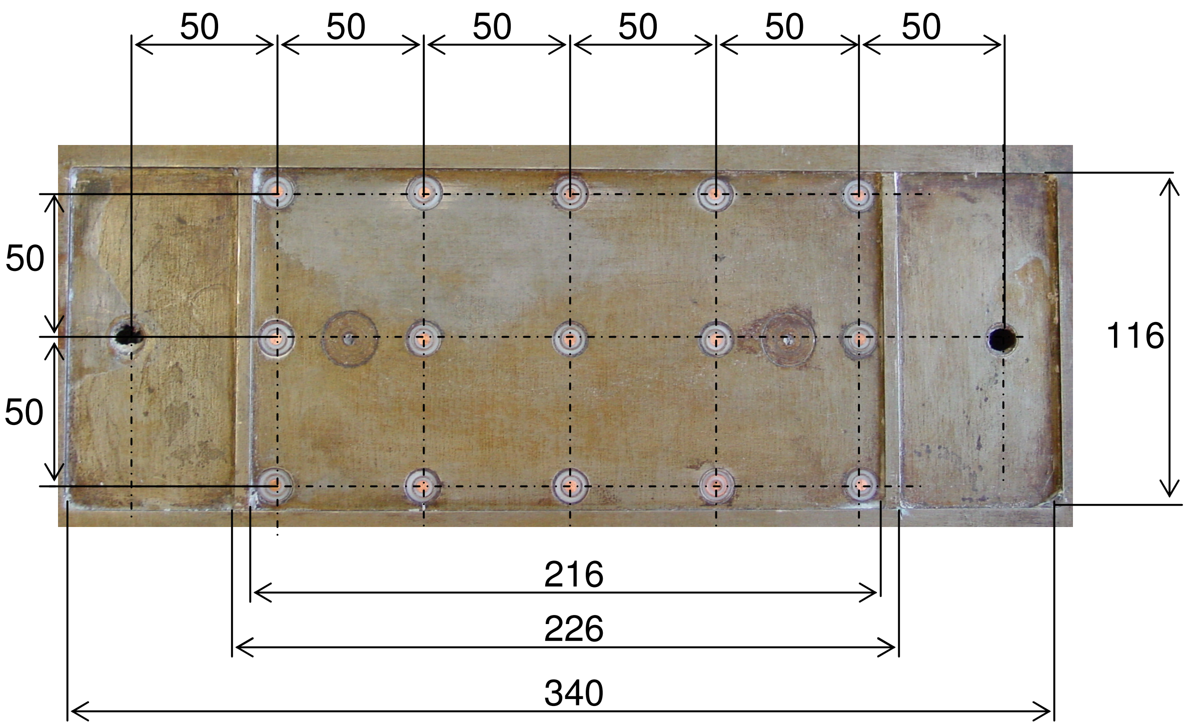

Figure 5.1 Top view of the mold with dimensions (in millimeters).

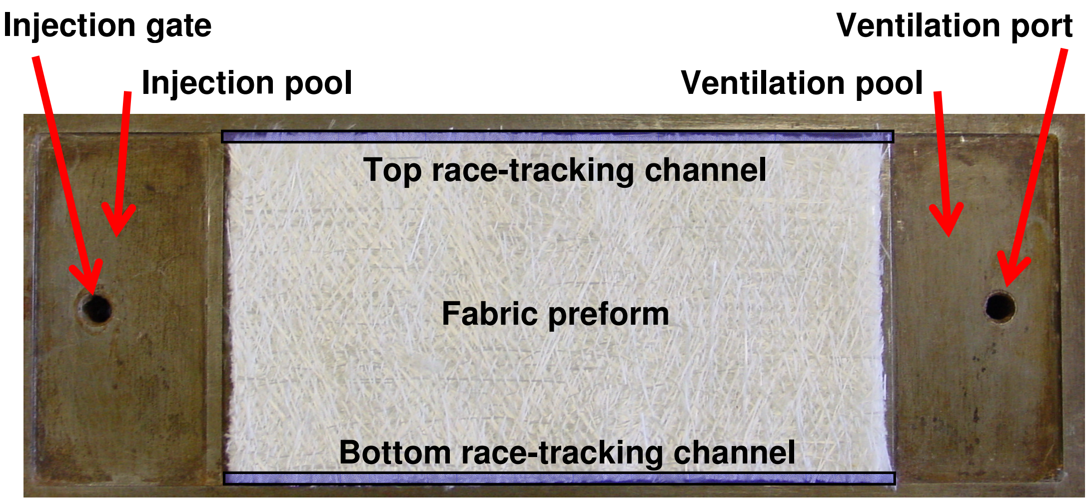

Figure 5.2 Potential race-tracking channels in the mold.

In Figure 5.3, mesh of the mold geometry is shown. LIMS uses a finite element method (FEM) to solve for the pressure distribution and flow front advancement. The density of the mesh alters in different regions of the mold. The regions where race-tracking channels are formed have dense meshes. Inlet and ventilation pools have a coarse mesh because the pressure gradient is expected to be very low there (no fabric is placed in them). Also, the bumps between the mold cavity and inlet / vent pools are defined in the mesh. In Table 5.1, details of the elements are presented.

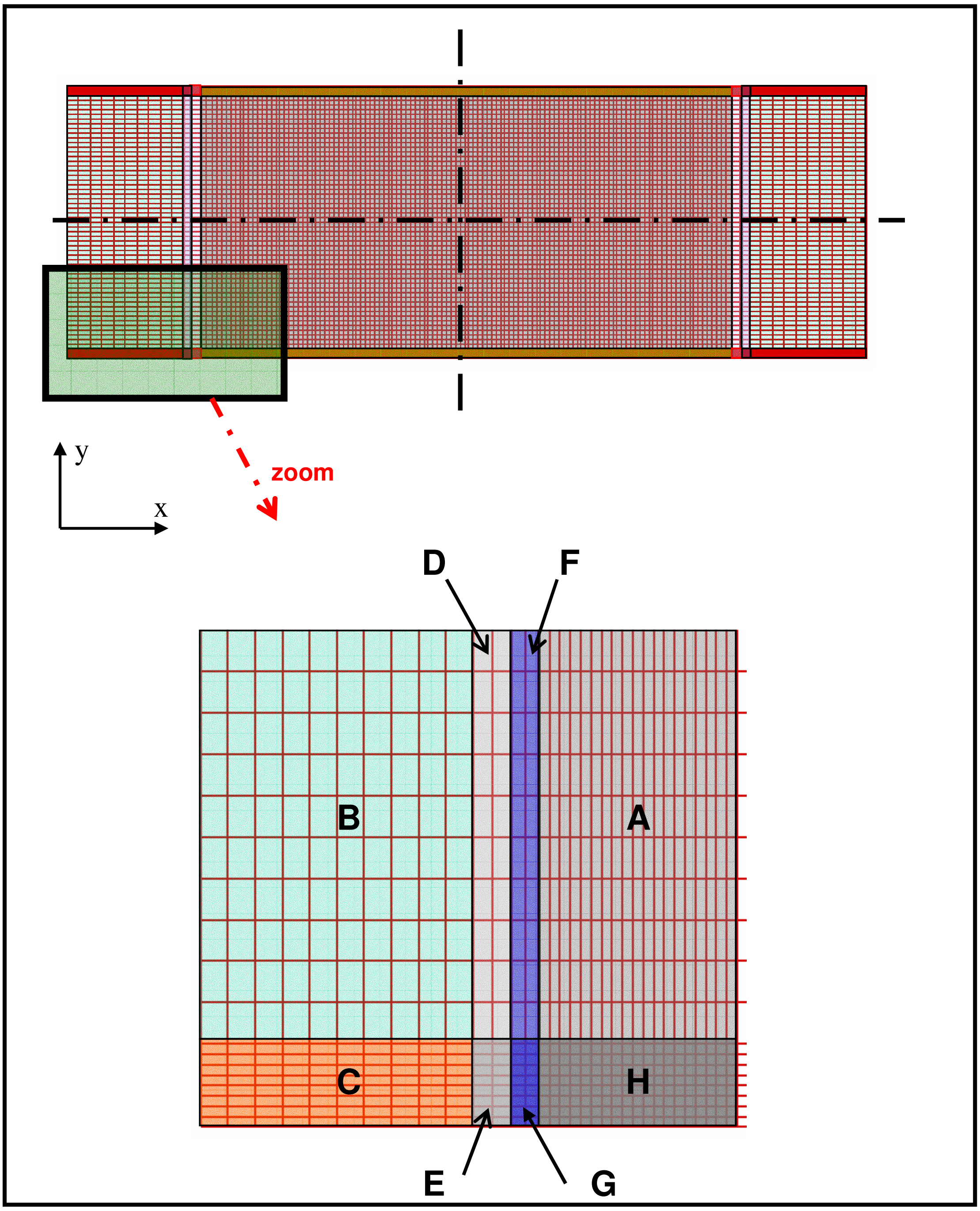

Figure 5.3 Meshed view of the mold cavity.

Table 5.1 Dimensions of regions and number of elements.

Region	**Number of elements in x- direction**	**Dimension of elements in x- direction (mm)**	**Number of elements in y- direction**	**Dimension of elements in y- direction (mm)**	**Explanation**
A	113	2	54	2	Mold cavity where the fabric perform is placed
B	10	5	54	2	Inlet / ventilation pool
C	10	5	8	0.5	Inlet / ventilation pool
D	2	3.5	54	2	Inlet / ventilation pool
E	2	3.5	8	0.5	Inlet / ventilation pool
F	2	2.5	54	2	Bump
G	2	2.5	8	0.5	Bump
H	113	2	8	0.5	Possible race-tracking channel region

The input mesh file has 10082 nodes and 9870 elements. The permeability values of elements in different sections of the mold (mold cavity, race-tracking channels, inlet/vent pools and bumps) are assigned separately.

In Figure 5.4, element numbers and node numbers at the corners of the mold are seen. Each box represents a quadrilateral element, and the number inside the box is the corresponding element number. The numbers around the boxes are node numbers; each element has 4 nodes.

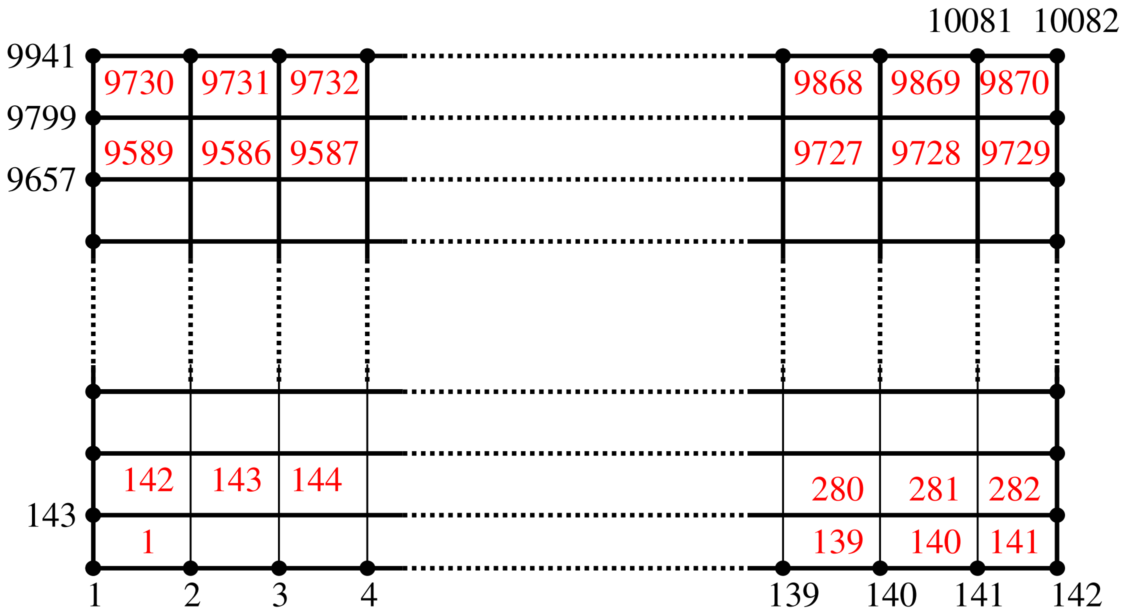

Figure 5.4 Node and element numbers at the corners of the mold (red numbers inside boxes are element numbers, and black numbers around boxes are node numbers).

5.2 Permeability Calculation

5.2.1 Permeability of fabric preform

A porous fabric preform has a resistance to the flow of a liquid resin. Inverse of the resistance is called permeability. Permeability values of different regions are input parameters in LIMS. To calculate the permeability of the fabric preform, 1-D injections are done in permeability measurement experiments [42]. 1-D Darcy law is:

$$\bar{u}_x = \frac{1}{\eta} K_{xx} \frac{\partial P}{\partial x} \tag{5.1}$$

where $\bar{u}_x$ is the average velocity of resin in x-direction, η is the viscosity of resin, K_{xx} is the permeability of the fabric preform and $\frac{\partial P}{\partial x}$ is the pressure gradient in x- direction.

The fabric preform is placed in a simple RTM mold. At constant flow rate injection, 1-D flow is obtained. $\frac{\partial P}{\partial x}$ and $\bar{u}_x$ are recorded. Then, permeability is calculated by using Darcy law (Equation (5.1)). For a more detailed description of the “steady” and “unsteady” 1-D flow permeability measurement experiments, it is suggested to read Reference [42]. In the simulations, fabric preform’s permeability is set to $2 \cdot 10^{-9}\ m^2$.

5.2.2 Permeability of race-tracking channels

Permeability of a race-tracking channel is calculated in [32]:

$$K = K^* \frac{h^2}{12} \tag{5.2}$$

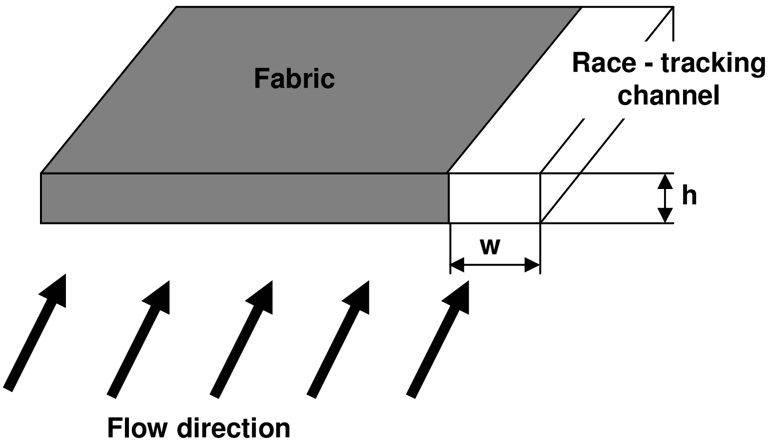

Figure 5.5 Race - tracking channel dimensions.

Hence K and K^* are the dimensional and non-dimensional permeability respectively. h is the height of the mold cavity, and $\frac{h^2}{12}$ is the reference permeability of an infinite channel (i.e., height is h and w → ∞). K^* is taken from Table 6.3 which was constructed from [32].

Table 5.2 Permeability of race-tracking channels with a fixed height of $h = 3\ mm$.

$w\ (mm)$	h/w	K^*	$K\ (m^2)$
0.3	10	0.00936	$0.70 \cdot 10^{-8}$
0.5	6	0.02480	$1.86 \cdot 10^{-8}$
1.0	3	0.08770	$6.58 \cdot 10^{-8}$
1.5	2	0.17100	$12.83 \cdot 10^{-8}$
2.0	1.5	0.26100	$19.56 \cdot 10^{-8}$
2.5	1.2	0.34600	$25.95 \cdot 10^{-8}$

5.2.3 Permeability of inlet / ventilation pools

As $h/w \to 0$, $\boldsymbol{K \to h^2/12}$ [8]. The width of the pools is much larger than the height of them ($w = 116\ mm$ whereas $h = 3\ mm$). The corresponding permeability is:

$$\boldsymbol{K \cong h^2/12 = 0.003^2/12 = 75 \cdot 10^{-8}\ m^2} \quad (5.3)$$

5.2.4 Permeability of the bumps

At the bumps, $w = 116\ mm$ and $h = 1\ mm$. For this $w >> h$ case.

$$\boldsymbol{K = h^2/12 = 0.001^2/12 = 8.33 \cdot 10^{-8}\ m^2} \quad (5.4)$$

5.3 Results of the Simulations

For 16 different race-tracking channel scenarios, 16 simulations are performed. In these simulations, injections are done at constant flow rate of $30\,cc/\min$. The differences between the scenarios are described in Figure 5.6. In each scenario, race-tracking channels have different width dimensions along the right and left sides.

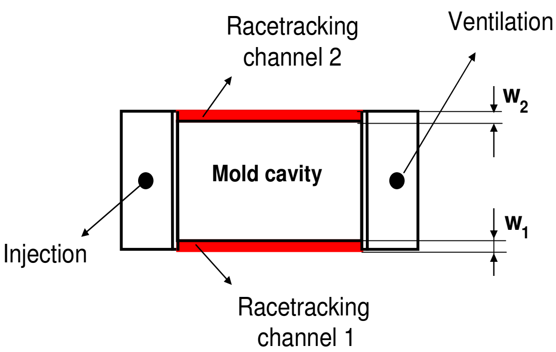

SCENARIO #	W_1 (mm)	W_2 (mm)
1	0	0
2	0	0.3
3	0	0.5
4	0	1
5	0.3	0
6	0.3	0.3
7	0.3	0.5
8	0.3	1
9	0.5	0
10	0.5	0.3
11	0.5	0.5
12	0.5	1
13	1	0
14	1	0.3
15	1	0.5
16	1	1

Figure 5.6 Race-tracking channel widths in different disturbance scenarios Scn 1-16.

For each simulation, a set of three figures are given. The first figure is inlet resin pressure. The second figure is flow front contours using 10082 nodes. The third figure is flow front contours created with using only 15 nodes (nodes at the locations of sensors).

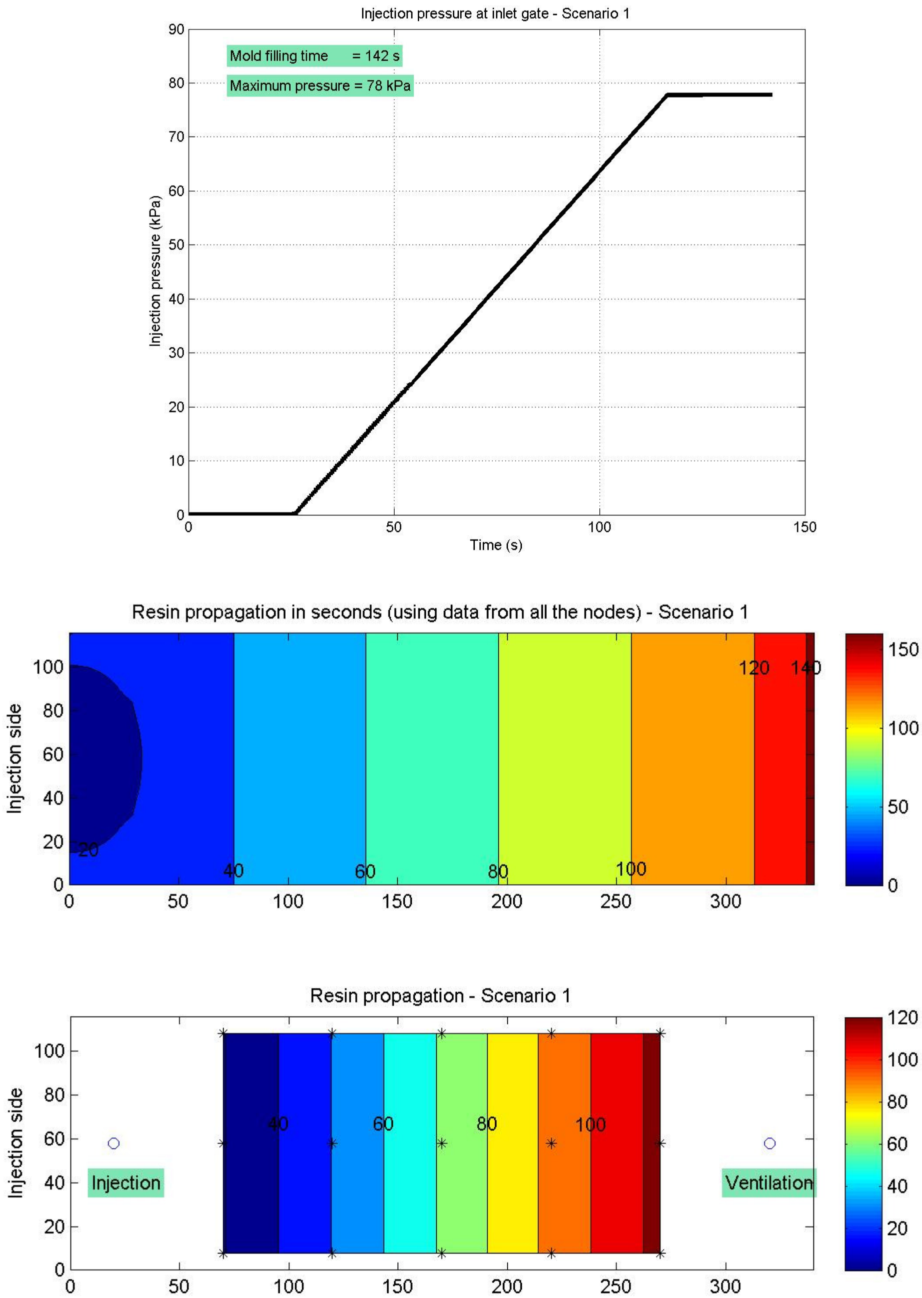

Figure 5.7 Simulation results for scenario 1.

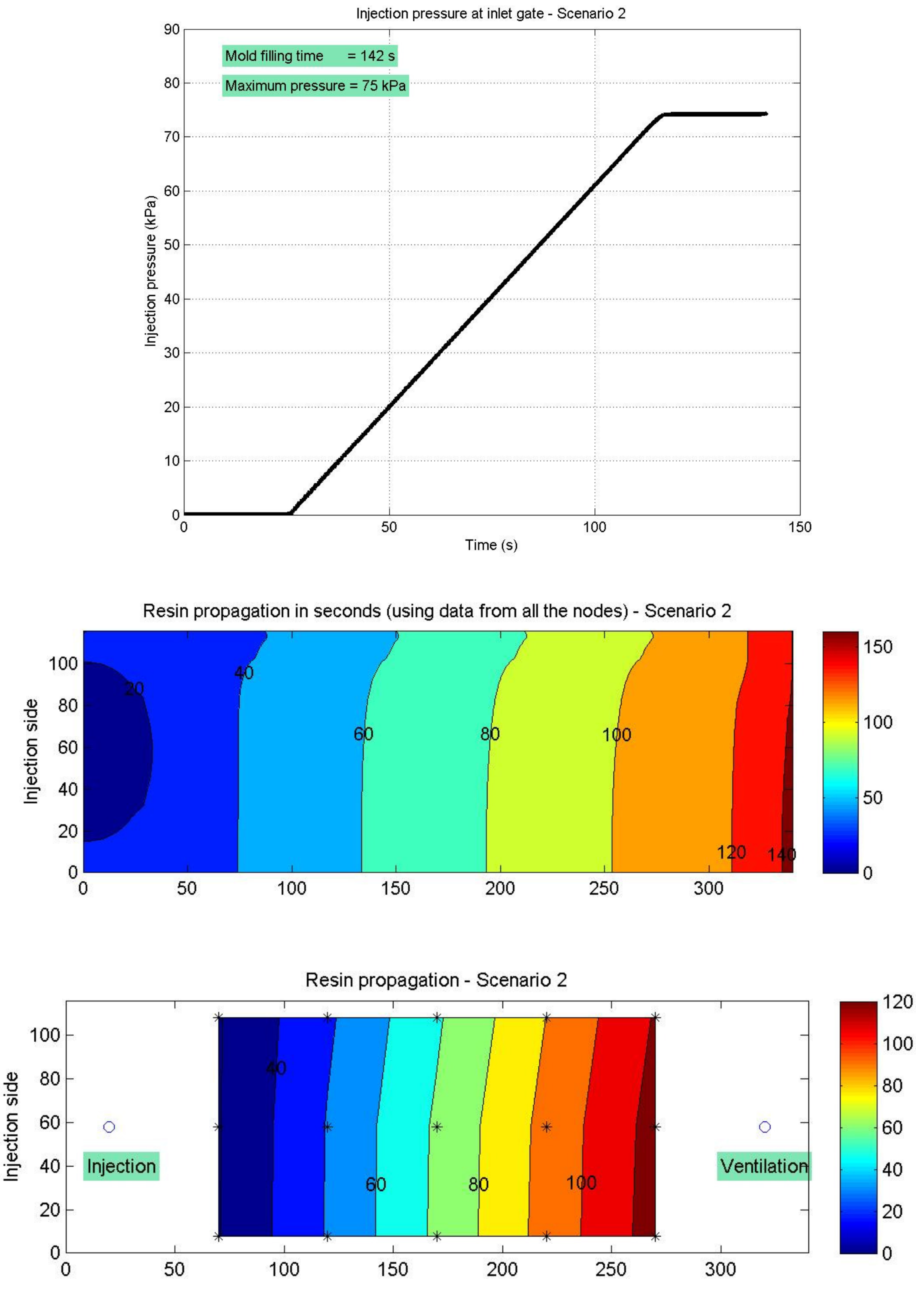

Figure 5.8 Simulation results for scenario 2.

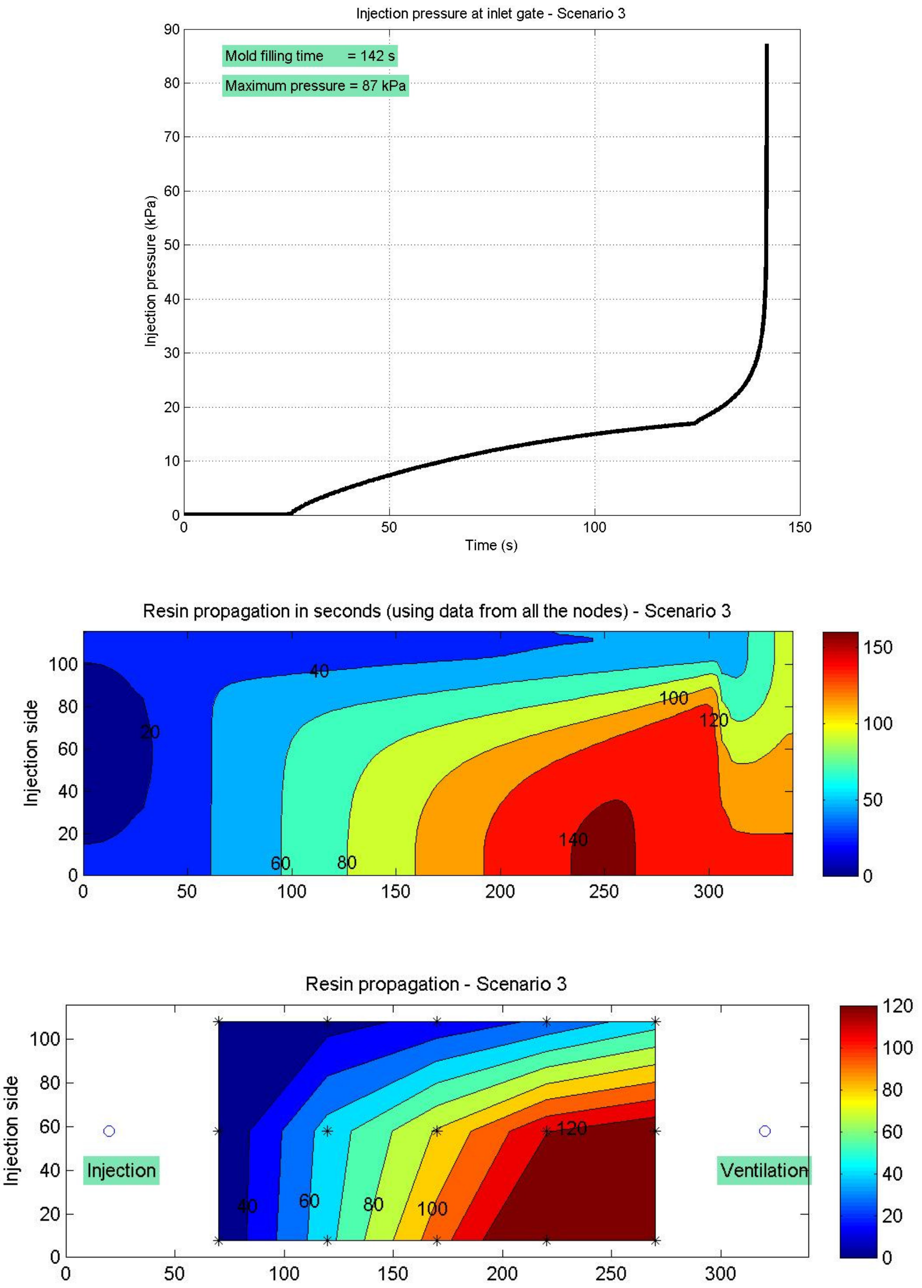

Figure 5.9 Simulation results for scenario 3.

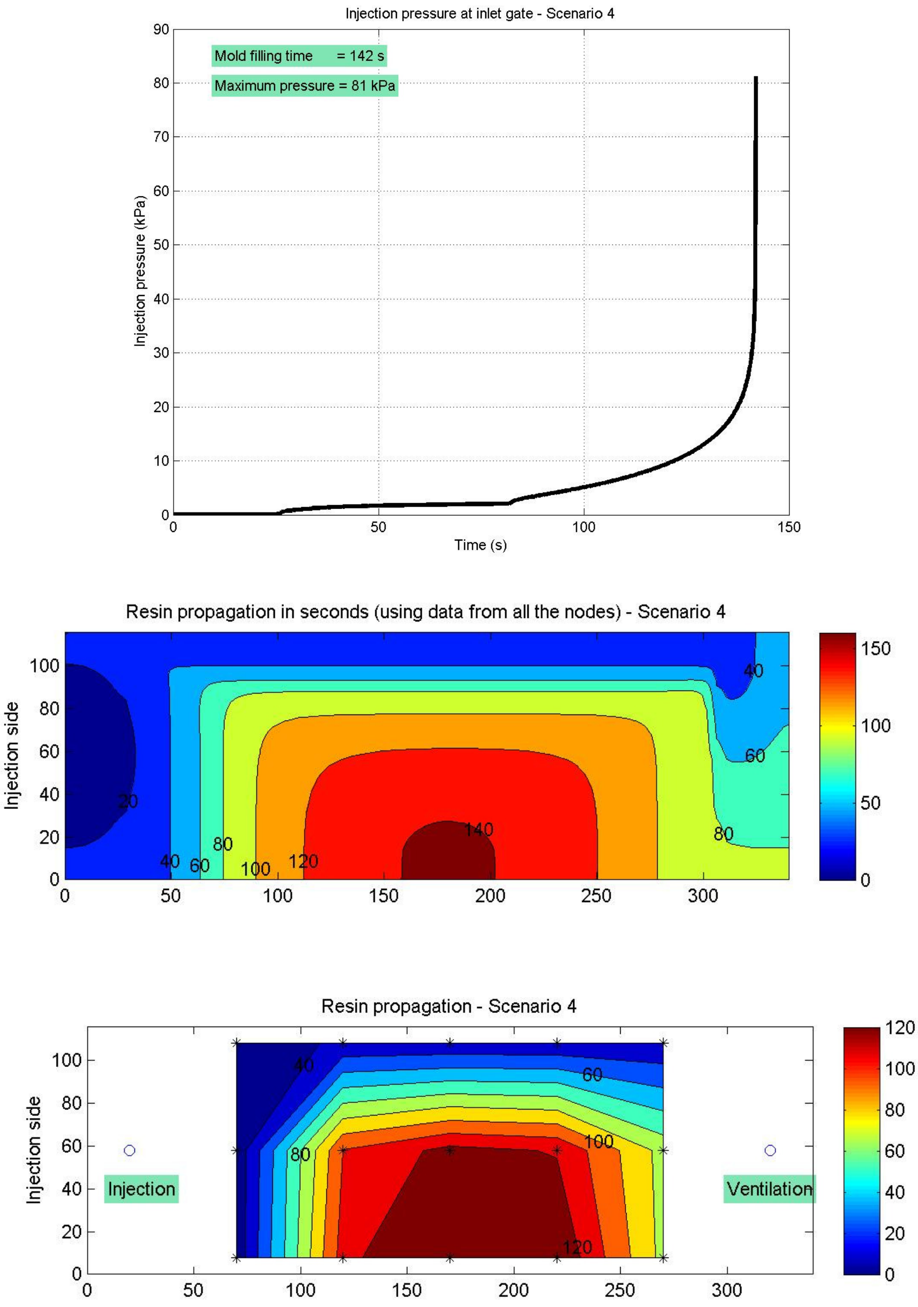

Figure 5.10 Simulation results for scenario 4.

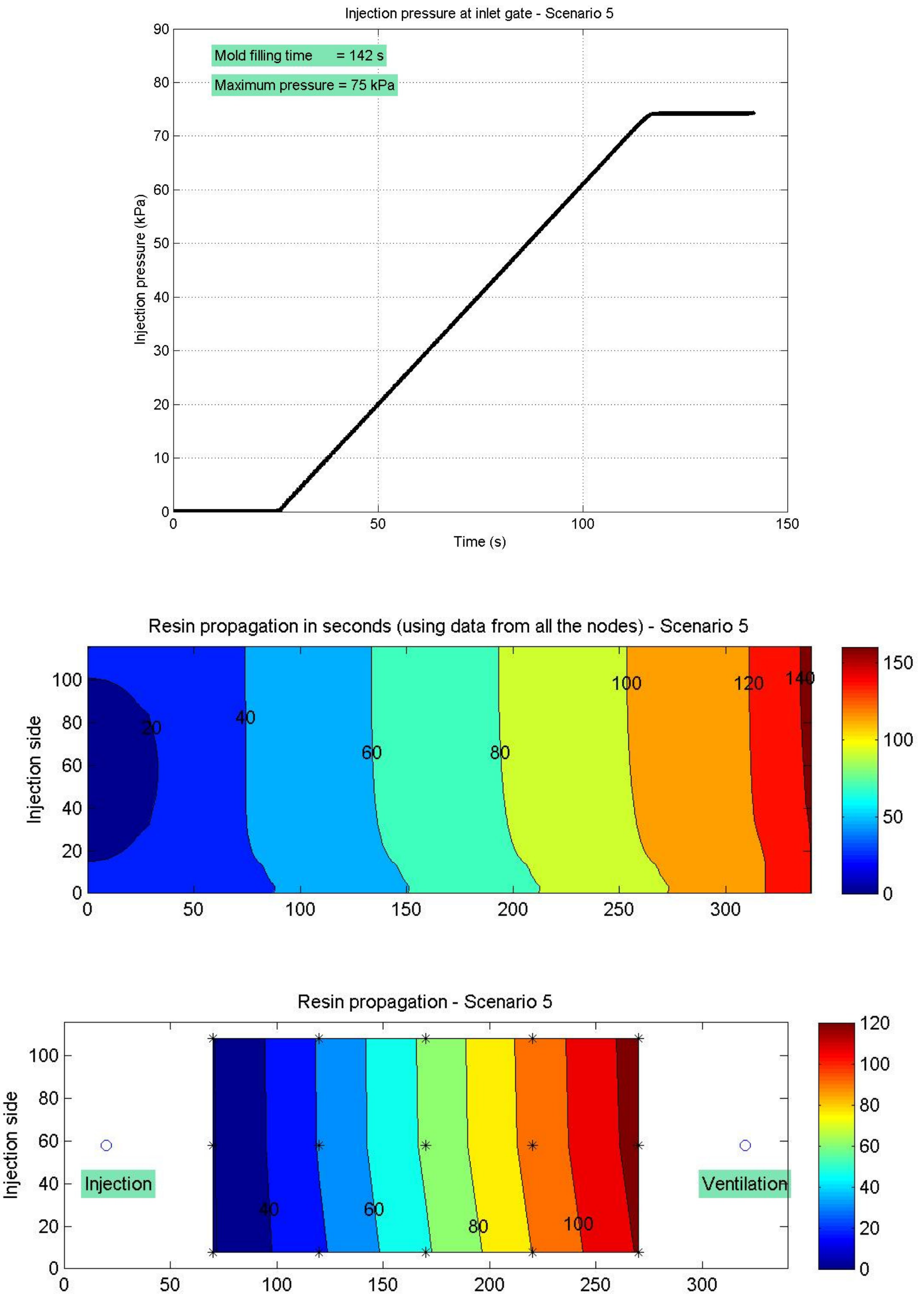

Figure 5.11 Simulation results for scenario 5.

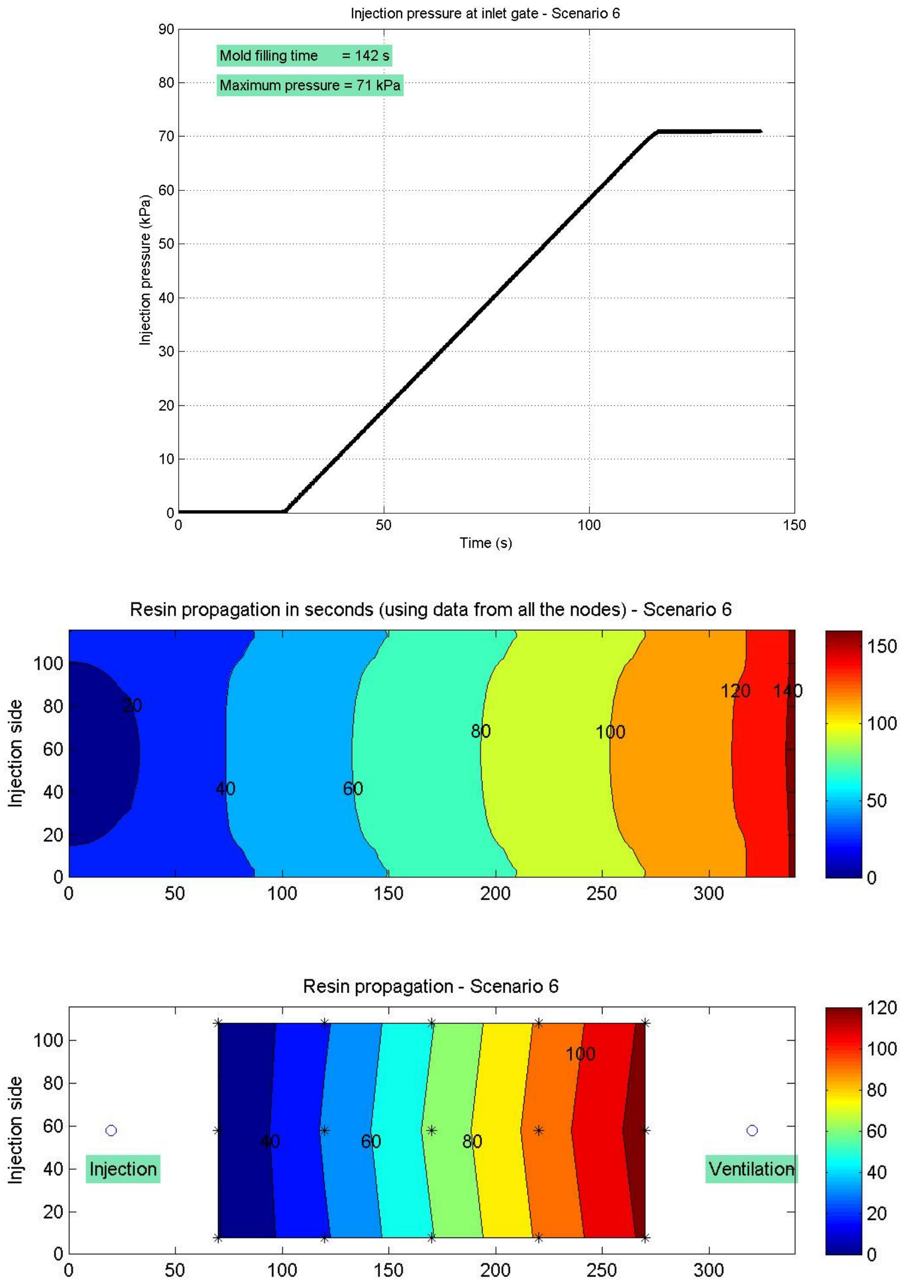

Figure 5.12 Simulation results for scenario 6.

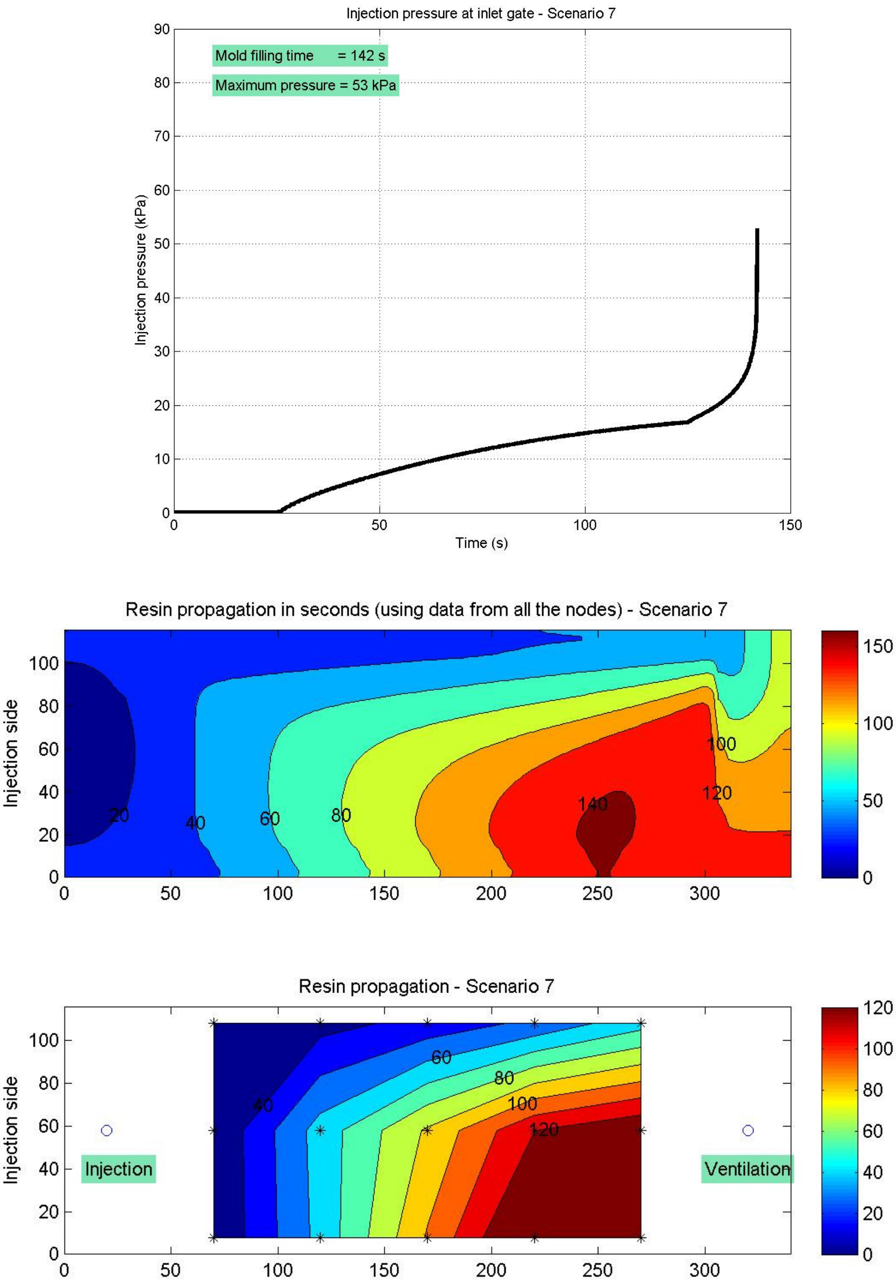

Figure 5.13 Simulation results for scenario 7.

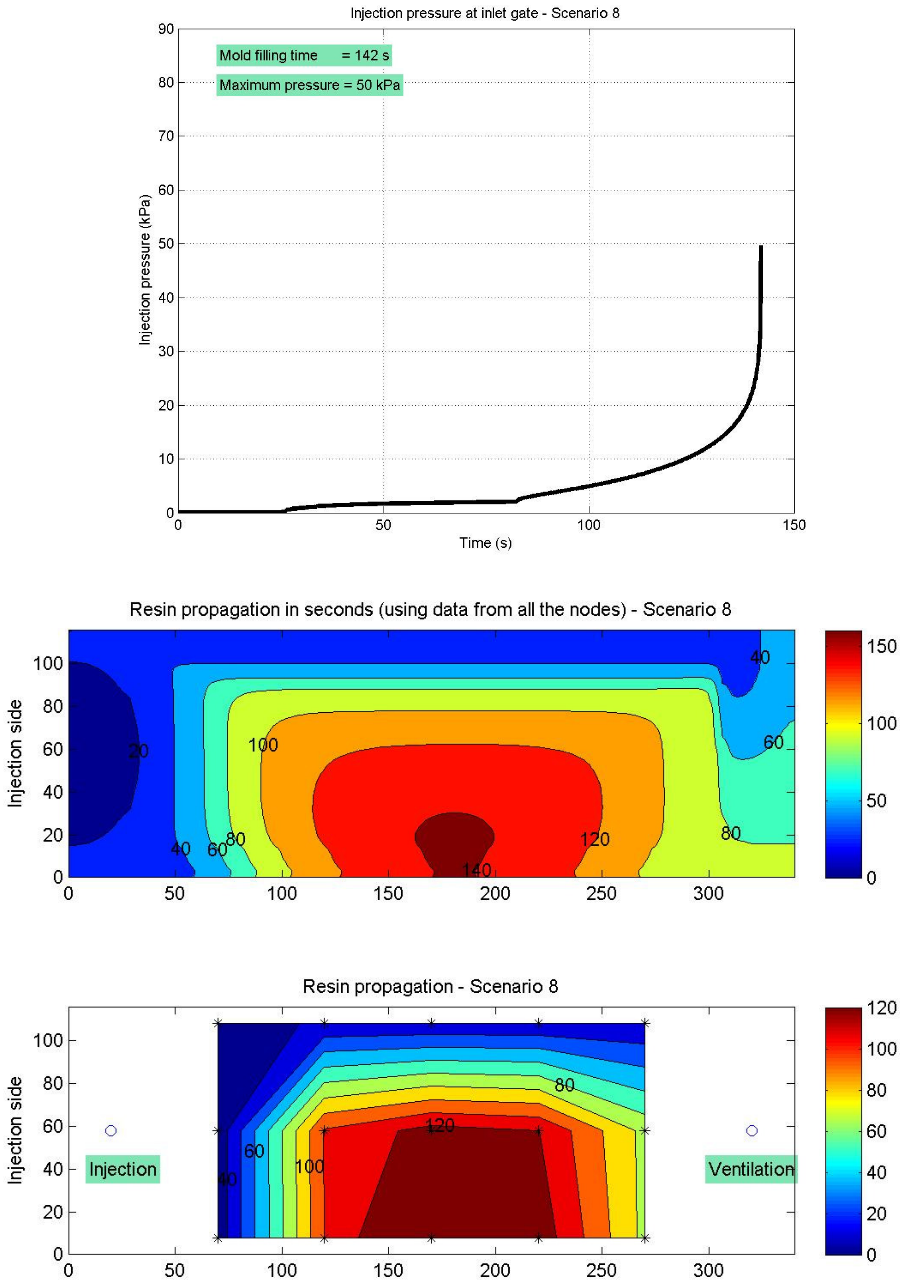

Figure 5.14 Simulation results for scenario 8.

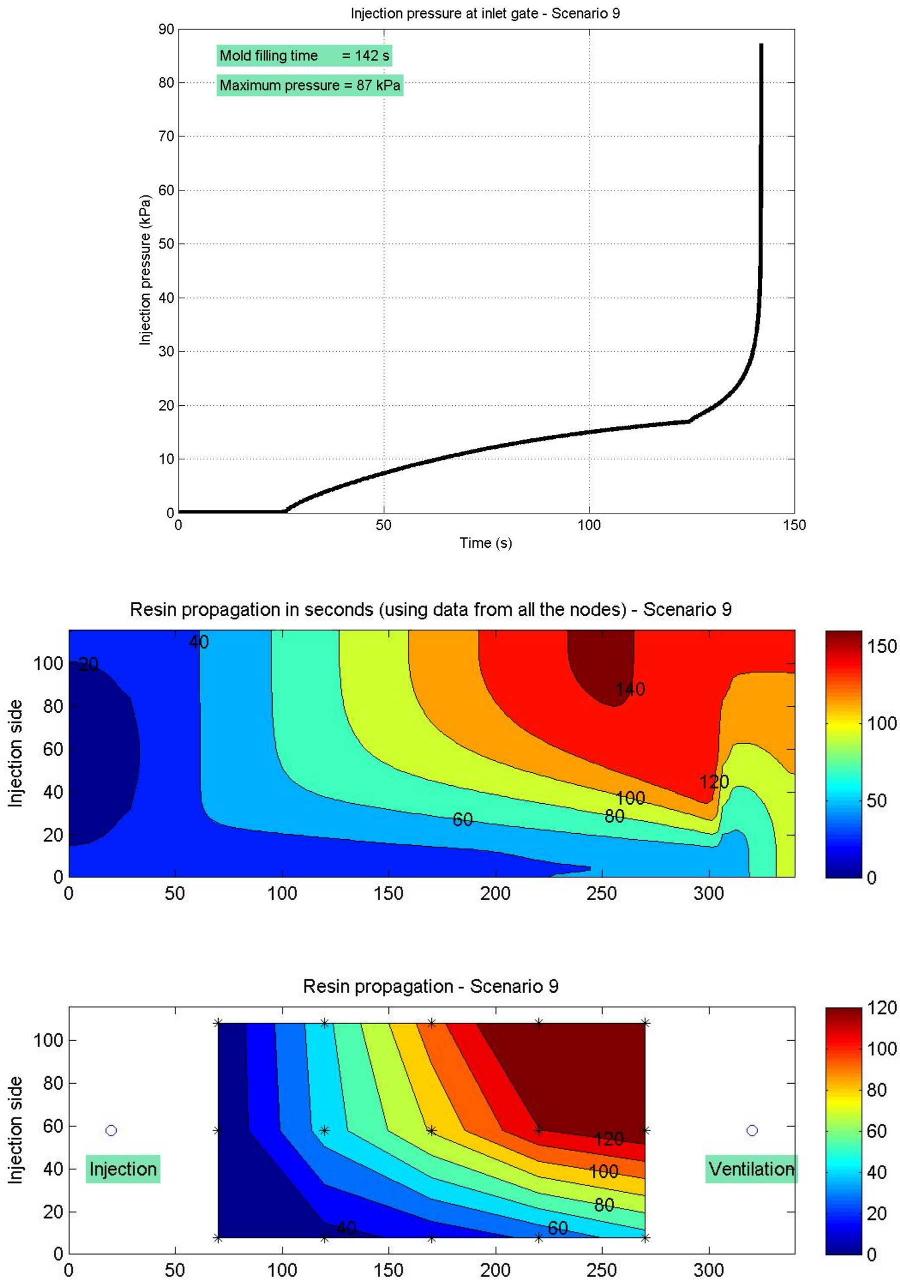

Figure 5.15 Simulation results for scenario 9.

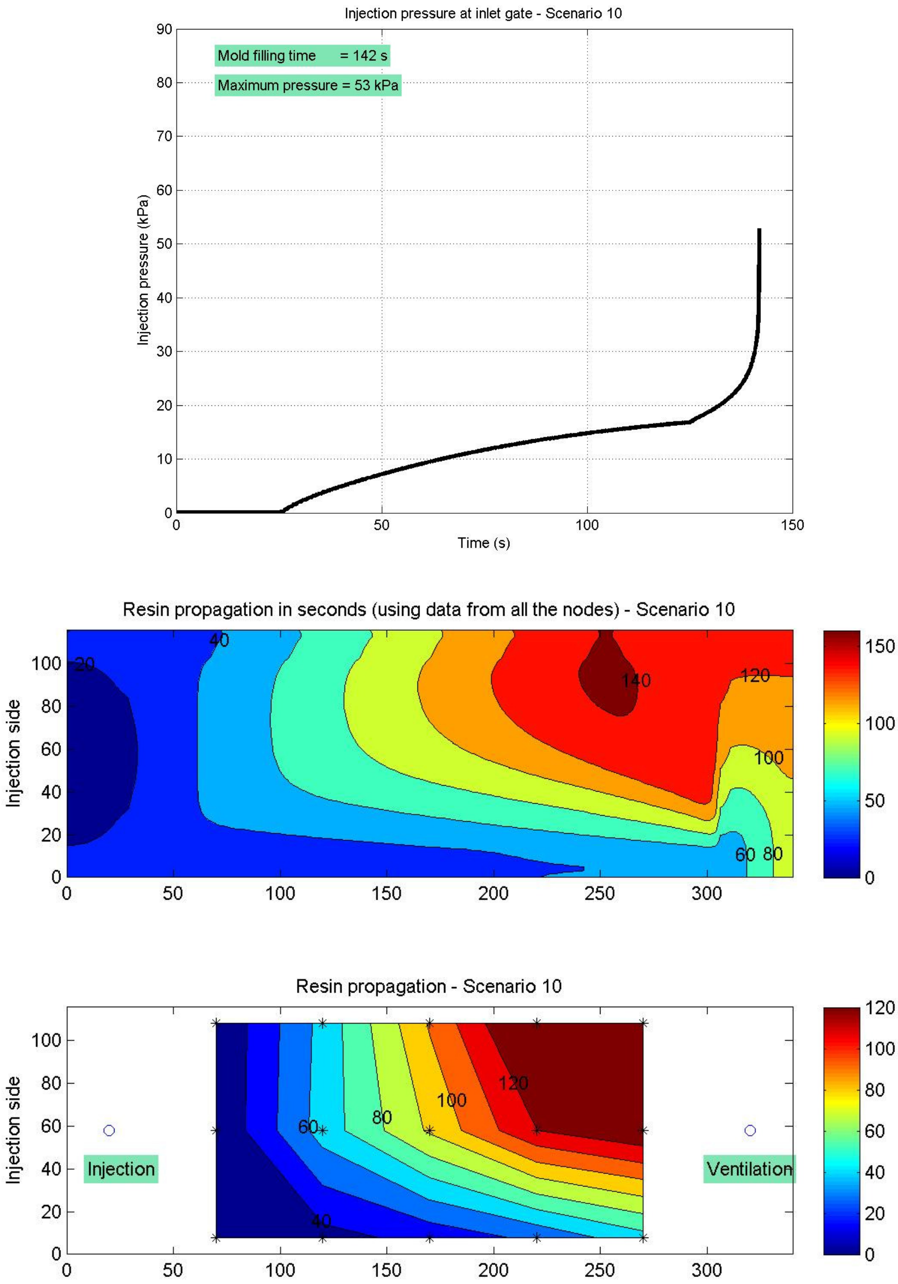

Figure 5.16 Simulation results for scenario 10.

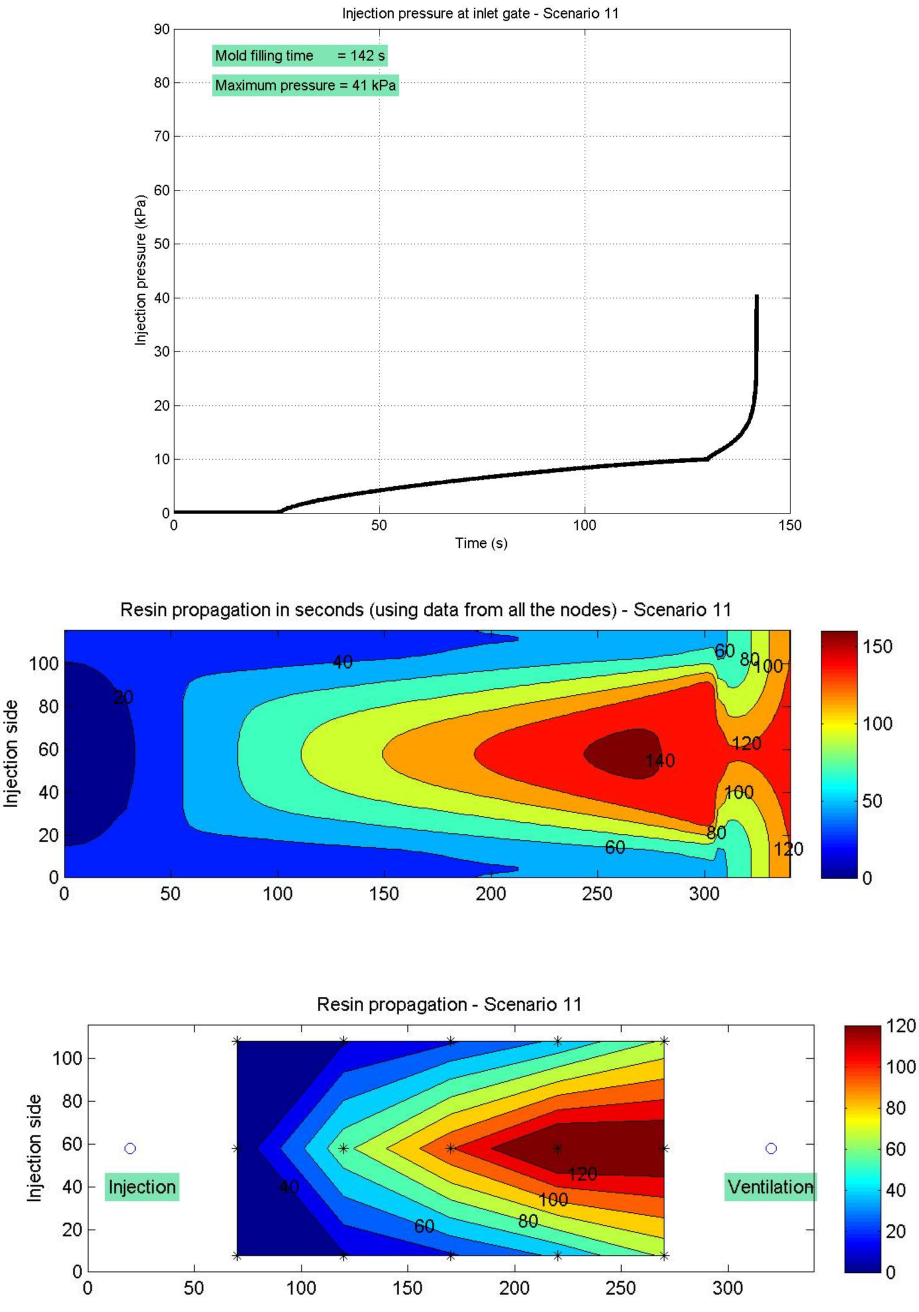

Figure 5.17 Simulation results for scenario 11.

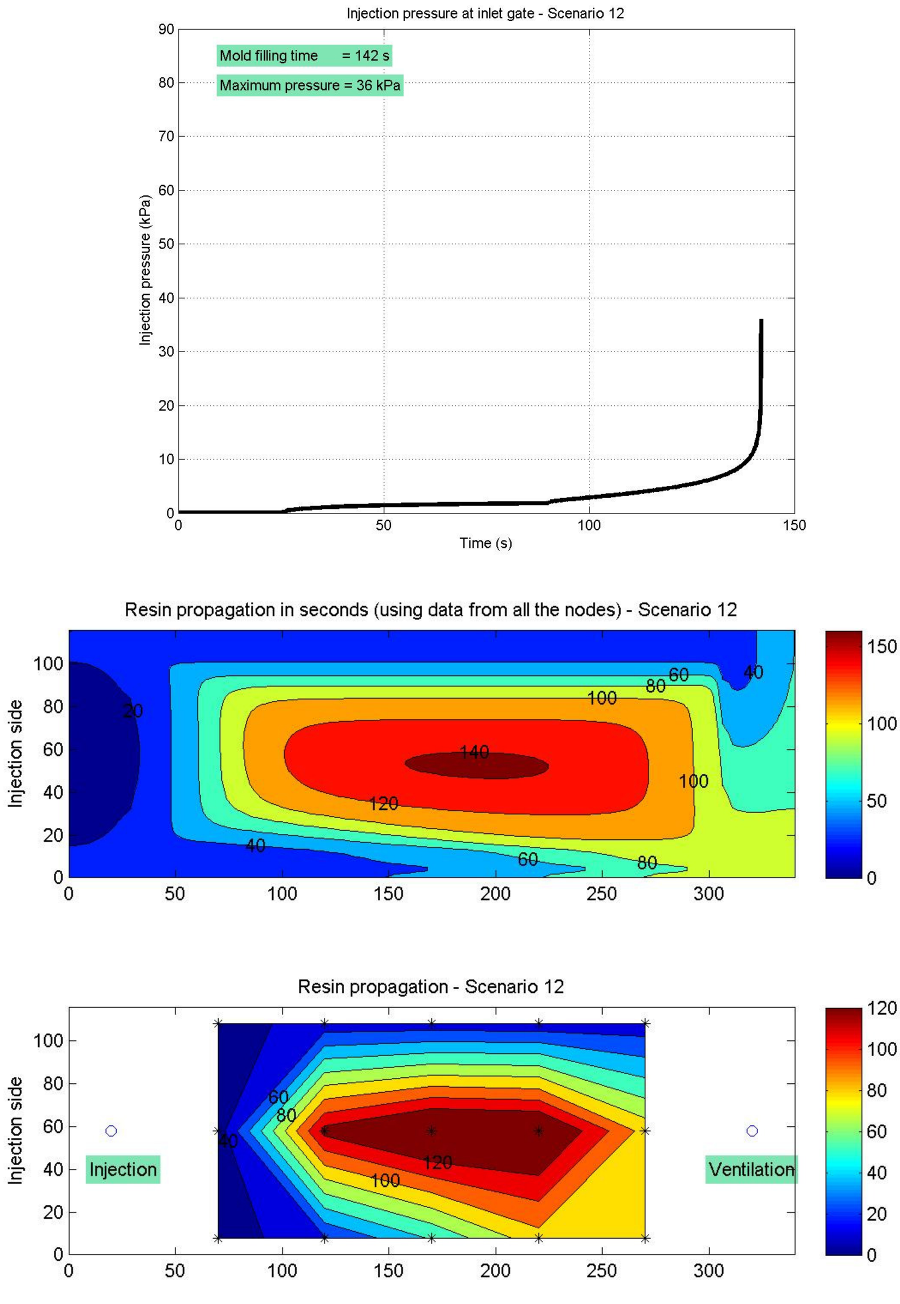

Figure 5.18 Simulation results for scenario 12.

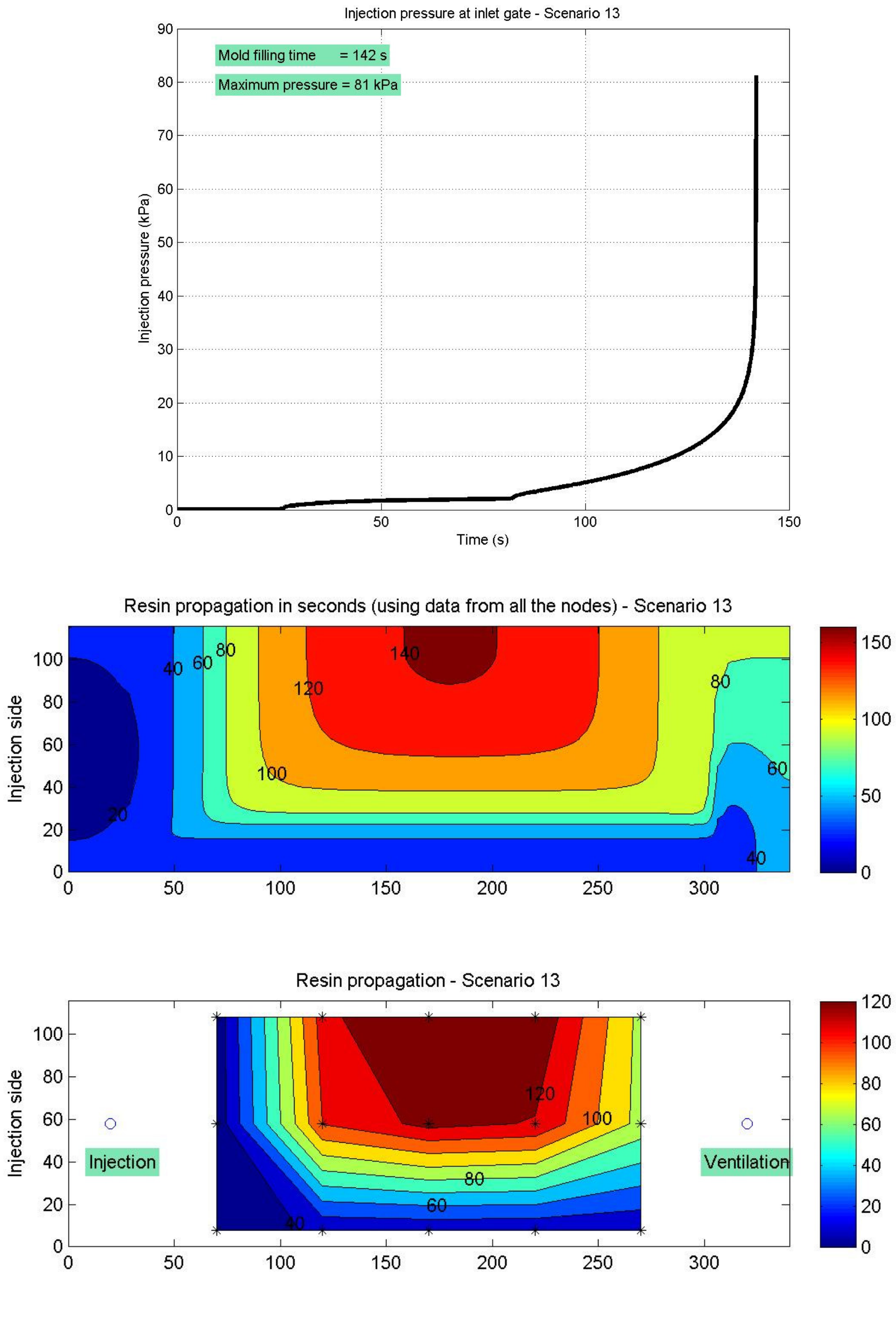

Figure 5.19 Simulation results for scenario 13.

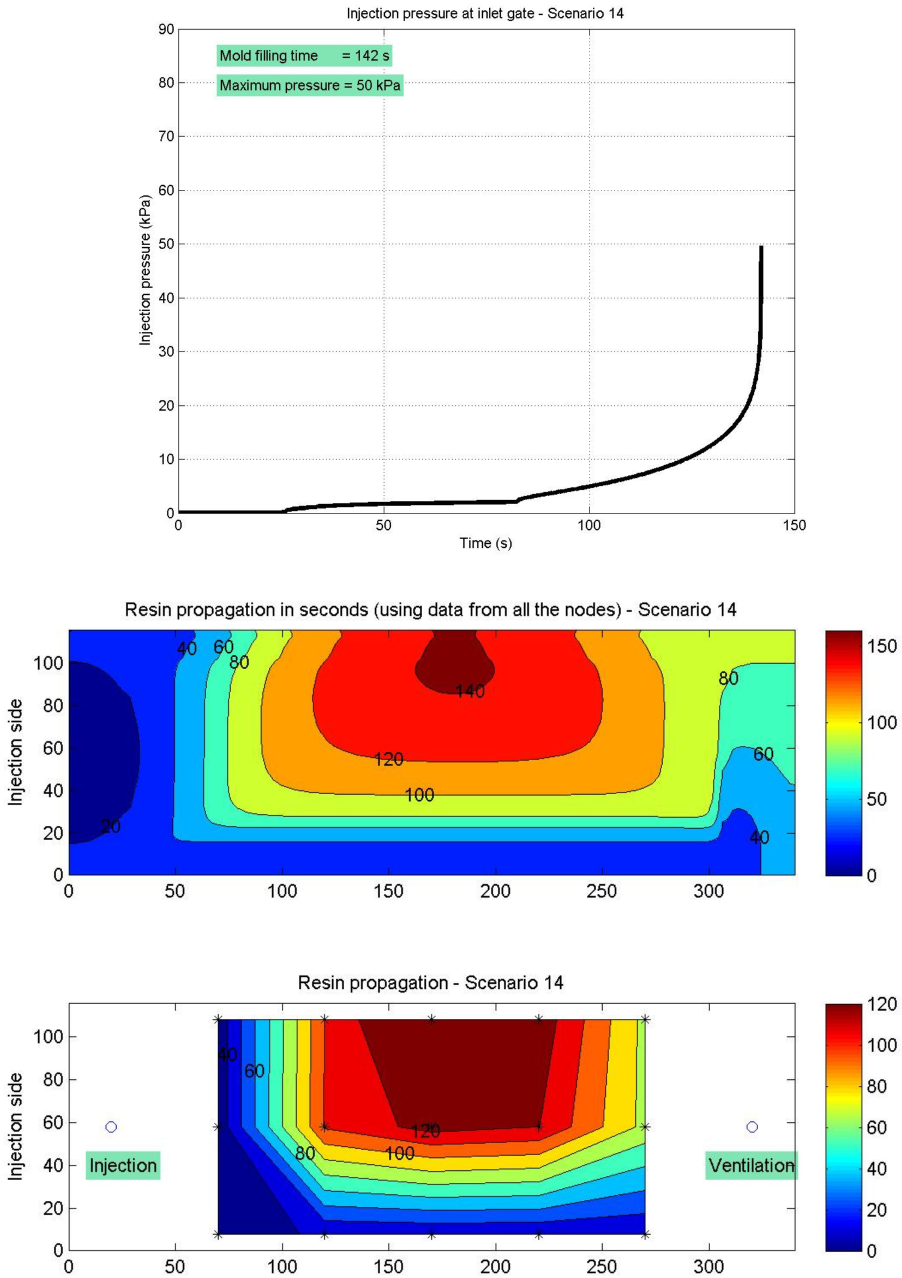

Figure 5.20 Simulation results for scenario 14.

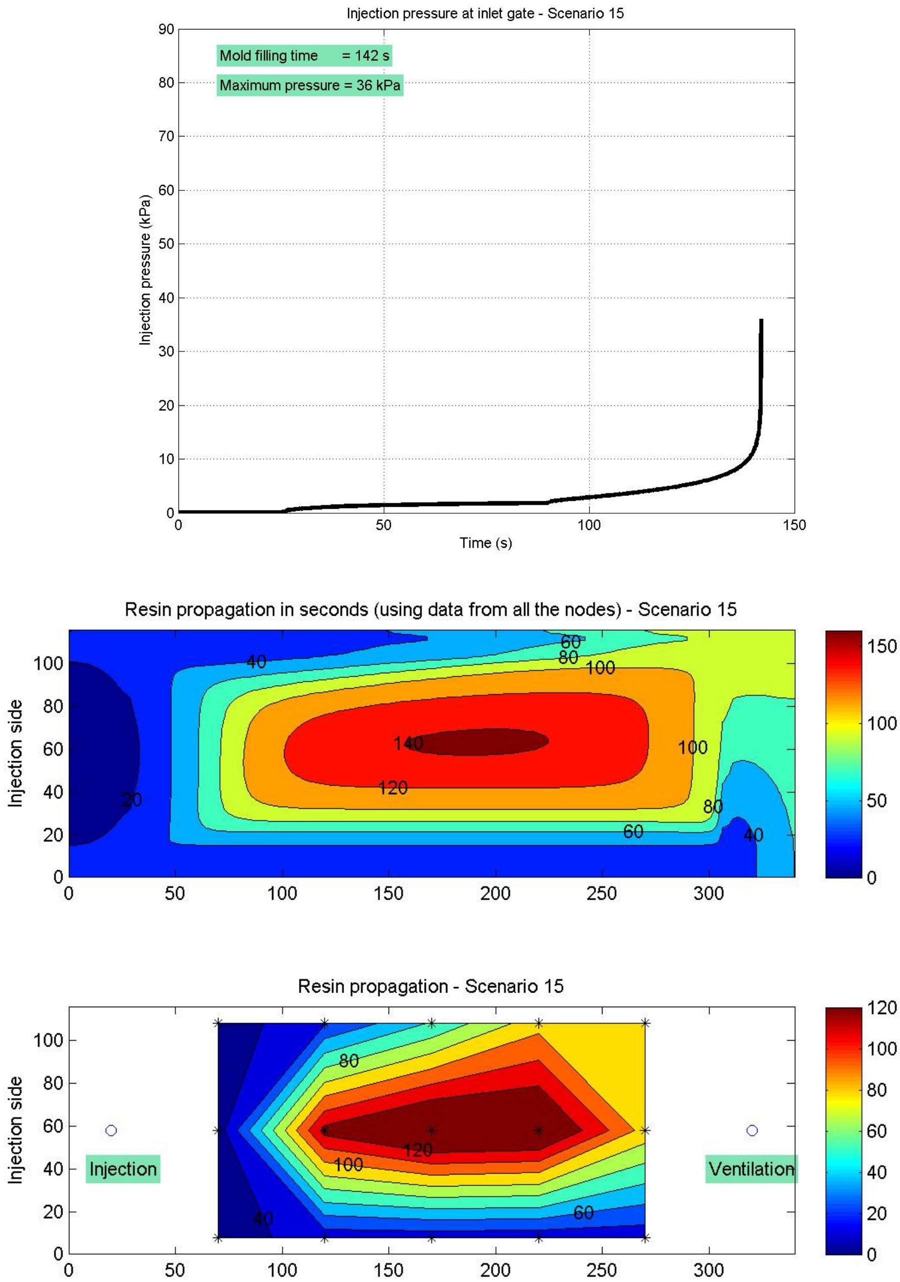

Figure 5.21 Simulation results for scenario 15.

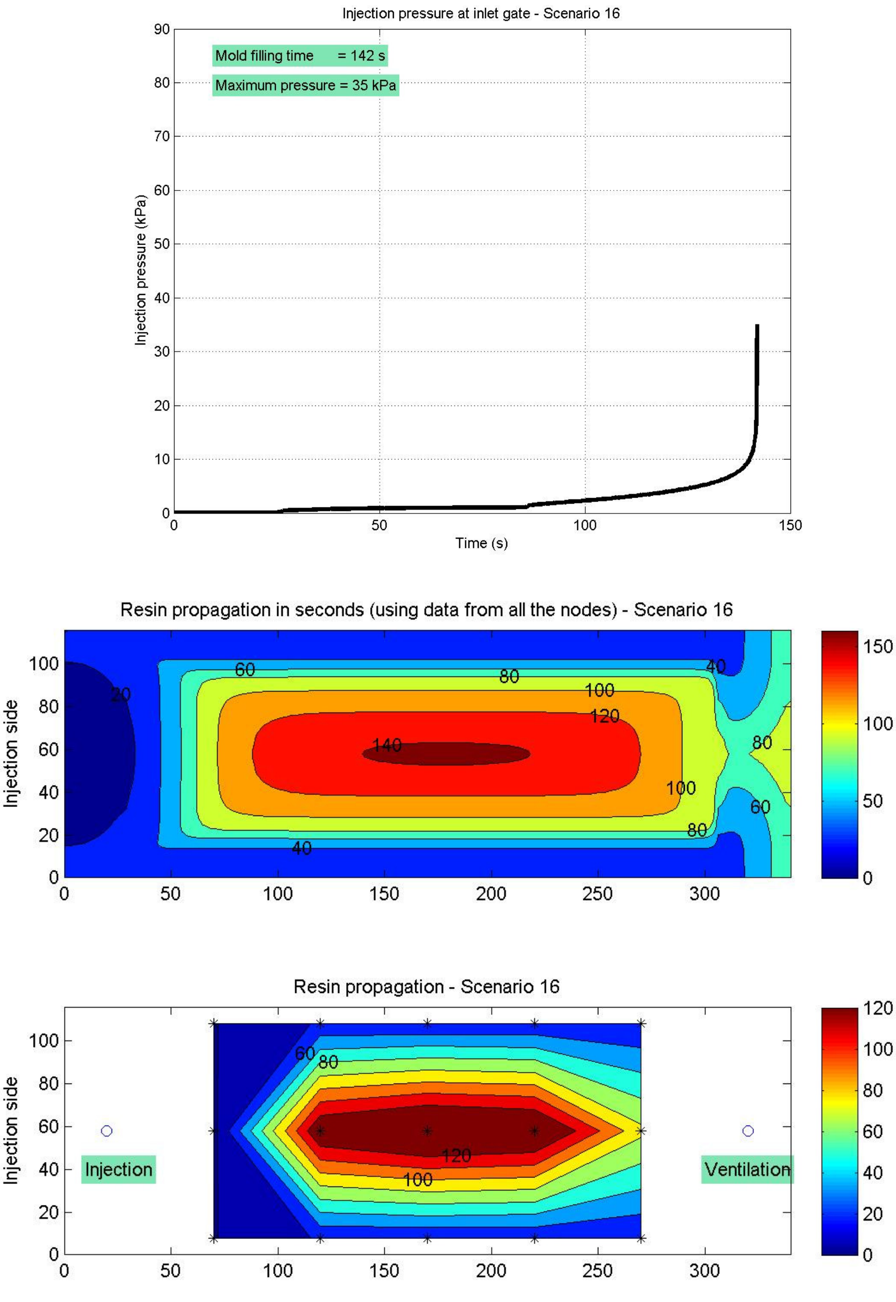

Figure 5.22 Simulation results for scenario 16.

5.4 Sensor Data Evaluation

In composite material manufacturing, it is common to have some disturbances such as race-tracking channels or non-uniform fabric compaction. These disturbances may result in void formation in the parts. To manufacture void-free parts, automation of the process is necessary. By evaluating in-situ sensor data, one can achieve two major objectives:

(i) on-line monitoring of currently dry region(s);

(ii) prediction if any section(s) of the mold cavity will not be filled when the injection is continued with the injection parameters.

Especially, the second objective is very crucial to control the process, and automate the adjustments of the injection conditions, such as changing the injection pressure or flow rate, and opening/closing gates or vents.

After collecting the triggering time data from the sensors, the behavior of the flow can be estimated by comparing the arrival times at the sensors with the predefined scenarios (Figures 5.7 – 5.22). These scenarios are determined before the manufacturing process, by taking into the considerations of possible major disturbances. In Figure 5.23, flow front contours are shown together for quick comparisons (also see Figure 5.6).

In on-line control strategy, triggering order and triggering time of the sensors are the two important variables. Triggering time of sensor i, t_i is the moment at which time the voltage reading of the sensor i exceed the critical value (= 9.5 V). The order of triggering for the sensor i is shown with s_i. For example, if only five sensors (1, 2, 3 ,4, 7) are triggered with t_1=20 s, t_2=25 s, t_3=18 s, t_4=30 s, t_7=35 s then s_1=2, s_2=3 ,s_3=1, s_4=4, s_7=5. That means, $sensor_3$ was triggered first (1), $sensor_1$ was triggered second (2), and so on. s_i= NA (not available) for the other sensors at that time. These data are taken via data acquisition system from the mold to the computer. During estimation of the resin flow pattern, these parameters are used in different algorithms.

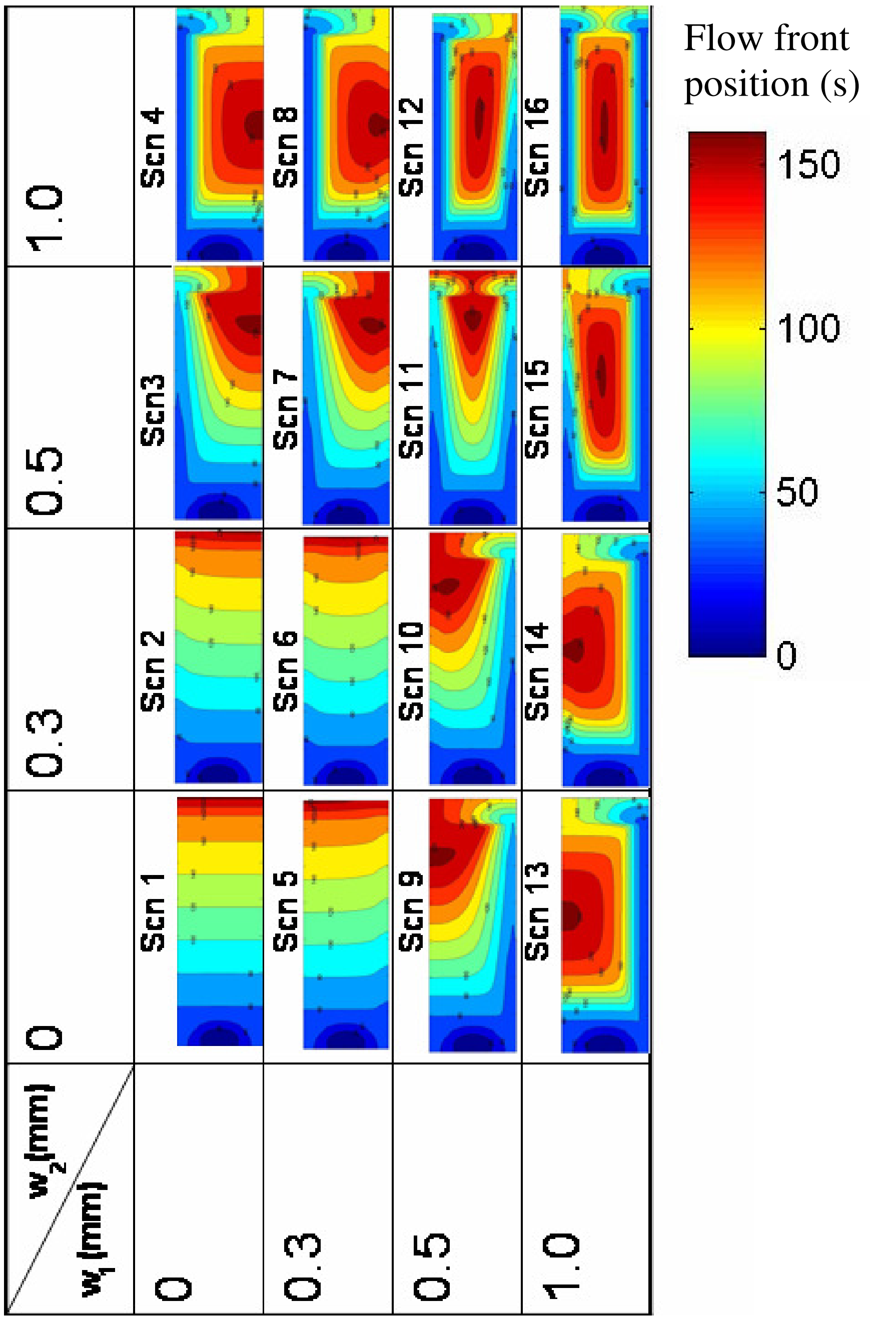

Figure 5.23 Flow front contours of the scenarios 1-16.

5.4.1 Time Normalization Algorithm

Hsiao et al. [33] used triggering times of the sensors in their algorithm for resin's flow pattern estimation. Normalized triggering times are found by:

$$\bar{t}_{j,\exp} = \frac{t_{j,\exp}}{\sum_i t_{i,\exp}} \tag{5.5}$$

$$\bar{t}_{j,Scn\ k} = \frac{t_{j,Scn\ k}}{\sum_i t_{i,Scn\ k}} \tag{5.6}$$

where $t_{i,exp}$ is the actual arrival time of resin at sensor i. Here, $\sum_i$ represents the set of triggered sensors only at the current experimental time. Table 5.3 was constructed for an experimental sensor data to illustrate how the normalization (Equation (5.5)) is applied. Notice that the analysis was done after all the sensors were triggered. All predefined scenarios are also normalized using Equation (5.6), and normalized triggering time database is created off-line. Comparison of the normalized triggering times of the experiment and the scenarios are done by using least square method:

$$P_{Scnk} = \sqrt{\sum_i (\bar{t}_{i,\exp} - \bar{t}_{i,Scnk})^2} \tag{5.7}$$

$P_{Scn\ k}$ is the penalty value for scenario Scn k. The scenario with the minimum penalty value is the best fit to the experimental data. For the same experimental data given in Table 5.3, penalty values of all scenarios are given in Table 5.4. Again, this analysis was done after all the 15 sensors were triggered. Scn 5 has the minimum penalty value.

Table 5.3 Normalized time values of the experiment.

SENSOR	TRIGGERING TIME (s)	NORMALIZED TRIGGERING TIME
S1	37	0.029
S2	38	0.030
S3	35	0.027
S4	66	0.051
S5	75	0.058
S6	55	0.043
S7	83	0.064
S8	109	0.085
S9	70	0.054
S10	113	0.088
S11	138	0.107
S12	89	0.069
S13	153	0.119
S14	128	0.099
S15	99	0.077

Table 5.4 Penalty values for the Predefined Scenarios, Scn 1-16.

Scenario #	Penalty
Scn 1	0.049
Scn 2	0.050
Scn 3	0.109
Scn 4	0.140
Scn 5	0.046
Scn 6	0.047
Scn 7	0.107
Scn 8	0.139
Scn 9	0.055
Scn 10	0.051
Scn 11	0.071
Scn 12	0.116
Scn 13	0.105
Scn 14	0.103
Scn 15	0.084
Scn 16	0.122

5.4.2 Sensor Triggering Order Based Algorithm

In our study, we used triggering order, not the normalized time, to compare the experiment with each scenario. The penalty value for scenario Scn k is given by

$$P_{Scn\,k} = \sqrt{\sum_i (s_{i,\exp} - s_{i,Scn\,k})^2} \qquad (5.8)$$

where $s_{i,exp}$ is the triggering order of sensor i in the experiment, and $s_{i,scenario}$ is the triggering order of that sensors in the predefined scenario Scn k. $\sum_i$ represents the summation on all the triggered sensors until the current experimental time. The result of this algorithm for a representative scenario, say Scn 15, is given in Tables 5.5 and Scn 10 has the minimum penalty value as seen in Table 5.6 when this method is performed on all the scenarios.

Table 5.5 Results of the triggering order based algorithm.

Sensor	Triggering Order		Penalty term $(s_{i,exp}-s_{i,scn\ 15})^2$
	Experiment, s_i, exp	Scenario, Scn 15, s_i, Scn 15	
S1	2	1	1
S2	3	2	1
S3	1	3	4
S4	5	8	9
S5	7	13	36
S6	4	5	1
S7	8	9	1
S8	11	15	16
S9	6	6	0
S10	12	10	4
S11	14	14	0
S12	9	7	4
S13	15	11	16
S14	13	12	1
S15	10	4	36
$P_{Scn\,15} = \sqrt{\sum (s_{i,\exp} - s_{i,Scn\,15})^2} = \sqrt{1+1+4+9+36....+1+36} =$ **11.4**			

Table 5.6 Penalty values for sensor triggering order based algorithm.

Scenario	Penalty, $P_{Scn\ k}$
Scn 1	9.6
Scn 2	9.3
Scn 3	14.3
Scn 4	18.8
Scn 5	6.2
Scn 6	7.1
Scn 7	12.9
Scn 8	18.5
Scn 9	7.1
Scn 10	5.7
Scn 11	7.9
Scn 12	15.2
Scn 13	14.7
Scn 14	14.7
Scn 15	11.4
Scn 16	15.3

5.4.3 Comparison of Algorithms

We would like to find the perfect match between the experimental sensor data and the virtual sensor-data of 16 scenarios. To do this, we developed an algorithm, and also used another algorithm in the literature [33]. Results of experiments 1, 2 and 3 were virtually generated by using a randomly selected disturbance in the mold filling simulations. These virtual experiments have been done with the same injection parameters (flow rate, mold geometry, etc, …) of the actual experiment. Experiment 4 is an actual experiment. It can be seen from Table 5.7 that the results of the two algorithms are usually consistent.

In experiment 1 and 2, the fabric was assumed to have a non-uniform bulk permeability in an inner region. In experiment 1, there are longitudinal race-tracking channels (each 0.6 mm width) at both sides of the mold cavity and also there is a race-tracking channel in the transverse direction (10 mm width) near the center of the mold. In experiment 2, there is a longitudinal race-tracking channel (0.6 mm width) at only one side of the mold cavity. The transverse direction race-tracking channel also exists in this simulation. Hence, the characteristic of the flow front propagation is much different than all the scenarios (Scn1-16) considered. Recall that all the scenarios correspond to the disturbances due to race-tracking channels along the upper and lower edges only. Among those 16 scenarios considered, Experiments 1 and 2 were best fitted to Scn 11 and Scn 4, respectively by using both Algorithm 1 and 2.

Experiment 3 has a race-tracking channel along both sides of the mold cavity with $w_1 = w_2 = 0.6$ mm which was not considered in scenarios Scn 1-16. However, this experiment was best fitted to Scn 6 by using both Algorithm 1 and 2.

The front contour of the actual experiment 4 is seen in Table 5.7. These contours were plotted by using MATLAB's built-in function "contourf".

Algorithms 1 and 2 resulted in different scenarios (Scn 5 and Scn 10, respectively) to best fit to this experiment. A qualitative comparison by naked eye favors Scn 10 which is the best fit of Algorithm 2.

Table 5.7 Comparison of two algorithms.

EXPERIMENT	**ALGORITHM 1 (Developed by Hsiao and Advani)**		**ALGORITHM 2 (Developed in Koc University)**	
Flow front contours of experiments	Sorted scenarios with descending penalty values	Flow front contours of the scenario with least penalty value	Sorted scenarios with descending penalty values	Flow front contours of the scenario with least penalty value
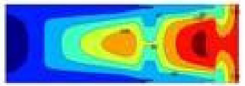	Scenario 11 (P=0.0367) Scenario 6 (P=0.0752) Scenario 2 (P=0.0771)	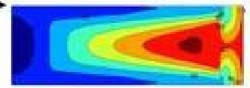	Scenario 11 (P=2.4495) Scenario 6 (P=7.7460) Scenario 7 (P=9.6954)	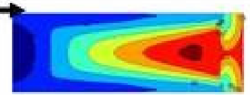
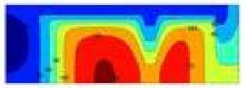	Scenario 4 (P=0.0169) Scenario 8 (P=0.0191) Scenario 12 (P=0.0927)	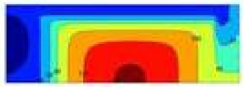	Scenario 4 (P= 4.0000) Scenario 8 (P= 4.6904) Scenario 12 (P= 10.5830)	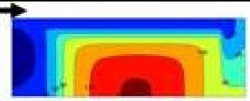
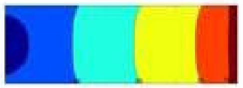	Scenario 1 (P=0.0153) Scenario 6 (P= 0.0154) Scenario 2 (P=0.0157)	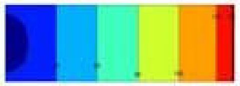	Scenario 6 (P=2.4495) Scenario 2 (P= 3.1623) Scenario 1 (P=3.4641)	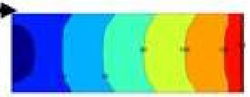
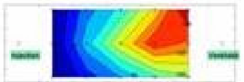	Scenario 5 (P= 0.0409) Scenario 6 (P= 0.0419) Scenario 1 (P=0.0434)	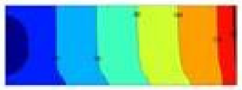	Scenario 10 (P=5.0990) Scenario 5 (P= 6.1644) Scenario 9 (P=7.8740)	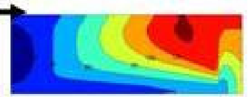

Chapter 6

MECHANICAL TESTS OF COMPOSITE MATERIALS

6.1 Introduction

Testing of mechanical properties of composite materials is required for quality control purpose. Quality control consists of methods to check if a product meets the standards or the needs of the customer. This chapter is about two different quality control tests for composite materials: (i) tensile test, and (ii) three-point bending test.

Before proceeding, it is important that all the quality control tests have to be performed according to a standard test method. Different institutions described test methods for quality control purposes. These tests may differ from each other, so an engineer must choose a method and perform the test with respect to the method limitations and descriptions. In Table 6.1, test methods are listed for tensile and bending properties.

Table 6.1 Equivalent test methods for tensile and bending properties of composite materials [34].

	CEN	**ASTM**	**DIN**	**BS**	**ISO**	**NF**
Tensile test	EN61	D 3039 D 638	53455	2782/10 1003	3268	T57-101
Three-point bending test	EN63	D790-03	53452	2782/10 335A	178	T57-105

6.2 Three-Point Bending Test

One of the mechanical tests applied on composite materials is the three-point bending test (also known as flexural test). With the three-point bending test, the following mechanical properties of a material can be determined [34]:

- maximum failure strength under bending, σ_F (flexural stress),
- bending modulus, E_F (flexural modulus),
- maximum bending deflection, y_M.

In Figure 6.1, it is shown how a three-point bending test is done. A specimen is simply supported as shown. Another external load is applied on the specimen from the middle of the specimen between the two supports. The specimen is deflected until (i) the moment when the specimen ruptures, or (ii) a critical deflection is reached before a rupture.

Maximum deflection (y_m) and the force (F_F) at that maximum deflection are recorded data the experiment.

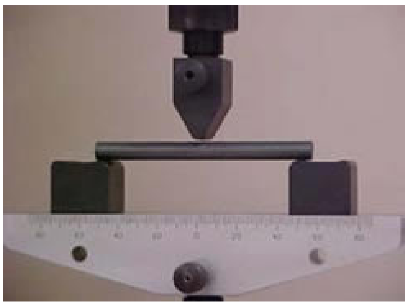

Figure 6.1 Three-point bending test [35].

In Figure 6.2, a schematic of the three-point bending test is shown. The bending stress at the surface of a rectangular beam is given by [6]:

$$\sigma_F = \frac{3F_F L}{2bd^2} \tag{6.1}$$

where

F_F = the value of the force when the specimen ruptures or the critical deflection is reached before rupture,

L = distance between two support spans,

d = thickness of the specimen,

b = width of the specimen.

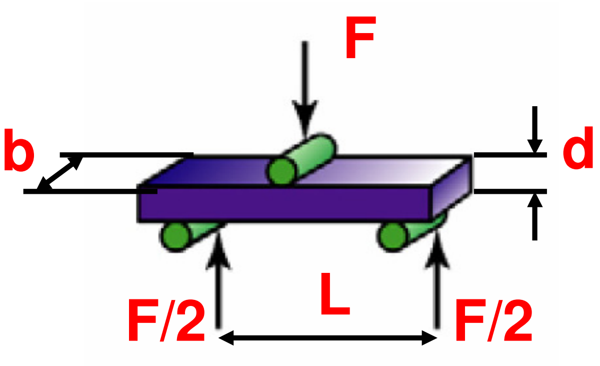

Figure 6.2 Schematic of the three-point bending test [6].

Also, one can get the flexural modulus by using [6]:

$$E_F = \frac{3}{4}\frac{F_F L^3}{bd^3 y_m} \tag{6.2}$$

Notice that all these equations are for rectangular prism specimens. The three-point bending tests for composite materials are done with rectangular cross-section specimens according to the standard test methods seen in Table 6.1. These test methods define all the experimental parameters. Some of the parameters described in ASTM D 790 – 03 are [36]:

- specimen geometry and dimensions,
- testing machine used to apply load on the specimen,
- the geometry and the dimensions of the loading nose and support spans,
- micrometer used to measure the specimen dimensions,
- testing conditions (air humidity and temperature),
- rate of the loading nose motion (speed of the loading nose).

Mechanical properties of reinforced plastics depend on many parameters: type of resin used, type of fibers, fiber volume fraction, fiber orientation and void content. For this reason, analytical methods or experiments are needed to estimate the mechanical properties. In Table 6.2, bending strength and modulus of elasticity for glass reinforced composites is shown from a reference [24]. The same resin type is used in all parts in the table; its aim is to present the effect of glass reinforcement type in bending properties. Neat cured resin is the cured polymer with no reinforcement in it. The other materials are composites with different types of reinforcements.

Table 6.2 Flexural properties for glass reinforced polyester composites [29].

Type of glass reinforcement	**Glass content, wt%**	**Bending strength, MPa**	**Bending modulus, GPa**
Neat cured resin	0	88	3.9
Roving fabric	60	317	15
Woven glass fabric	70	403	17.38
Unidirectional roving fabric	70	403	29.44

In our university, we have a three-point bending apparatus seen in Figure 6.3.

Figure 6.3 The three-point bending apparatus in our university.

We did tests on specimens cut from composite parts that we manufactured. The dimensions of the specimen are seen in Figure 6.4. The geometry complies with the ASTM D 790-03. But, we encountered a problem during the test: the capacity of our load cell was too high that, it could not sense the force at the moment of rupture. That means, the force F_F was only a few percent of the machine capacity or less, and since this value is lower than much 5-10% of the capacity, the data is not reliable. Two alternative solutions can be offered to resolve this problem: (i) increase the thickness of our specimens so that the rupture will occur at a higher force or (ii) to change the load cell with a more sensitive one.

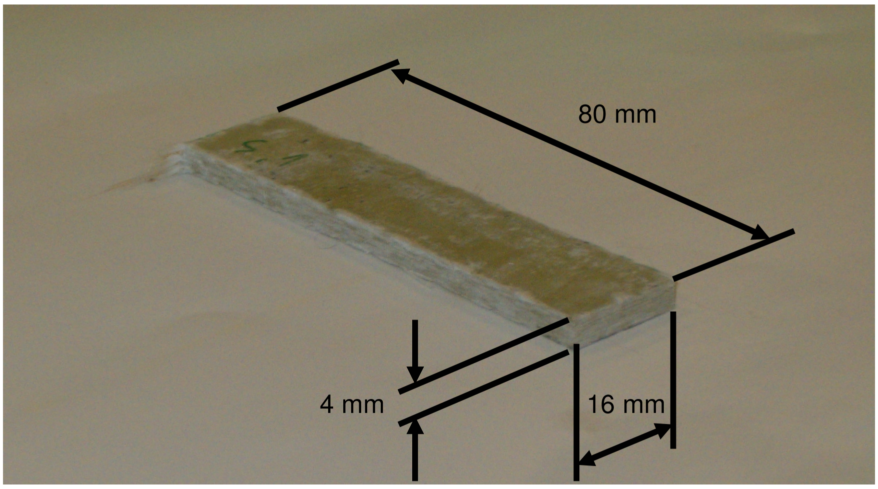

Figure 6.4 Specimen for three-point bending test.

As a continuation of this study, it is recommended to apply the former modification.

6.3 Tensile Test

Tensile test is a universal test to measure the following mechanical properties of a material [6]:

- modulus of elasticity, *E*
- yield strength, σ_Y
- ultimate strength, σ_U
- whether the material is ductile or brittle,
- modulus of thoughness, u_t
- ranges of elastic and plastic deformations.

A typical stress versus strain (or stress – strain) diagram for a composite material is schematically shown in Figure 6.5.

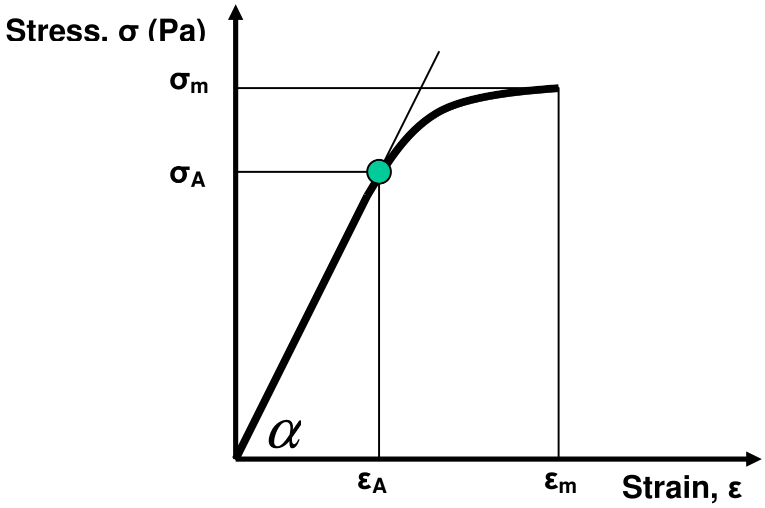

Figure 6.5 A typical stress versus strain plot for reinforced plastics.

where

$$\varepsilon = \frac{\Delta l_0}{l_0} \tag{6.3}$$

$$\sigma_m = \frac{F_m}{A_0} = \frac{F_m}{b \cdot e} \tag{6.4}$$

$$\sigma_A = \frac{F_A}{A_0} = \frac{F_A}{b \cdot e} \tag{6.5}$$

$$E = \frac{\sigma_A}{\varepsilon_0} = \frac{F_A}{b \cdot e} \tag{6.6}$$

where

$\varepsilon =$ strain of the material under load,

Δl = elongation,

l_0 = initial gage length of the material,

σ_m = maximum ultimate stress of the material,

A_0 = initial cross-sectional area,

$F_{m =}$ load at the instant of fracture,

e = initial thickness of the specimen,

b = initial width of the specimen,

σ_A = yield strength,

F_m = force at the instant of yield,

E = elastic modulus.

In Figure 6.6, a composite a specimen under tensile test is seen [37]. The specimen is placed between the grips of the test machine. The upper jaw moves upward with a defined rate of motion. During loading, both the strain, ε and the stress, σ are recorded.

This specimen (shown in Figure 6.6) is cut according to ASTM D 638 [43]. Standard dimensions for ASTM D 638 are seen in Figure 6.8 for a specimen with a thickness smaller than 7 mm.

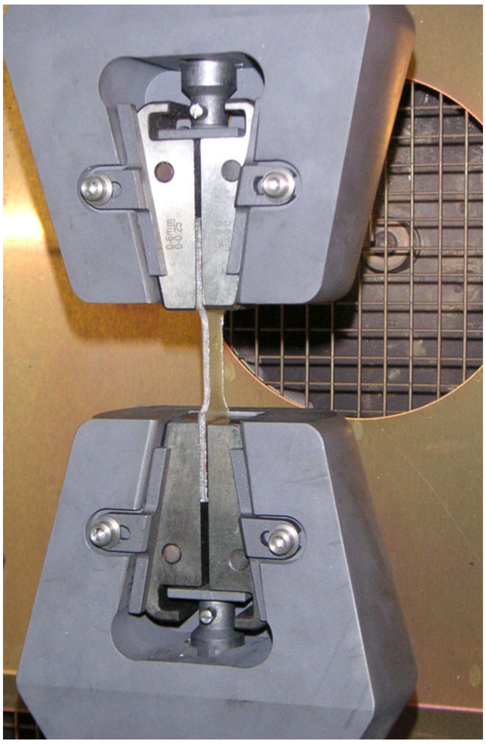

Figure 6.6 Composite material under tensile test [37].

In Table 6.1, standard test methods for tensile properties are listed. ASTM D 3039 (standard test method for tensile properties of polymer matrix composite materials) is one of the standards for tensile tests. This standard explains all the tensile test procedure such as [38]:

- Specimen geometry: The shape is constant rectangular geometry. The exact dimensions are not defined, but ratio of length and width is recommended in the text.
- Tabs are used if required (see Figure 6.8).

- rate of strain (duration of the test before fracture occurs),
- test environment (temperature and moisture).

In Table 6.3, tensile properties of a typical composite material are shown. Like the flexural properties, tensile properties depend on many parameters of the part as described above. In Table 6.3, neat cured resin is unreinforced cured plastic. The other materials are composite materials with different types of reinforcements.

Table 6.3 Tensile properties of glass reinforced polyester composites [29].

Type of glass reinforcement	**Glass content, wt%**	**Tensile strength, MPa**	**Tensile modulus, GPa**
Neat cured resin	0	59	5.40
Roving fabric	60	314	19.50
Woven glass fabric	70	331	25.86
Unidirectional roving fabric	70	611	32.54

In our laboratory, we performed tensile tests on composite material specimens (seen in Figure 6.7), but we had gripping problems during the tests. Grips in the machine were designed for metals. When the composite specimens are placed between the grips, the grips damage the specimen and the part fractures at a section near the grips. In Figure 6.9, a specimen is shown with this type of fracture. According to the ASTM D3039, this is a failure of the test method. The fracture section must be at least 1 w away from the grip where w is the width of the specimen. We bonded tabs to the specimens (compatible with the standard) using an epoxy glue (see Figure 6.10). However, the bonded area was not strong enough, and the tabs slipped away from the specimen. Then, we put pieces of clothes between the specimen and the tab, but again the specimen slipped away. The optimum solution for this problem is to change the grips. So, these tests are left as future work.

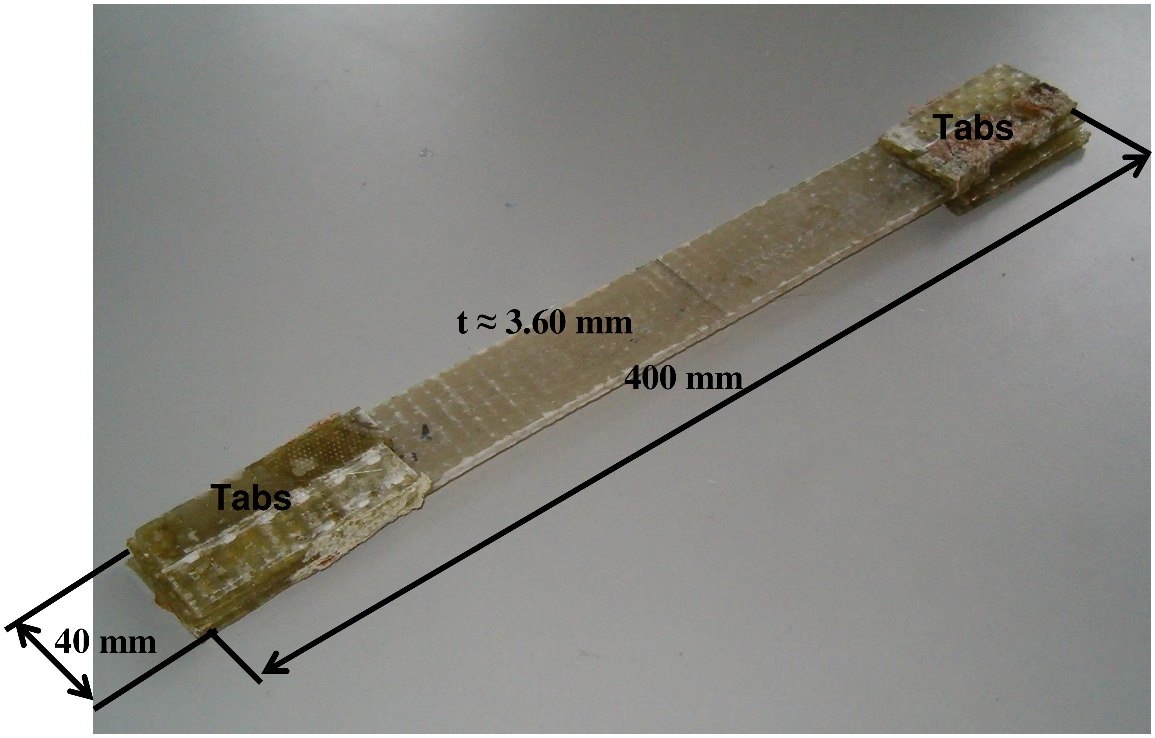

Figure 6.7 Specimen manufactured according to ASTM D3039.

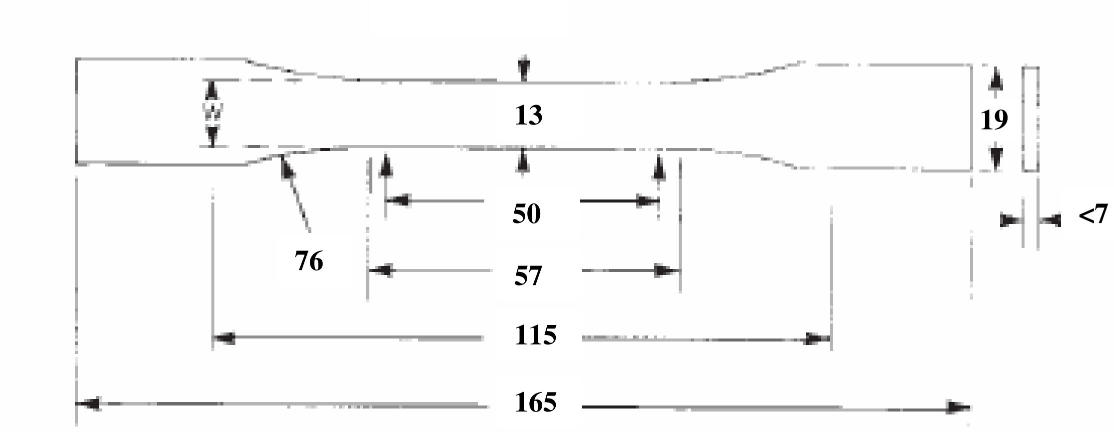

Figure 6.8 Specimen geometries according to ASTM D 638 [43]

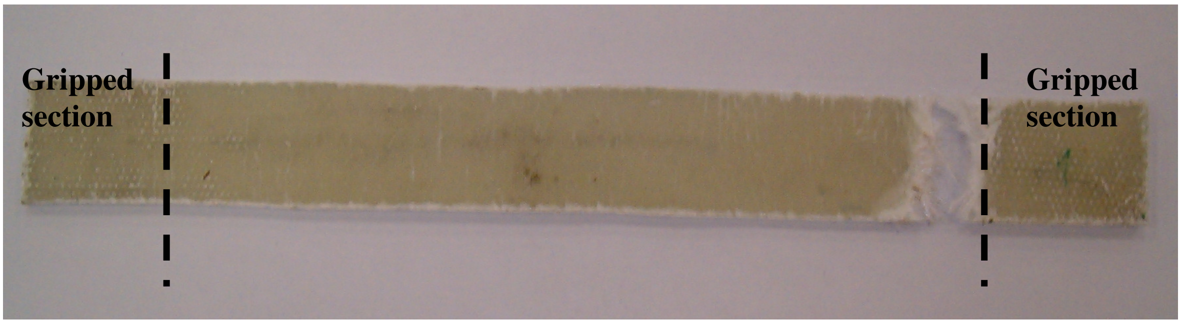

Figure 6.9 A specimen which fractured with failure.

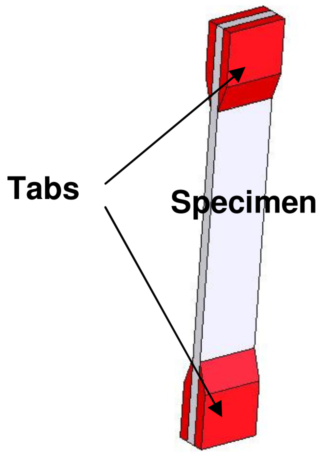

Figure 6.10 A specimen with tabs.

6.4 Future Work

If the problems with data acquisition and gripping are resolved, the following items can be done as a future work:

- How the process parameters affect the mechanical properties of composite materials?
- Distribution of mechanical properties, as a function of spatial coordinates and also fiber volume fraction.
- Effect of micro-size voids on mechanical properties.

Chapter 7

CONCLUSION

A progress was made in this study for the automation of the RTM process. RTM automation requires monitoring of mold filling and resin cure. Point-voltage sensors were developed and investigated in a recent study. In this study, a modification was made in the circuit of point–voltage sensors to improve these sensors. In the previous version of the sensors, only a single gain factor was used both for resin flow and resin cure monitoring. By having an adjustable gain factor in this work, the sensor's sensitivity can be adjusted for two different stages: (i) high gain (and hence a quick response rate) during flow monitoring, and (ii) relatively moderate gain factor (and hence higher sensitivity on resin's electrical resistance and its cure degree) during cure monitoring.

A literature survey about mold design and was done. A new mold was designed and manufactured by following the general guidelines, and the idea of having a modular mold. Currently, 30 point–voltage sensors are embedded on the mold. The sensor holes on the mold are modular, the sensors can be replaced with inlet / ventilation bolts. In this mold, monitoring of resin flow and resin cure were successfully achieved by having repeated experiments.

Off-line disturbance simulations were done to predict the resin flow patterns during injections under disturbance scenarios. These scenarios correspond to different degrees of race-tracking channels at both sides of the mold cavity. By automating the process, it is going to be possible to evaluate the sensor data, and to make control actions by changing injection parameters. An algorithm was developed to evaluate in-situ sensor data and to relate it to the closest virtual sensor response of many potential mold filling scenarios which correspond to different disturbances.

To sum up, a modular mold was designed and manufactured. Resin flow and resin cure monitoring were achieved. An algorithm was introduced to evaluate the in-situ sensor data. As future work, the most accurate algorithm should be determined to fit the actuat sensor data to the closest scenario's sensor data. Also, additional injection gates / ventilation ports with automatic valves should be connected to the RTM mold. Besides off-line disturbance scenarios, on-line scenarios should be simulated for a more accurate and realistic investigation of disturbances. Optimum control actions should be determined to affect the flow front propagation such that the mold can be filled completely even if a disturbance exists in the mold cavity.

BIBLIOGRAPHY

[1] M. Danışman, Use of Thermocouples and Voltage Sensors to Monitor the Resin Transfer Molding Process, M. Sc. Thesis, Koc University, (2006)

[2] http://www.aviationexplorer.com/eclipse_aircraft/eclipse_500_aircraft.jpg

[3] http://www.exoticcars.ws/cars/ferrari-enzo.jpg

[4] http://www.tfhrc.gov/focus/may04/images/bridge4.jpg

[5] http://www.biziworks.com.au/aeroshop/graphics/docimages/lazerhelmet.gif

[6] S. Kalpakjian and S. R. Schmid, Manufacturing Engineering and Technology, Prentice Hall, 4th edition, (2001).

[7] P.K.Mallick, Fiber-Reinfoced Composites,Marcel Dekker, 2nd Edition, (1993).

[8] S.G. Advani, E.M. Sozer, Process modeling in Composites Manufacturing, New York, Marcel Dekker, Inc., (2003).

[9] Polipol™ 336-RTM, Product Technical Bulletin.

[10] K. Potter, Resin Transfer Moulding, Chapman & Hall, 1st edition, (1997).

[11] Polyethylene tube, model no: 4HM16 from www.grainger.com

[12] M. Danisman, G. Tuncol, A.Kaynar and E.M. Sozer, Monitoring of resin flow in the resin transfer molding (RTM) process using point-voltage sensors, Composites Science and Technology, 67 (2007), 367–379.

[13] G. Tuncol, M. Danisman, A. Kaynar and E.M. Sozer, Constraints on monitoring resin flow in the resin transfer molding (RTM) process by using thermocouple sensors, Composites: Part A, 38 (2007), 1363–1386.

[14] http://www.compositesworld.com/hpc/issues/2003/November/282/3

[15] SMARTweave monitors resin flow and cure in RTM, Reinforced Plastics Periodical 41 (1997), 24.

[16] McIlhagger A, Brown D, Hill B. The development of a dielectric system for the online cure monitoring of the resin transfer molding process. Composites Part A, 31 (2000), 1373–81.

[17] E. Schmachtenberg, J. Schulte zur Heide and J. Töpker, Application of ultrasonics for the process control of Resin Transfer Moulding (RTM), Polymer Testing, 24(3) (2005) 330-338.

[18] S.T. Lim and W. Lee, An analysis of the three-dimensional resin-transfer mold filling process, Composites Science and Technology, 60 (2000), 961-975.

[19] J.P. Dunkers, J.L. Lenhart, S.R. Kueh, J.H. van Zanten, S.G. Advani and R.S. Parnas, Fiber-optic flow and cure sensing for liquid composite molding, Opt Lasers Engineering, 35(2) (2001), 91–104.

[20] P. Barooah, B. Berker and J.Q. Sun, Lineal Sensors for Liquid Injection Molding of Advanced Composite Materials, J Mater Process Manuf Sci, 6 (2003), 169–84.

[21] J.M. Lawrence, K. Hsiao, R.C. Don, P. Simacek, G. Estrada, E.M. Sozer, H.C. Stadtfeld and S.G. Advani, An approach to couple mold design and on-line control to manufacture complex composite parts by resin transfer molding, Composites Part A: Applied Science and Manufacturing, 33 (2002), 981-990.

[22] S. Bickerton, H.C. Stadtfeld, Karl V. Steiner and Suresh G. Advani, Design and application of actively controlled injection schemes for resin-transfer molding, Composites Science and Technology, 61(11) (2001), 1625-1637.

[23] E.M. Sozer, S. Bickerton and S.G. Advani, On-line strategic control of liquid composite mold filling process, Composites: Part A, 31 (2000), 1383–1394.

[24] William D. Callister, Materials Science and Technology, John Wiley & Sons, Inc., Fifth edition.

[25] S. Bickerton and M.J. Buntain, Modeling forces generated within rigid liquid composite molding tools. Part B: Numerical analysis, Composites: Part A, 38 (2007), 1742–1754.

[26] http://www.ase.uc.edu/mmccs/3.jpg

[27] http://www.destaco.com/greng/products.asp?loc=TU&lang=ENG&products=Manual%20Clamps&Category_1=Pull+Action+Latch+Clamps&Category_2=Standard+Horizontal+U%2DHook

[28] Y. Luo and I. Verpoest, Compressibility and Relaxation of a New Sandwich Textile Preform for Liquid Composite Molding, Polymer Composites, (1999), Vd. 20, No. 2.

[29] ASM Metals Handbook, Vol. 21, (2001).

[30] Douglas M. Bryce, Plastic Injection Molding, Society of Manufacturing Engineers, (1998).

[31] http://www.dogma.org.uk/vtt/process/text/process_monitoring_files/image010.jpg

[32] G. Tuncol, Monitoring of Resin Flow and Cure in Resin Transfer Molding (RTM) Process, M. Sc. Thesis, Koc University, (2005).

[33] K. Hsiao1 and S.G. Advani, Flow sensing and control strategies to address race-tracking disturbances in resin transfer molding. Part I: design and algorithm development, Composites: Part A, 35 (2004), 1149–1159.

[34] M.H. Geier, Quality Handbook for Composite Materials, Chapman and Hall, (1994)

[35] http://www.testedandproven.com/images/clip_image001_003.jpg

[36] Standard Test Methods for Flexural Properties of Unreinforced and Reinforced Plastics and Electrical Insulating Materials (ASTM D 790 – 03).

[37] http://www.engr.uky.edu/~asme/hpv/archive/pics/tensile_test.jpg

[38] Standard Test Method for Tensile Properties of Polymer Matrix Composite Materials (ASTM D 3039/D 3039M - 00).

[39] S.M. Walsh, In-situ Sensor Method and Device, United States Patent No: 5210499, (1993).

[40]http://upload.wikimedia.org/wikipedia/commons/thumb/d/d5/Opampdifferential.svg/280px-Opamp-differential.svg.png

[41] LIMS (Liquid Injection Molding Simulation), University of Delaware, S. Advani.

[42] M. Senan, Monitoring of Part Dimensions and Fiber-Volume Content in Vacuum Assisted Resin Transfer Molding (VARTM) Process, M. Sc. Thesis, Koc University, (2007).

[43] Standard Test Method for Tensile Properties of Plastics (ASTM D 638 - 03).

VITA

Galip Tarkan Güçlü was born in Kayseri, Turkey on 22.01.1983. He received his B.S. degree in Mechanical Engineering from Istanbul Technical University, Istanbul, in 2005. Since 2005, he has enrolled to the M.S. program in Mechanical Engineering at Koc University as a teaching and research assistant. He has been studying in the "Mold Design in Resin Transfer Molding Process (RTM) Using Point-Voltage Sensors" project since September 2005. He is planning to continue his career as a Mechanical Engineer in the industry.

APPENDIX A

A1. Polyester [9]

Polipol™ 336-RTM

SIVI HALDEKİ ÖZELLİKLERİ
PROPERTIES OF LIQUID FORM

TEST TEST	METOD METHOD		DEĞER VALUE
Renk Colour	ISO 2211	-	**max. 100 Hazen**
Yoğunluk Density	ISO 1675	±%5	**1,094 gr/cm^3**
Kırılma Indisi Refraction Index	ISO 0489	±%5	**1,532**
Asit Değeri Acid Value	ISO 2114	±%10	**23 mg KOH/gr**
Viskozite [1] Brookfield® Viscosity Brookfield®	ISO 2555	±%30	**300 cp**
Tiksotropi Thixotropy	-	±%30	**N/A**
Jel Süresi [2] Gel Time	ISO 2535	±%40	**14'**
Monomer Oranı Monomer Content	-	±%12	**37 %**
Parlama Noktası Flash Point	Abel-Pernsky	-	**28 °C**
Raf Omrü Shelf life in months	-	-	**4 ay**

1 **23 °C de, 4 uç, 50 devir ile ölçülmüştür.**
It is measured at 23 °C, 50 rpm with spindle 4.

2 **23 °C de, % 1 ml % 1 lik Co, % 1 ml Mek-p (Butanox M 60) ile ölçülmüştür.**
It is measured at 23 °C added 1 % ml Co (1 % con.) and 1 % ml Mek-p (Butanox M 60).

SERTLEŞME VERİLERİ [3]
CURING DATA

TEST TEST	METOD METHOD		DEĞER VALUE
$t_{65°C \rightarrow 90°C}$ $t_{65°C \rightarrow 90°C}$	ISO 0584	±%10	**6'13"**
$t_{65°C \rightarrow T maks}$ $t_{65°C \rightarrow T max}$	ISO 0584	±%10	**8'38"**
t_{maks} t_{max}	ISO 0584	±%10	**11'36"**
T_{maks} T_{max}	ISO 0584	±%10	**222 °C**

3 **Reçine 80 °C sıcaklığındaki banyoda, %2 oranında %50 lik Benzoil Peroksit Pasta (Lucidol BT-50,Akzo) ile sertleştirilmiştir.**
Resin cured in 80 °C bath with 2% Benzoyl Peroxide Paste (50% con,Lucidol BT-50,Akzo)

SERTLEŞMİŞ REÇİNENİN ÖZELLİKLERİ [4]
PROPERTIES OF CURED RESIN

TEST TEST	METOD METHOD		DEĞER VALUE
Yük Altında Eğilme Sıcaklığı (HDT) Heat Deflection Temperature (HDT)	ISO 0075-A ISO 0075-B	±%10	77 °C 91 °C
Su Absorbsiyonu Water Absorption	ISO 0062	±%10	0,185 %
Barkol Sertliği (Barcol 934-1) Barcol Hardness (Barcol 934-1)	ASTM-D 2583	±%10	44
Toplam Hacimsel Çekme Total Volume Shrinkage	ISO 2114	±%10	9,04 %

SERTLEŞMİŞ REÇİNENİN MEKANİK ÖZELLİKLERİ [5]
MECHANICAL PROPERTIES OF CURED RESIN

TEST TEST	METOD METHOD		SAF REÇİNE DEĞERİ PURE RESIN VALUE
Eğilme Dayanımı Flexural Strength	ISO 0178	±%10	113 MPa
Elastiklik Modülü Flexural Modulus	ISO 0178	±%10	3110 MPa
Kopmadaki Uzama Elongation at Break	ISO 0178	±%10	4,3 %
Çekme Dayanımı Tensile Strenght	ISO 0527	±%10	64 MPa
Elastiklik Modülü Modulus of Elasticity in Tensile	ISO 0527	±%10	2801 MPa
Kopmadaki Uzama Elongation at Break	ISO 0527	±%10	2,8 %
Izod Darbe Dayanımı Izod Impact Strength	ISO 0180	±%10	9 kj/m^2

4 5 **Sertleşmiş reçinenin testleri için reçine sertleştikten sonra post-kür işlemine tabi tutulmuştur.**
Before the mechanical tests, the cured resin is post-cured.

A2. Sensor circuit

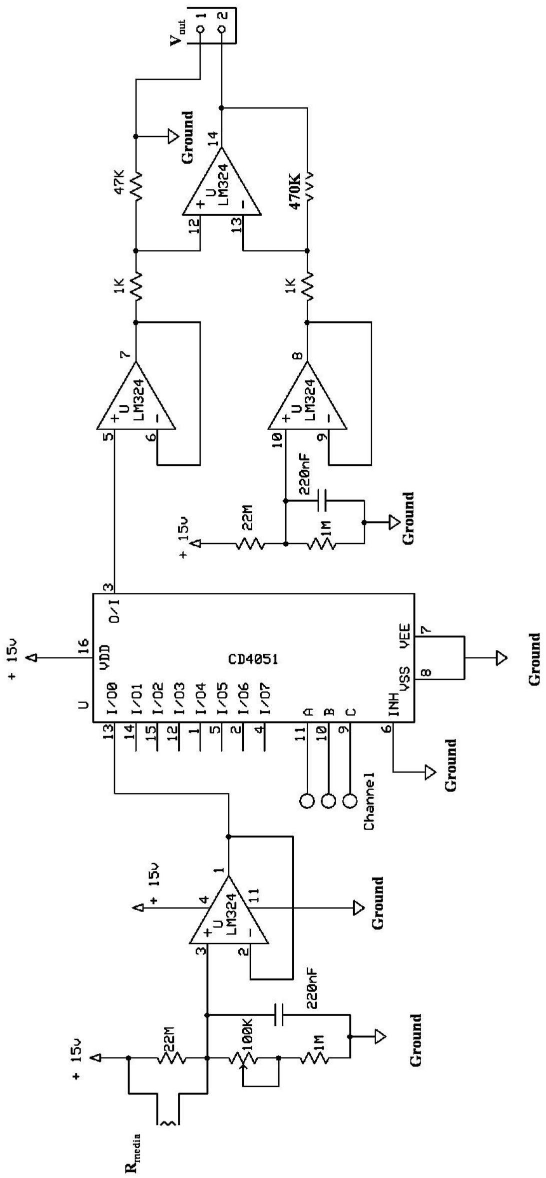

APPENDIX B

B1. Part list of RTM Mold

PART LIST

Part code	Part name	Material	Pcs.	Notes
A	Lower mold plate	Tool steel	1	
B	Upper mold plate	Tool steel	1	
C	Connection plate	Tool steel	1	
D	Spacer	Steel	10	8 spacers for this mold and +2 as spare
E	Sensor bolt	Steel	30	
F	Inlet/Vent bolt	Steel	6	2 bolts for this mold and +4 spare
G	Stiffening bar	Steel	3	2 for this mold and +1 spare
H	Hydraulic press		1	
I	Washer	Brass	36	
J	RTM Injection machine		1	http://www.plastech.co.uk/Megaject_Sprinter-SSB.html
K	Support frame	Steel (painted)	1	
L	O-ring	Silicon	1	Φ7 mm, L=1200 mm

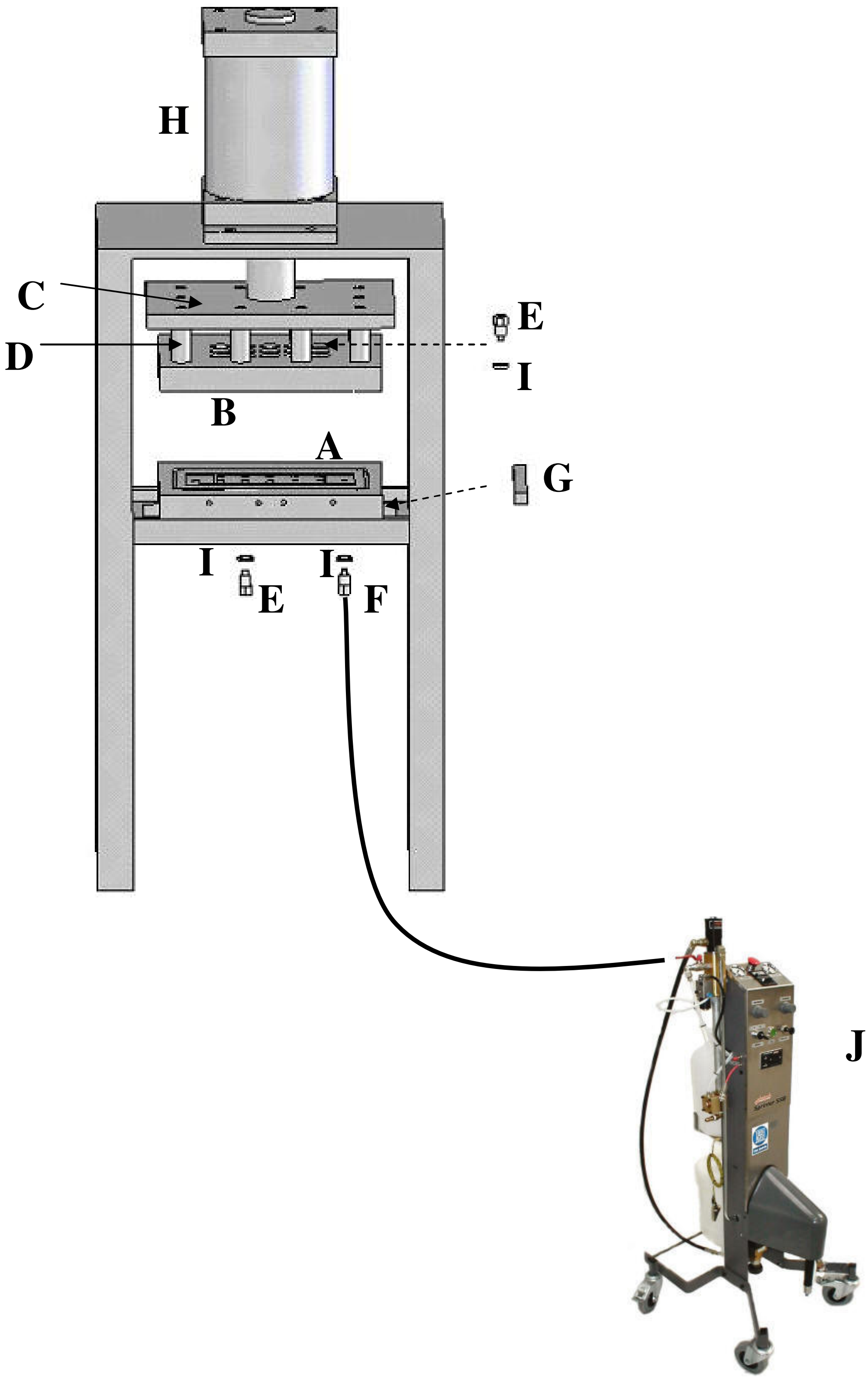
H
C
D
E
I
B
A
G
I
I
E
F
J

B2. Lower Mold Plate

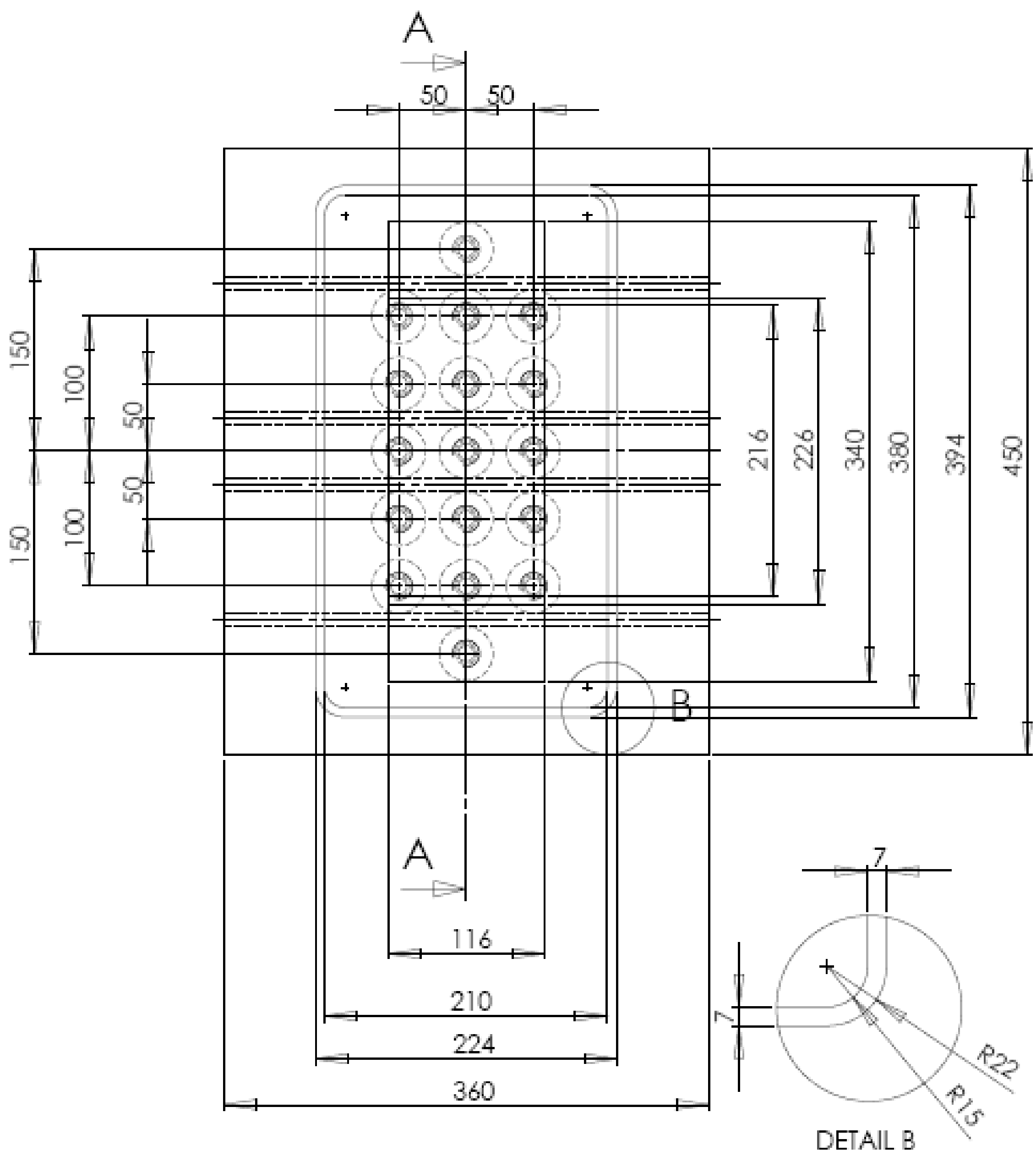

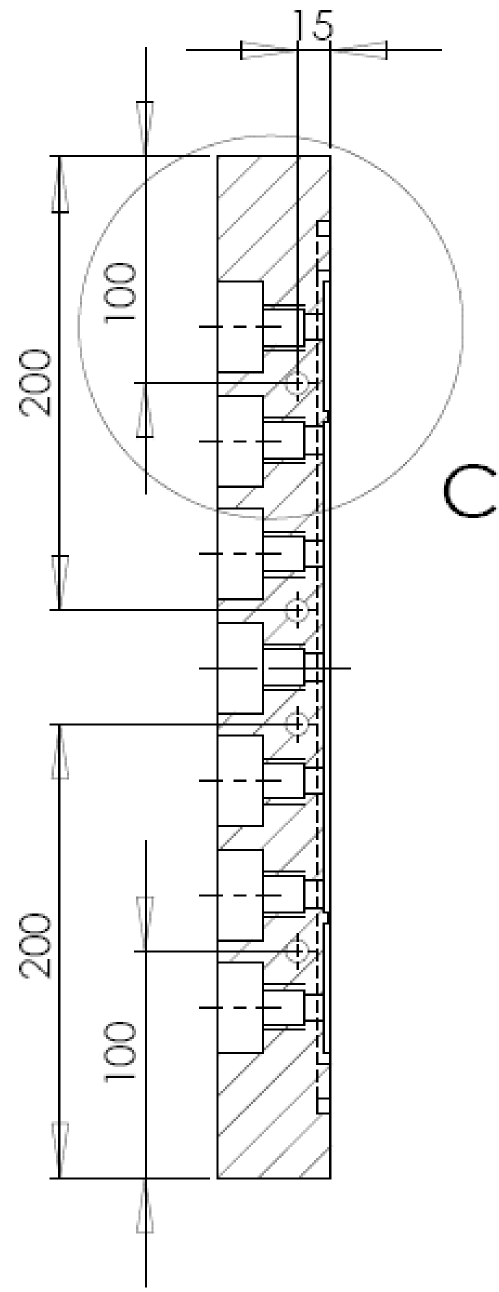

SECTION A-A

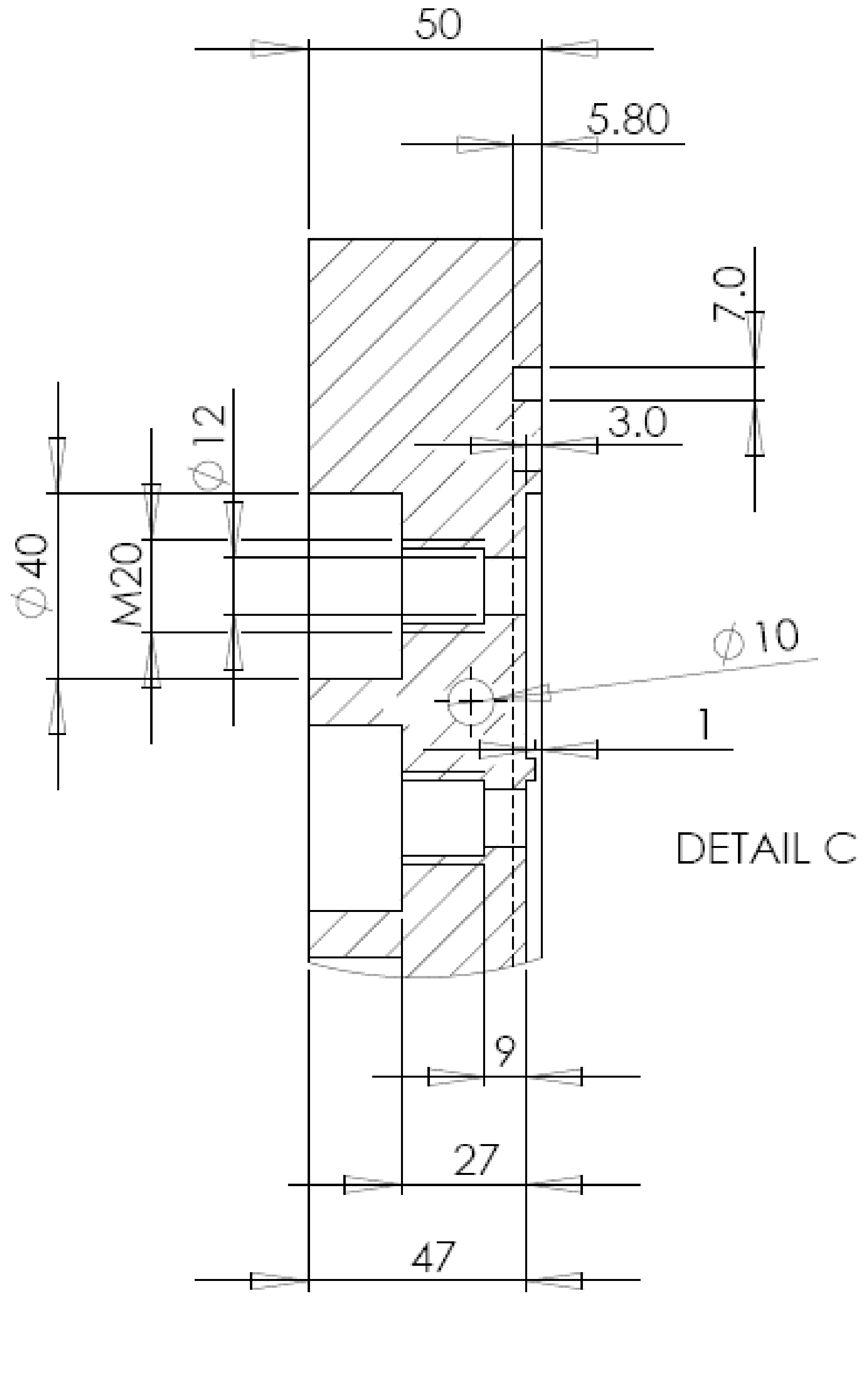
50
5.80
7.0
3.0
Ø12
Ø40
M20
Ø10
1
DETAIL C
9
27
47

B2. Upper Mold Plate

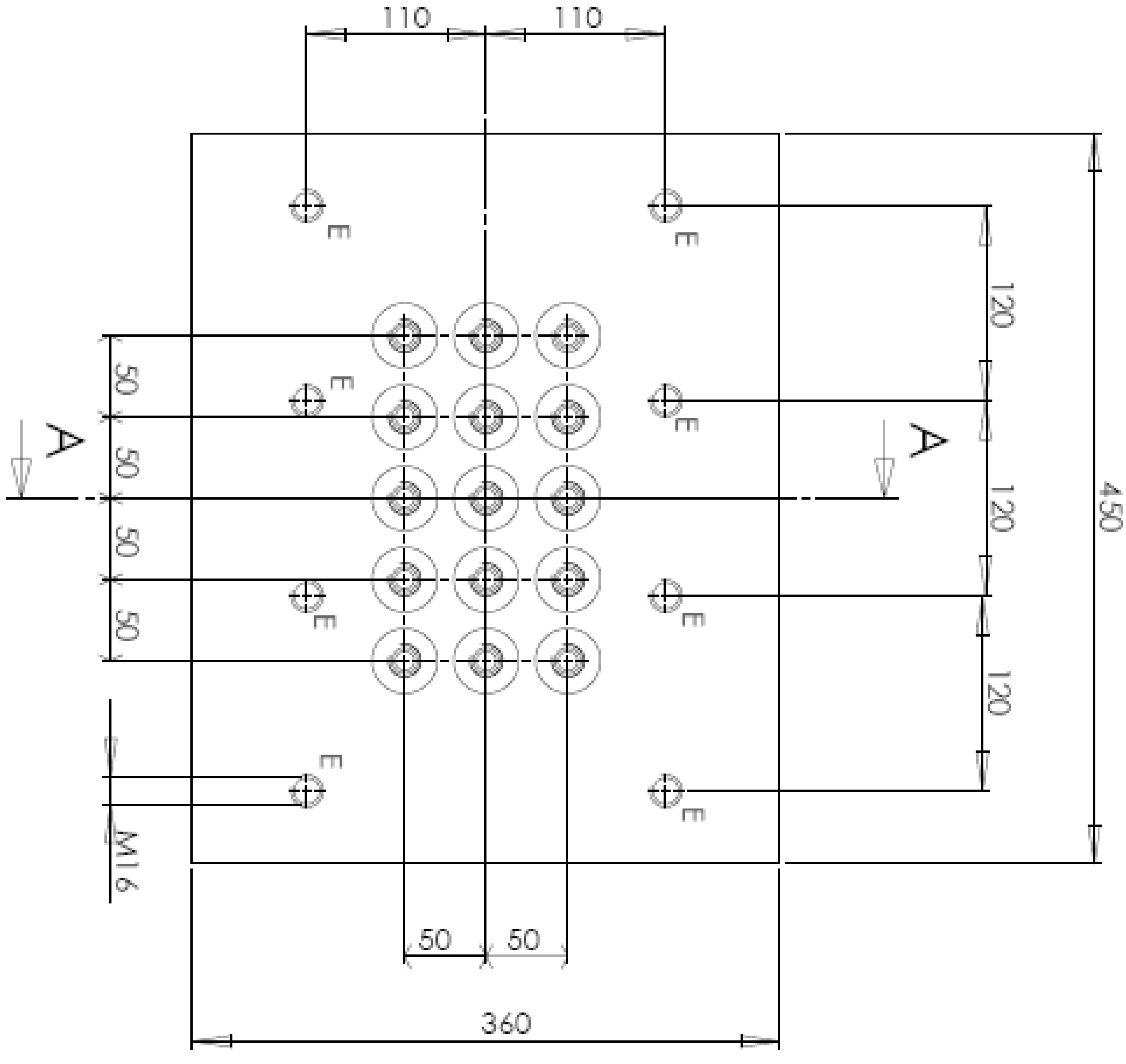

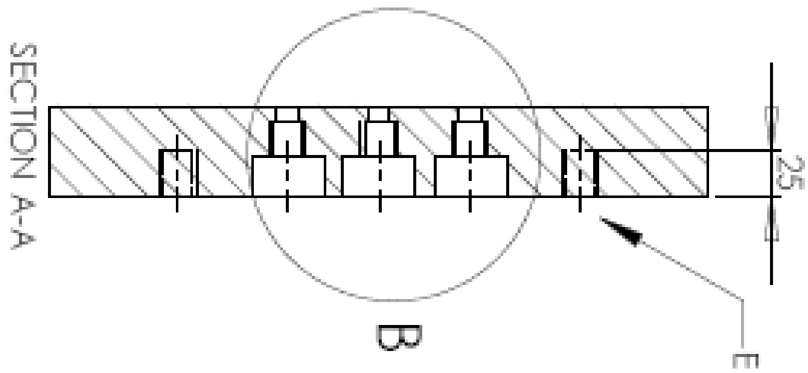
SECTION A-A
B
E
25

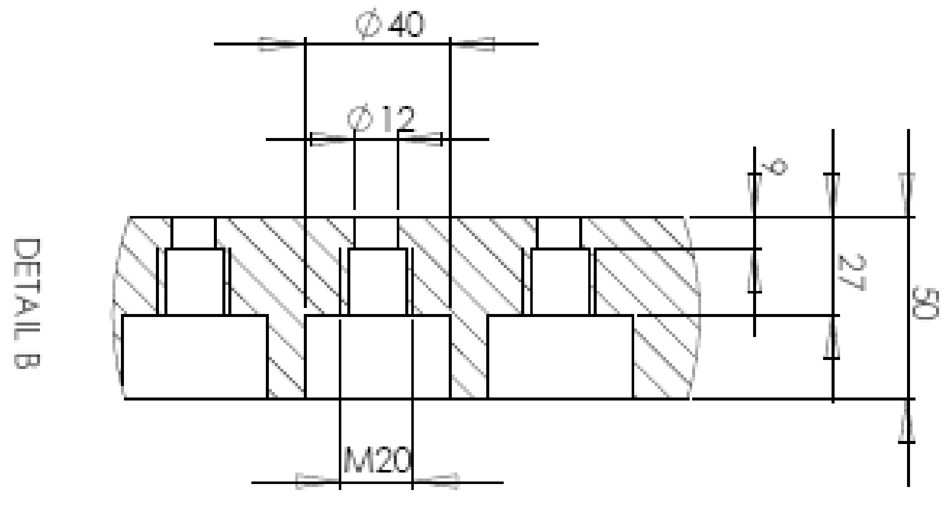
DETAIL B
Ø 40
Ø 12
9
27
50
M20

B3. Sensor Bolts

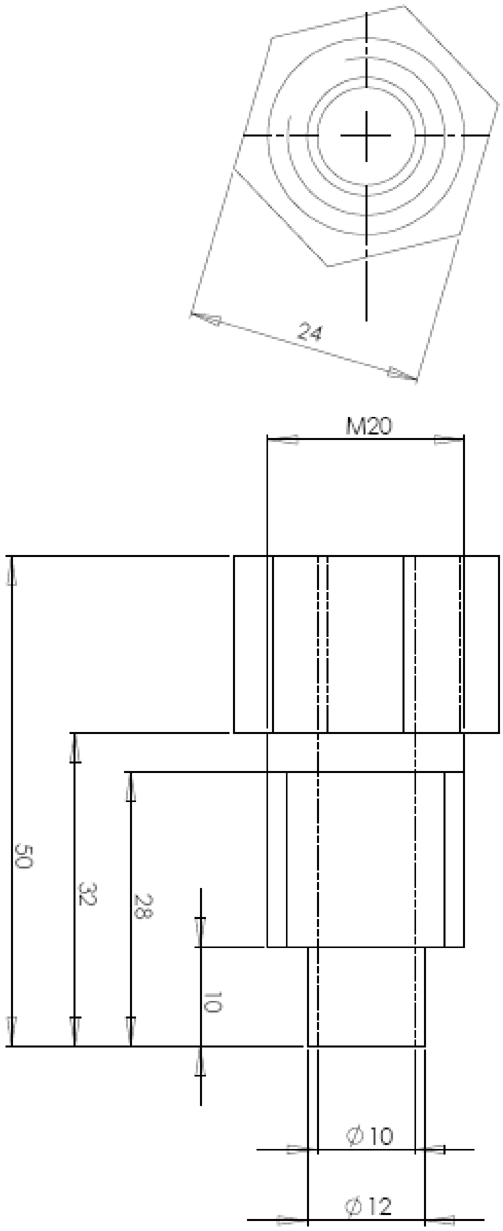

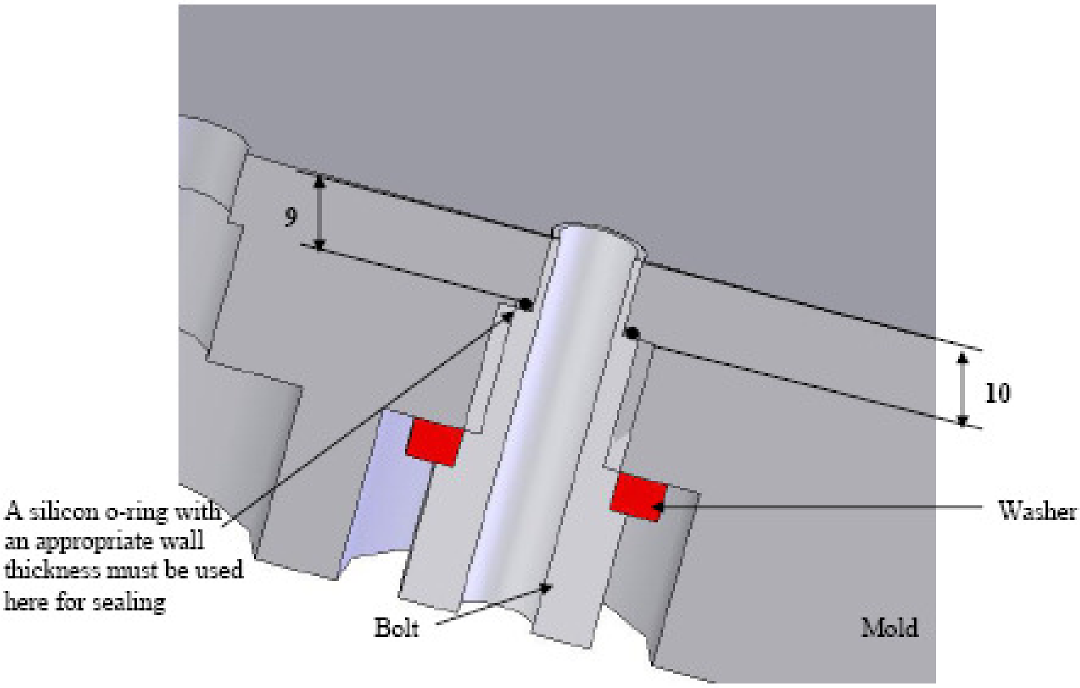

Sensor bolt mounted on the mold plate (internal parts; copper rode, delrin and copper tube not shown).

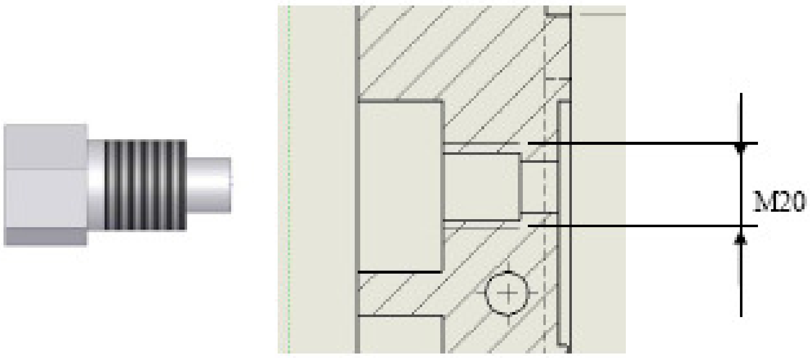

Sensor hole cross-section on the mold.